The dual use of cohesin and its protector Sgo1 contributes to the choreography of the chromosome and the centrosome cycle

DISSERTATION

Zur Erlangung des Grades
- Doktor der Naturwissenschaften (Dr. rer. nat) -
an der Bayreuther Graduiertenschule für Mathematik und
Naturwissenschaften (BayNat)

vorgelegt von
Laura Schöckel
aus Cottbus

Bayreuth 2012

Die vorliegende Arbeit wurde in der Zeit von April 2009 bis April 2012 am Lehrstuhl für Genetik der Universität Bayreuth unter Betreuung von Herrn Prof. Dr. Olaf Stemmann angefertigt.

Vollständiger Abdruck der von der Bayreuther Graduiertenschule für Mathematik und Naturwissenschaften (BayNat) der Universität Bayreuth genehmigten Dissertation zur Erlangung des akademischen Grades eines Doktors der Naturwissenschaften (Dr. rer. nat.).

Dissertation eingereicht am: 02.05.2012
Zulassung durch die Prüfungskommission: 03.05.2012
Wissenschaftliches Kolloquium: 09.07.2012

Direktor: Prof. Dr. Franz-Xaver Schmid

Prüfungsausschuss:
Prof. Dr. Olaf Stemmann (Erstgutachter)
PD Dr. Stefan Geimer (Zweitgutachter)
Prof. Dr. Wulf Blankenfeldt
Prof. Dr. Benedikt Westermann

Für Benny

1. SUMMARY

Supernumerous centrosomes cause chromosome mis-segregation and genomic instability, thereby likely contributing to the development of cancer. Centrosome duplication in S phase requires the preceding licensing step in late mitosis/early G1 phase, centriole disengagement. Reminiscent of the control of chromosome number, this dependence usually ensures that centrosomes are duplicated only once per cell cycle.

The multi-subunit protein complex cohesin forms a tripartite Scc1-Smc1-Smc3-ring around sister chromatids. In early mitosis cohesin is removed from chromosome arms by the phosphorylation-dependent prophase pathway. During this time, centromeric cohesin is protected by shugoshin 1 and protein phosphatase 2A (Sgo1-PP2A). It is opened only in anaphase by separase-dependent cleavage of Scc1, which triggers chromosome segregation. Shortly thereafter, centrioles loosen their tight orthogonal arrangement, which licenses later centrosome duplication in S-phase. While a role of separase in centriole disengagement has been reported, the molecular details of this process remain enigmatic. Extending recent studies on cultured cells, this work reveals in a reconstituted system that the proteolytic activity of separase is required for centriole disengagement, while its other known function as Cdk1-inhibitor is dispensable. Consistent with previous reports, cohesin is found to be associated with centrosomes and its centrosomal localization is further fine-mapped by electron microscopy. Importantly, a hitherto unknown function of cohesin in centriole engagement is unraveled. Both premature sister chromatid separation and centriole disengagement are induced *in vivo* by premature activation of separase or depletion of Sgo1. These unscheduled events are suppressed by expression of non-cleavable Scc1 or inhibition of the prophase pathway. Moreover, centriole disengagement can be artificially triggered by a site-specific protease unrelated to separase when endogenous Scc1 has previously been replaced by a correspondingly engineered variant. Separation of centrioles can even be induced by ectopic cleavage of cohesin, i.e. within an engineered Smc3. Thus, the chromosome and centrosome cycles exhibit extensive parallels and are coordinated with each other by dual use of the cohesin ring complex.

The second part of this thesis comprises the analysis and functional characterization of differently spliced Sgo1 isoforms. The data presented in this thesis identified a short alternatively spliced exon that not only directs human Sgo1 to centrosomes but

at the same time abrogates also its association with centromeres. The change of just three consecutive amino acids within the corresponding peptide inactivates both the pro-centrosomal as well as the anti-centromeric targeting effect. Importantly, localization closely correlates with function as revealed by knockdown-rescue experiments: Depletion of all Sgo1 isoforms by RNAi resulted in unscheduled loss of sister chromatid cohesion as well as centriole engagement. Selective expression of individual Sgo1 isoforms from siRNA resistant transgenes demonstrated that centromere-associated Sgo1 variants shield only sister chromatid cohesion. Contrary, centrosomally bound isoforms of Sgo1 exclusively preserve centriole engagement. Expression of the relevant exon in fusion with eGFP or shugoshin 2 (Sgo2) directs both proteins to centrosomes but enables only the Sgo2-based chimera to now protect centriole engagement. This demonstrates that 1) the centrosome localization signal of Sgo1 is transferable, and 2) targeting *per se* is necessary but not sufficient for protection of centrosomal cohesin. Consistent with shugoshin´s mode of action at centromeres, centrosome-associated variants with an altered PP2A binding site are compromised in their ability to sustain centriole engagement.

Based on these findings, it is tempting to speculate that an expression imbalance between the differently specialized Sgo1 isoforms could interfere with the crucial synchrony between the chromosome- and the centrosome cycles.

Zusammenfassung

Eine Überzahl an Zentrosomen ist ein häufiges Kennzeichen von Krebszellen und trägt vermutlich zur Tumorgenese bei. Die Zentriolentrennung am Ende der Mitose ist eine Voraussetzung für eine akkurate Zentrosomenverdopplung während der S Phase und damit ein wichtiger Prozess zur Kontrolle der Zentrosomenanzahl. Dieser Lizenzierungsschritt stellt sicher, dass sich die Zentrosomen nur einmal pro Zellzyklus verdoppeln und erinnert an die Kontrolle der Chromosomenanzahl. Die Schwesterchromatide eines jeden Chromosoms werden in der S Phase synthetisiert und gleichzeitig von einem sie ringförmig umschließenden Multi-Proteinkomplex, Kohäsin genannt, miteinander verbunden. Ihre Trennung in der nachfolgenden Mitose erfolgt bei Vertebraten in zwei Stufen. Zunächst wird Kohäsin von den Chromosomenarmen durch den phosphorylierungsabhängigen Prophaseweg entfernt. Zentromerisches Kohäsin wird während der Prophase durch Shugoshin 1 und Protein Phosphatase 2A (Sgo1-PP2A) geschützt und erst in der Anaphase entfernt, wenn Separase die Scc1 Untereinheit schneidet. Unmittelbar nach der Schwesterchromatidtrennung folgt die Trennung der Zentriolen, ein Prozess in dem Separase eine Rolle zukommt, wobei jedoch die zugrunde liegenden molekularen Mechanismen nicht geklärt sind. Offen bleibt außerdem die Frage, welches zentrosomale Protein dabei von Separase geschnitten wird. In der vorliegenden Arbeit ist in einem zellfreien System gezeigt worden, dass die proteolytische Aktivität von Separase für die Zentriolentrennung benötigt wird während seine Cdk1-inhibierende Aktivität entbehrlich ist. Verschiedene zell- und molekularbiologische Experimente machen deutlich, dass Kohäsin die Zentriolen zusammenhält und das gesuchte Zielsubstrat von Separase darstellt. Wie bereits in der Literatur beschrieben, lokalisiert Kohäsin an die Zentrosomen, was in dieser Arbeit durch Elektronenmikroskopie präzisiert wird. Außerdem konnten sowohl die frühzeitige Schwesterchromatidtrennung als auch die verfrühte Zentriolentrennung durch ektopische Aktivierung von Separase oder Depletion von Sgo1 ausgelöst werden. Beide unplanmäßigen Trennungen werden unterdrückt, wenn ein durch Separase nicht-spaltbares Scc1 exprimiert oder der Prophaseweg inhibiert wird. Wenn endogenes Kohäsin durch ein artifizielles Kohäsin ersetzt wird, welches durch eine Separase-unverwandte Protease geschnitten werden kann, so führt die Zugabe der betreffenden Protease zur spezifischen Trennung beider Zentriolen. Dabei ist es

interessanterweise unerheblich, welche Untereinheit des Kohäsin geschnitten wird, solange sich dabei nur der Kohäsin-Ring öffnet. Die Entfernung des gleichen Kohäsin Komplexes koordiniert also die Trennung der Schwesterchromatiden und die Lizenzierung der späteren Zentrosomenverdopplung. So werden der Chromosomen- und Zentrosomenzyklus sinnvoll aufeinander abgestimmt.

Der zweite Teil dieser Arbeit beinhaltet die Analyse und funktionelle Charakterisierung von unterschiedlich gespleißten Sgo1 Isoformen. Es wurde berichtet, dass eine durch alternatives Spleißen entstandene Isoform von Sgo1 nicht am Zentromer sondern vielmehr am Zentrosom lokalisiert und dort die vorzeitige Trennung der Zentriolen verhindert. Inspiriert von dieser Studie wurden stabile Zelllinien generiert, die verschiedene induzierbare Sgo1 Varianten von siRNA-resistenten Transgenen exprimieren. Dies ermöglichte es, alle endogenen Sgo1 Varianten durch RNAi zu depletieren und durch einzelne Isoformen zu ersetzen. Die erhaltenen Ergebnisse zeigen, dass ein alternativ gespleißtes Exon nicht nur humanes Sgo1 zu den Zentrosomen rekrutiert sondern gleichzeitig auch die Assoziation mit dem Zentromer verhindert. Der Austausch von drei aufeinanderfolgenden Aminosäuren in dem entsprechenden Peptid unterdrückten die Rekrutierung an das Zentrosom und zwangen Sgo1 an das Zentromer. Es konnte außerdem gezeigt werden, dass die Lokalisation von Sgo1 mit dessen Funktion korreliert. Demzufolge schützt Zentromer-assoziertes Sgo1 die Kohäsion der Schwesterchromatide, während Zentrosomen-gebundenes Sgo1 ausschließlich den Zusammenhalt der Zentriolen bewahrt. Die Expression von Fusionskonstrukten verdeutlichte, dass die zentrosomale Lokalisationssequenz des bifunktionellen Peptides zum einen übertragbar und notwendig für die Rekrutierung an das Zentrosom ist, zum anderen jedoch alleine nicht ausreicht, um das zentrosomale Kohäsin zu schützen. Übereinstimmend werden Zentrosomen-assoziierte Sgo1 Varianten, die eine mutierte PP2A Bindestelle besitzen, in ihrer Fähigkeit eingeschränkt, den Zusammenhalt der Zentriolen zu gewährleisten. Basierend auf diesen Daten lässt sich mutmaßen, dass ein Ungleichgewicht im Expressionsstärke der unterschiedlich spezialisierten Sgo1 Isoformen die Synchronisation von Chromosomen- und Zentrosomenzyklus beeinträchtigt und dadurch möglicherweise zur Krebsentstehung beiträgt.

2.   INTRODUCTION

"*Omnis cellula e cellula*" - an important dogma in cell biology was popularized in 1858, when Rudolf Virchow published that every cell originates from a pre-existing cell. Indeed, cell division and, with it, the transmission of the genetic information form the elementary basis for life.

2.1. The eukaryotic cell cycle and mitosis in general

The major function of the cell cycle is the accurate duplication of chromosomal DNA and the precise segregation thereof into two genetically identical daughter cells. With a definite directionality, the cell cycle depends on elementary principles such as cyclic synthesis of key regulatory proteins, post-translational modifications as well as irreversible, switch-like protein degradation events. Correct regulation of the cell cycle is critical since mistakes can lead to aneuploidy, cellular transformation and cancerogenesis.

The eukaryotic cell cycle is divided into four main phases (Fig. 1): DNA replication takes place during S phase (synthesis) while subsequent chromosome segregation and cytoplasmic division, or cytokinesis, occur later in M phase (mitos greek for movement). S and M phase of the eukaryotic somatic cell cycle are separated by G1 and G2, two gap phases of cell growth, which ensure that conditions are suitable before passing through the major upheavals of S and M phase. G1, S and G2 phase are collectively referred to as interphase and together occupy up to 95% of the time of a classical human somatic cell cycle. Following differentiation or deprivation of growth factors, cells can leave the cell cycle in G1 to enter a quiescent state known as G0. Here, they can remain for days, weeks, or even years and still sometimes resume proliferation thereafter. If extracellular conditions are favorable and signals to grow and divide are present, cells from G0 progress into G1 and from there through a restriction point, which commits them to cycling. Crucial cell cycle transitions are controlled by surveillance mechanisms (so-called checkpoints), which are highly regulated and constitute all-or-nothing switches to ensure faithful DNA replication in S phase and subsequent accurate DNA segregation in M phase. The cell cycle is driven by various cyclin dependent kinases (Cdks) and their regulatory cyclins,

whose concentrations typically oscillate. Extra- and intracellular cues as well as checkpoints ensure that these kinase complexes are activated only when the conditions for growth and division are favorable and when the previous cell cycle phase has been successfully completed.

In mammalian cells, mitosis is subdivided into five distinct phases and begins with chromosome condensation during prophase: The thin and highly elongated interphase chromosomes of higher eukaryotes condense into much more compact transport forms, which become visible in the light microscope as well-defined structures (Fig. 1). In late prophase, the nuclear envelope breaks down. This allows that the replicated chromosomes, each consisting of a pair of sister chromatids, are captured in a bipolar fashion by MTs of the mitotic spindle apparatus. The cell pauses briefly in that state, while the chromosomes are aligned at the equator of the mitotic spindle, the metaphase plate. Within a metaphase chromosome where two sister chromatids come in close contact a region of DNA called centromere is found. Centromeres can be identified in particular during the metaphase stage as a constriction at the chromosome. At this centromeric constriction the two identical halves of the chromosome, the sister chromatids, are held together until late metaphase. On top of the centromeres, a complex trilaminar structure called kinetochore (KT) is formed, which acquire the ability to assemble microtubules (MTs) emanating from the spindle poles. The two poles of the bipolar spindle are fromed by centrosomes, which act as microtubule organizing centers (MTOC) in animal cells. Every chromosome is now held under tension due to attachment of the two sister KTs to opposite centrosomes. From early mitosis until metaphase an ubiquitous safety device, the spindle assembly checkpoint (SAC), halts mitotic cells until they have attached all kinetochores to the mitotic spindle. Sister chromatids are paired by virtue of a ring-shaped multi-protein complex, cohesin, which likely encloses the two DNA double strands in its middle. Proteolytic cleavage of cohesin causes the sudden separation of sister chromatids and marks the beginning of anaphase, while every chromatid is pulled towards opposing spindle pole. Mitosis is completed in telophase, when the chromosomes have reached the poles. Then, the spindle disassembles and the nuclear envelope reforms around the decondensing chromatin. During cytokinesis, the cytoplasm is divided, leading to two identical daughter cells with identical sets of DNA.
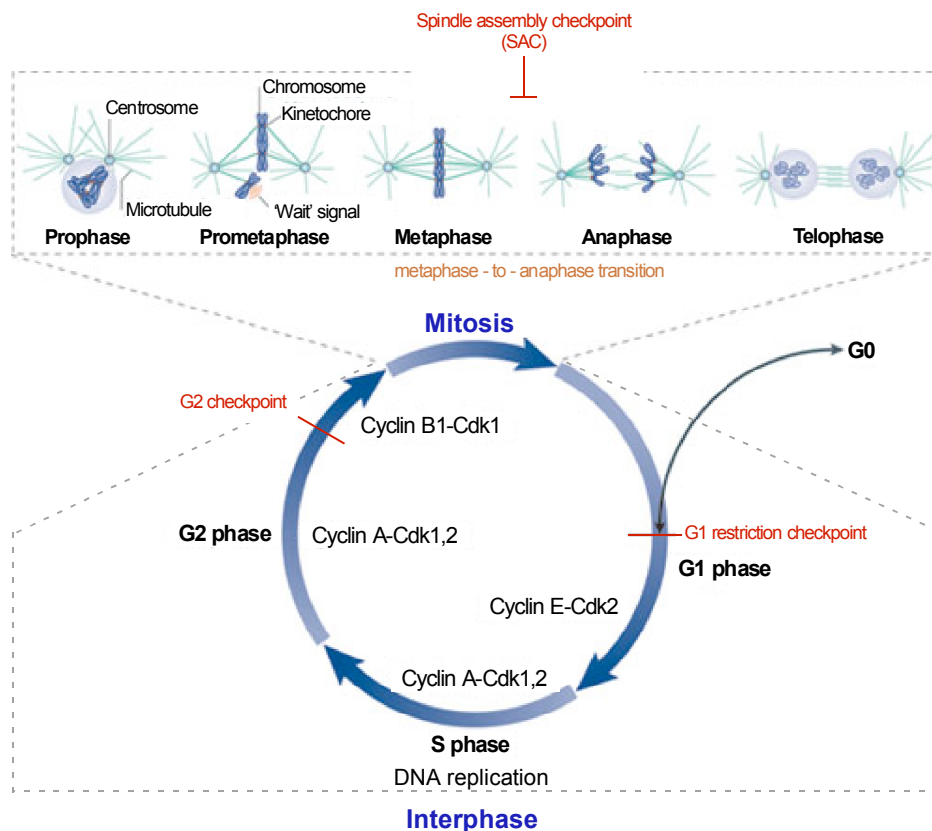
Figure 1. Overview of the eukaryotic cell cycle. The eukaryotic cell cycle consists of four main phases: G1, S (when DNA replication takes place), G2 phase and mitosis, which are all controlled by the corresponding complex of Cdk (cyclin-dependent kinase) and regulatory cyclin (light blue). Cdk1-cyclin B1 triggers entry into mitosis, which is further divided into five important sub-phases. During prophase, chromosomes condense, centrosomes separate to form a bipolar spindle and the nuclear envelope breaks down. In prometaphase, chromosomes are attached to the mitotic spindles via their kinetochores and align along the equator of the cell. Any unattached chromosome generates a 'wait anaphase' signal. When all chromosomes are properly attached in metaphase, then sister chromatid separation occurs in anaphase. During telophase, the chromatin decondenses, the nuclear envelope reforms and the two daughter cells are formed. Highlighted in red are critical checkpoints, which supervise crucial cell cycle transitions. Figure taken and modified from Pines et al. (2011).

2.2. Sister chromatid cohesion

How do cells avoid the entanglement of sister chromatids and make sure that identical chromatids are not separated, instead lying organized side by side until sister chromatid separation occurs in anaphase. The key to faithfully mastering these steps is cohesion in which sister DNAs remain physically tied with each other from the time of their synthesis in S phase until their separation in anaphase. Two

mechanisms contribute to hold sister chromatids together: intertwining (catenation) of sister DNAs (Sundin and Varshavsky, 1981; Surosky et al., 1986) and a proteinaceous bonding mediated by the cohesin complex (Losada et al., 1998; Michaelis et al., 1997). Both are established already during S phase, however, in yeast most catenation within sister DNAs of circular minichromosomes is resolved by the time of mitotic entry while cohesion is still maintained (Koshland and Hartwell, 1987).

In human cells, decatenation of DNA double strands is mediated by Topoisomerase II (Topo II), primarily by Topo IIa. Since most catenations along chromosome arms are already resolved before metaphase, cohesion is predominantly mediated by the cohesin complex (Porter and Farr, 2004). Interestingly, mutations within the cohesin complex fully abolished sister DNA catenation in mitotic 26 kb minichromosomes leading to the hypothesis that intertwining depends on direct cohesin linkages but not *vice versa*. Complete decatenation by Topo II is presumably hampered by cohesin until its removal at the metaphase to anaphase transition (Farcas et al., 2011; Wang et al., 2010).

2.3. Cohesin – the mediator of sister chromatid cohesion

Sister chromatids of replicated chromosomes are linked by a conserved multi-protein complex called cohesin. The association of cohesin along DNA differs between yeast and higher eukaryotes. In budding yeast cohesin was found to associate with chromosomes from late G1 phase until metaphase, but not in anaphase when sister chromatids separate (Michaelis et al., 1997). In contrast, vertebrate cohesin was found to localize onto chromatin already in telophase following reformation of the nuclear envelope (Gerlich et al., 2006; Losada et al., 1998; Sumara et al., 2000). These differences are due to different regulatory mechanisms of cohesin in diverse organisms. Accordingly, most of the cohesin in yeast dissociates from chromatin through proteolytic cleavage by a giant cysteine protease separase and cohesin then slowly re-accumulates during G1 phase (Uhlmann et al., 1999). This process is conserved in higher eukaryotes, however, most of the vertebrate cohesin is removed in a protease independent manner (Sumara et al., 2000; Waizenegger et al., 2000). As a result, cohesin is already available to be loaded onto chromatin in late mitosis. Interestingly, elegant studies from the Nasmyth lab indicate that sister chromatid

pairing requires the cohesin ring to embrace the two DNA double strands in its middle (see below).

Although well established, the maintenance of sister chromatid cohesion is not the only function of the cohesin complex. Numerous studies implicate cohesin in a wide range of other functions. These include, for example, formation and repair of double-strand breaks in mitotic (Sjögren and Nasmyth, 2001) and meiotic cells (Kim et al. 2010; Klein et al., 1999), organization of replication factories in S phase (Guillou et al., 2010) and regulation of gene expression in several organisms (Lin et al., 2011; Wendt et al., 2008).

2.3.1. Components of the cohesin complex

The first proteins to be required for sister chromatid cohesion were identified by yeast genetic screens (Guacci et al., 1997; Michaelis et al., 1997). At least four evolutionary conserved subunits compose the cohesin complex: Smc1, Smc3, Scc1 and Scc3 (Fig. 2). The two core subunits, Smc1 and Smc3, are members of a conserved family of 'structural maintenance of chromosomes proteins' (SMC), whose polypeptide chains fold back onto themselves. The resulting 50 nm long, anti-parallel coiled coils are flanked by a globular ATP-binding cassette (ABC)-like nucleotide-binding domain (NBD) at the one end and a dimerization or 'hinge' domain at the other end (Nasmyth and Haering, 2005). Interaction between the dimerization domains creates a V-shaped Smc1-Smc3 heterodimer. Within the cohesin complex, the positively charged 'hinge' domains of Smc1 and Smc3 bind tightly to each other, whereas the ABC-like ATPase 'heads' of both proteins are physically connected by the Scc1 subunit (Haering et al. 2002). Scc1 (Rec8 in meiotic cells) is a member of a protein family, called a-kleisins (Greek: bridge) because these subunits 'bridge' the ATPase heads in different SMC complexes (Schleiffer et al., 2003). The amino- and carboxy-terminal domains within Scc1 bind to the NBDs of Smc3 and Smc1, respectively. Scc1 is further associated with the fourth peripheral cohesin subunit, Scc3. In higher eukaryotes, Scc3 occurs in two paralogs, called stromal antigens 1 and 2 (SA1 and SA2). The cohesin complex contains either SA1 or SA2, but never both proteins (Losada et al., 2000).

In addition to these core subunits, three further proteins are associated with cohesin. These include Pds5, Wapl and sororin. In general, Pds5 and Wapl promote the dissociation of chromosomal cohesin an activity referred to as releasin, while sororin

antagonizes this anti-establishment activity by competing with Wapl for Pds5 binding (Kueng et al, 2006; reviewed by K. Nasmyth, 2011).

Pds5 has been identified as a substoichiometric cohesin component whose sequence is well conserved and is characterized by numerous HEAT repeats needed for protein interactions (Panizza et al., 2000). In vertebrate cells, there are two homologs of Pds5, Pds5A and Pds5B, which can either associate with SA1 or SA2 (Losada et al., 2005; Sumara et al., 2000). Pds5 function seems to be dispensable in sister chromatid cohesion of vertebrates since only minor effects have been observed upon Pds5 depletion (Losada et al., 2005). Cohesin was found to be associated also with wings apart-like protein (Wapl), which was initially discovered in *Drosophila.* Wapl and Pds5 form a heterodimer that interacts with cohesin (Kueng et al., 2006). In vertebrate cells and *S. pombe*, Wapl is needed for the removal of chromosomal cohesin whereas a different situation has been observed in *Drosophila* and budding yeast (Bernard et al., 2008). Here, slight cohesion defects have been observed upon Wapl inactivation (Verni et al., 2000). Sororin was identified as a third interactor in vertebrates, which is required for stable binding of cohesin to chromatin and for sister chromatid cohesion (Rankin et al., 2005; Schmitz et al., 2007). Moreover, it was found that sororin causes a conformational change within cohesin by competitively replacing Wapl from its binding partner Pds5. Thus, sororin leads to stabilization and maintenance of cohesin onto chromatin (Nishiyama et al., 2010).

Interestingly, in mammals, there are two types of Smc1 subunits (Smc1a and Smc1b), three types of Scc1 (Rad21, Rad21L, Rec8), three types of Scc3 (SA1, SA2 and STAG3) and two types of Pds5 (Pds5a and Pds5b) potentially giving rise to 18 different cohesin complexes.
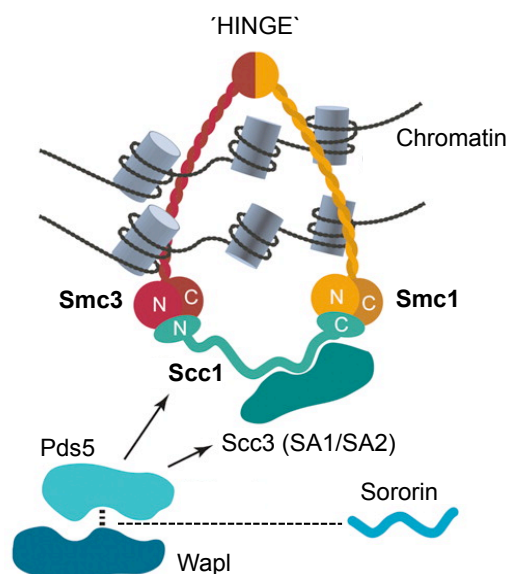
Figure 2. The cohesin ring complex. The cohesin core subunits are two large, anti-parallel coiled coil proteins, Smc1 and Smc3, which dimerize via a hinge domain (´HINGE) and from ABC-like ATPases from their N- and C-termini. A tripartite ring is created through binding of the Scc1 subunit with its N- and C-terminal ends to the ATPase head domains of the V-shaped Smc1-Smc3 heterodimer. The core complex is further associated with Scc3 (SA1/2) and Pds5 through binding to the central domain of Scc1. Wapl and sororin compete for the binding to Pds5. According to the ring model, cohesin acts as a topological device that entraps the two sister chromatids. Image with modifications from Peters et al. (2008).

2.3.2. The cohesin ring model

How does cohesin interact with DNA? It has been assumed for a long time that cohesin mediates sister chromatid cohesion by direct DNA interaction. Although the ATPase head domains of Smc1 and Smc3 may directly interact with chromatin (McIntyre et al., 2007; Nasmyth et al., 2000), integrity of Scc1 is clearly required for cohesin function (Uhlmann et al., 1999). Furthermore, it has been found that proteolytic cleavage of either Scc1 or Smc3 destroys cohesin binding to DNA *in vivo* (Gruber et al., 2003). Cohesin forms a tripartite Scc1-Smc1-Smc3 ring, whose cleavage by separase triggers the loss of sister chromatid cohesion. Due to appropriate molecular dimensions, it was suggested that DNA strands might be topologically entrapped by the cohesin complex (Gruber et al., 2003; Haering et al., 2002; Haering et al., 2008). The existence of an annular arrangement of cohesin having an outer diameter of 50 nm is well supported by electron microscopic images of purified vertebrate cohesin complexes (Anderson et al., 2002) as well as by crystal structures of cohesin subcomplexes or SMC relatives (Haering et al, 2002 and 2004). Instead of connecting sister chromatids physically through DNA interaction,

substantial proof for the ring model was contributed by several elegant studies from Nasmyth and colleagues. It explains why proteolytic cleavage of either Scc1 or Smc3 leads to dissociation of cohesin from DNA and results in loss of sister chromatid cohesion (Gruber et al., 2003; Uhlmann et al., 2000). It also explains why linearization of circular minichromosomes by restriction enzymes leads to its dissociation from associated cohesin (Haering et al., 2008; Ivanov and Nasmyth, 2005, 2007). According to the ring model, cohesin should be capable of sliding along entrapped chromatin. This is consistent with the finding that cohesin relocates from places of chromosomal loading to convergent transcription sites (Ciosk et al., 2000; Lengronne et al., 2004; Watanabe et al., 2004).

Cohesin acting as a topological device that entraps sister chromatids is a very attractive model. The simplest version supposes that a single monomeric ring encloses the two DNA double strands in its middle. However, it is also conceivable that cohesin forms dimeric rings either by cohesin ring concatenation or by binding of the ATPase heads from different Smc1-Smc3 heterodimers to Scc1 proteins (reviewed by Nasmyth, 2011).

2.3.3. Cohesin loading and establishment of sister chromatid cohesion

In humans, daughter cells inherit a huge pool of intact cohesin complexes, since cohesin that was removed by the action of the prophase pathway is spared separase-mediated cleavage and re-associates with chromatin already in telophase (Sun et al., 2009; Waizenegger et al., 2000). Establishment of cohesion is a two-step process starting with cohesin loading onto DNA - during telophase in human cells and in late G1 phase in budding yeast - and subsequent establishment of cohesion between newly synthesized sister chromatids by topological embracement in S phase (Haering et al., 2008; reviewed in Nasmyth and Haering, 2009).

The prereplicative complex (preRC) is a multi-protein complex that assembles at particular sequences in the genome, the origins of replication (ORIs), in telophase, thereby licensing forthcoming DNA replication in S phase. A second function of the preRC has been discovered in *Xenopus*, where it recruits the kollerin (after Greek meaning 'to attach with glue') complex Scc2 and Scc4 (Takahashi et al., 2004). In binding to Scc3, the kollerin complex somehow facilitates initial loading of cohesin onto chromosomes (Ciosk et al., 2000). In budding yeast, there is little evidence that cohesin loading onto core centromeres is necessary and sufficient to recruit cohesin

to adjacent pericentric regions (Hu et al., 2011; Tanaka et al., 1999; Weber et al., 2004). Chromosome spreads (Gruber et al., 2006) and chromatin-immunoprecipitation studies (ChIP) studies in yeast indicate that the kollerin and cohesin complexes are arranged at different loci suggesting that the cohesin ring slides from so called 'loading sites' occupied by kollerin to its final genomic destinations, like intragenic sites of convergent transcription (Kogut et al., 2009).

It has been suggested that cohesin rings most likely entrap individual chromatin fibers by opening the ring at the Smc1/3-hinge (Gruber et al., 2006). Recently, a new model supposes that cohesin loading to core centromeres requires kollerin and opening of the Smc1/3 hinge. The engagement of the NBDs of Smc1 and -3 is driven by ATP binding (Hu et al., 2011). Subsequent ATP hydrolysis disconnects NBDs, which is somehow communicated to the opposite site of the ring and triggers Smc1/3 hinge opening. Re-association of the hinge domain allows proper DNA entrapment and enables translocation along chromosome arms.

How is cohesin stabilized onto chromosomes to promote enduring sister chromatid cohesion? In humans, two key regulators facilitate cohesins stabilization to maintain stable entrapment of sister chromatids: Cohesin acetyltransferase (CoAT) and sororin. A robust cohesion between sisters depends on the *de novo* acetylation of lysine residues within the NBD of Smc3 mediated by CoAT (Ben-Sharhar et al., 2008; Unal et al., 2008). In humans, two CoATs Esco1 and -2 acetyltransferase concomitantly recruit sororin to chromatin-bound cohesin complexes (Lafont et al., 2010; Nishiyama et al., 2010; Rankin et al., 2005) in order to maintain establishment. Remarkably, mutations within the Smc1/Smc3 hinge region impaired Smc3 acetylation and establishment of cohesion, suggesting that establishment requires opening at the Smc1/Smc3-hinge (Kurze et al., 2011). Not until cohesin dissociates from chromatin in anaphase, deacetylation is mediated by cohesin deacetylase (CoDAC). Hos1 carries out deacetylation in yeast upon Scc1 cleavage (Borges et al., 2010), while deacetylation by HDAC8 in humans occurs in two steps presumably during pro- and anaphase (reviewed by Nasmyth, 2011).

However, the exact mechanism by which cohesin rings co-entrap newly replicated sister DNAs during S phase has not been elucidated yet. It remains also elusive how replication forks pass through the rings or whether they can trigger them to open and close properly without chromatid loss.

2.3.4. Resolution of sister chromatid cohesion in mitosis

In vertebrate mitosis, the removal of cohesin from chromosomes occurs in two steps (Fig. 3). The bulk of cohesin is removed from the chromosome arms but not from the centromeres by the action of the so-called prophase pathway (Sumara et al., 2000). In contrast the majority of cohesin in yeast remains bound until metaphase (Ciosk et al., 2000).

The prophase pathway involves the phosphorylation dependent opening of the cohesin ring promoted by the releasin complex Wapl and Pds5 and further requiring activity of polo-like kinase 1 (Plk1) and phosphorylation of Scc3 (Kueng et al., 2006; Nishiyama et al., 2010; Sumara et al., 2002). Interestingly, expression of an Scc3 (SA3) variant, which has 12 threonine and serine residues mutated to alanines prevents cohesin´s release from chromosome arms in prophase (Hauf et al., 2005). However, separase activity is sufficient to remove all cohesin from chromosome arms when the prophase pathway fails. The releasin complex mainly drives efficient release of cohesin since inhibition of Wapl function abrogated this process completely (Gandhi et al., 2006; reviewed by Peters et al., 2008). Preliminary studies from the Stemmann lab indicate that opening of the Smc3-Scc1 linkage is needed for accurate execution of the prophase pathway (Buheitel, personal communication). However, a small centromeric fraction of cohesin is insusceptible to the prophase pathway and maintains pairing of the chromatids at centromeres until all chromosomes have properly bioriented on the mitotic spindle. This is due to a centromeric protein complex consisting of protein phosphatase 2A (PP2A) and shugoshin 1 (Sgo1) (Japanese for 'guardian spirit'), which likely protects this subpopulation of cohesin by constitutive dephosphorylation of the Scc3 subunit of cohesin (Kitajima et al., 2006; McGuinness et al., 2005; Watanabe, 2005). The second step in cohesin removal is triggered by the activation of separase at the metaphase to anaphase transition. This large cysteine endopeptidase then cleaves the Scc1 subunit of remaining centromeric cohesin, which enables sister chromatids to spring apart (Uhlmann, 2003).
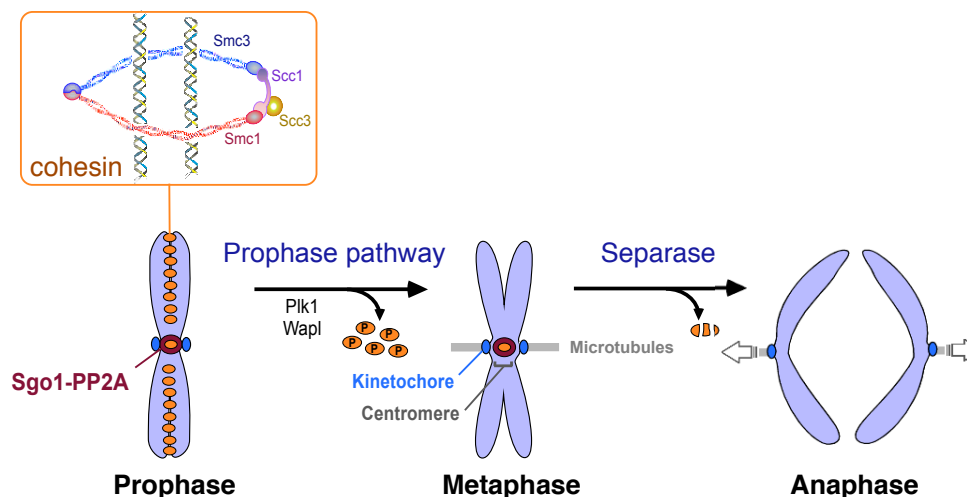
Figure 3. Resolution of sister chromatid cohesion in mitosis. The removal of cohesin is a two-step process. The bulk of cohesin complexes is removed early in mitosis from chromosome arms by the phosphorylation-dependent prophase pathway. Opening of the cohesin ring at this stage requires presence of Wapl, Plk1 kinase activity and phosphorylation of Scc3 (and possibly other cohesin subunits). Centromeric cohesin is not targeted by the prophase pathway due to protection by shugoshin 1 (Sgo1), which counteracts the phosphorylation of cohesin by recruiting protein phosphatase 2A (PP2A). Separase becomes active at the metaphase to anaphase transition and then cleaves Scc1 of centromeric cohesin, thereby opening the ring and allowing sister chromatids to be pulled apart. Figure modified from Stemmann.

2.3.5. Shugoshin – the guardian of centromeric cohesion

As previously described, centromeric cohesion must be protected from the proteolytic onslaught by separase in early prophase of mitosis. The same is true for meiosis, a special type of cell division in germ cells (see 2.5). More specifically, the removal of cohesin from arms and centromeres, respectively, triggers separation of homologs in meiosis I and of sister chromatids in meiosis II (Petronczki et al., 2003; Stemmann et al., 2005). Both waves of meiotic cohesin displacement are triggered by separase-dependent cleavage of Rec8, the meiotic counterpart of Scc1. Obviously, centromeric cohesion is protected during meiosis I by a factor that is lost during anaphase of meiosis II. Based on these facts, Kitajima et al. (2004) screened for genes that were lethal only when ectopically expressed with Rec8 in mitotic fission yeast because sister chromatids were unable to separate efficiently. They isolated such a gene and named its encoded protein Sgo, short for 'shugoshin' - 'guardian spirit' in Japanese. The Sgo proteins belong to a functional conserved protein family and are hallmarked by an N-terminal coiled coil domain and a C-terminal basic motif (Kitajima et al., 2004; Watanabe et al., 2005).

By means of different model systems, it could be shown that Sgo proteins localize to centromeres, thereby protecting centromeric cohesin during early mitosis and anaphase of meiosis I (Katis et al., 2004; Kitajima et al., 2004; McGuinness et al., 2005; Rabitsch et al., 2004; Salic et al., 2004; Tang et al., 2004). In mammals, Sgo was identified and studied in HeLa cells, in which Sgo had been depleted by siRNA. Consequently, cells failed to retain cohesin at centromeres leading to premature separation of sister chromatids (Kitajima et al., 2004; Watanabe, 2005). Two Sgo orthologs have been identified in mammals, Sgo1 and Sgo2. While the former is required for the maintenance of centromeric cohesion during early mitosis (McGuinness et al., 2005; Salic et al., 2004; Tang et al., 2004), the latter has a corresponding function in meiosis I (Lee et al., 2008; Llano et al., 2008). Despite their division of labor, vertebrate Sgo1 and Sgo2 are both expressed in somatic and germline cells (Huang et al., 2007; Lee et al., 2008).

As mentioned above, dissociation of cohesin in early prophase requires phosphorylation of Scc3 and probably other cohesin subunits (Hauf et al., 2005). Consistently, Rec8 is recognized and efficiently cleaved by separase only when phosphorylated (Brar et al., 2006; Kudo et al., 2009). Sgo proteins counteract this phosphorylation dependent displacement by recruiting the ubiquitous protein phosphatase 2A (PP2A) to centromeres (Kitajima et al., 2006; Riedel et al., 2006; Tang et al., 2006). The tight Sgo-PP2A complex is essential to protect the subpopulation of centromeric cohesin, most probably by keeping cohesin constitutively dephosphorylated in humans (Kitajima et al., 2006; Tang et al., 2006).

The centromeric localization of both, Sgo1 and Sgo2 during early mitosis significantly depends on the mitotic kinase Bub1 (Huang et al., 2007; Kitajima et al., 2005; Tang et al., 2004). Depletion of Bub1 is associated with re-localization of Sgo1 to chromosomal arms, which results in cohesion along chromosome arms while centromeric cohesion is lost (Kitajima et al., 2005; Tang et al., 2004). The primary signal to allure Sgo1 and -2 to centromeres is the phosphorylation of histone H2A (Thr 120 in humans and Ser 121 in fission yeast) by Bub1 (Kawashima et al., 2010). The C-terminal conserved Sgo C-Box features a binding motif specific for phosphorylated H2A. The Sgo C-Box mediates proper binding to this phosphorylated H2A tail since a K491I mutation in humans or K298I in *S. pombe* completely abrogated Sgo1´s centromeric localization (Kawashima et al., 2010). Additionally, the mitotic kinase Aurora B also contributes to the centromeric localization of Sgo in

Metazoan (Boyarchuk et al., 2007; Huang et al., 2007; Pouwels et al., 2007; Resnick et al., 2006).

However, mammalian Sgo2 localization is far more complex since it relocates from centromeres to kinetochores in prometaphase (Gomez et al., 2007; Lee et al., 2008). Re-localization might be due to DNA stretching caused by pulling forces, and thereby probably uncovers the remaining centromeric fraction of cohesin in order to trigger sister chromatid separation in anaphase of meiosis II (Lee et al., 2008).

2.3.6. Clinical relevance of shugoshin

Chromosome instability (CIN) is a common hallmark of cancer and is caused by chromosome mis-segreagtion, SAC disorders, and sister chromatid cohesion defects or the presence of extra centrosomes. It has been reported that human shugoshin is implicated in a series of cancers. Discussed as a cancer antigen, human Sgo1 was observed to be overexpressed in 90% of examined breast cancers tissues (Scanlan et al., 2001). Futhermore, human Sgo1 was shown to be significantly downregulated in colorectal cancer tissue (Iwaizumi et al., 2009). Depletion of Sgo1 from colorectal cells (HCT116) caused a delay in mitosis. Extended depletion of Sgo1, however, resulted in mitotic slippage, leading to tetraploidy and an increase of centrosome number (Iwaizumi et al., 2009). More recently, Yamada and colleagues generated Sgo knock-out mice and tested whether this knock-out leads to CIN and tumor formation (Yamada et al., 2012). As expected, due to the key role of Sgo1 in protecting cohesin, homozygous Sgo1 knock-out mice were embryonic lethal. However, heterozygous Sgo1$^{+/-}$ mice were viable. It was further reported that cells from these mice showed chromosome segregation defects and centrosome amplification, which led to an increase in the number of aneuploid and polyploidy cells. Since haploinsufficiency of *sgo1* in mice causes an increase in CIN and tumorigenesis, suggests that Sgo1 is essential for the suppression of CIN and tumor formation (Yamada et al., 2012).

2.4. Molecular players of mitosis

2.4.1. Mitotic entry is regulated by cyclin dependent kinase 1 (Cdk1)

The master regulator of mitosis is cyclin dependent kinase 1 (Cdk1) in association with its activating and regulatory subunit cyclin B1. Cyclin B abundance and the removal of Cdk1 inhibitory phosphorylations are the main parameters that drive mitotic entry: During S and G2 phase, cyclin B1 slowly accumulates and binds Cdk1. The activation of Cdk1 not only depends on cyclin B1 binding but also on phosphorylation by Cdk activating kinase (CAK). Moreover, inhibitory phosphorylations, imposed by the kinases Wee1 and Myt1, need to be removed by the dual specificity phosphatase Cdc25 (Mueller et al., 1995; Parker et al., 1992).

The active Cdk1-cyclin B1 complex phosphorylates several cellular targets leading to morphological changes, alterations in microtubule dynamics and molecular mechanisms characteristic for mitotic cells. For example, chromosome condensation requires Cdk1-cyclin B1 activity (Hirano, 2005). Phosphorylation of nuclear lamins by Cdk1-cyclin B1 leads to their depolymerisation and subsequent nuclear envelope breakdown (Heald and Mc Keon, 1990). Cdk1 activity is essential for spindle morphogenesis since microtubule dynamics are up-regulated when active Cdk1 is added to *Xenopus* cell-free extracts (Verde et al., 1990). Furthermore, mitotic spindle formation depends on phosphorylation of microtubule-associated proteins (MAPs) (Crasta et al., 2006).

2.4.2. The mitotic spindle and chromosome attachment

One of the major hallmarks of mitosis is the reshaping of the microtubule network, leading to the formation of the mitotic spindle (Gadde and Heald, 2004). In most animal cells, centrosomes are the main microtubule organizing centers (MTOC) and form the two poles of the bipolar mitotic spindle. Microtubules (MTs) are long hollow tubes (25 nm in diameter), formed by the lateral association of 13 protofilaments, each being a polymer of α- and β-tubulin dimers. MTs start to nucleate from the spindle poles in a highly dynamic fashion. More precisely, they emanate from the g-tubulin ring complex (γ-TuRC) or related γ-tubulin complexes, e.g. γ-tubulin small complex (γ-TuSC) (reviewed by Kollman et al., 2011). With an inherently polar

structure, MTs exhibit a plus end distal of the MTOC and a minus end at the MTOC. Elongation of the MTs occurs at the plus end. Three types of MTs can be distinguished: 1) Polar MTs are directed towards the opposing spindle pole. They overlap in an antiparallel fashion, where they are cross-linked by multivalent motors and microtubule-associated proteins (MAPs) to stabilize the bipolar spindle. 2) Astral MTs are directed towards the cell cortex and ensure proper spindle positioning. 3) Kinetochore MTs (K-fibers) dynamically polymerize from the centrosome towards the chromosomes, where they attach to kinetochores in a 'search and capture' like manner (Kirschner and Mitchison, 1986; Wittmann et al., 2001). The kinetochore (KT) establishes the connection between K-fiber MTs and chromosomes (Cleveland et al., 2003).

A correct bipolar (amphitelic) arrangement, in which the two KTs of a chromosome attach to opposing poles of the spindle, is essential to faithfully segregate chromosomes in anaphase. However, the stochastic nature of this 'search and capture' mechanism, in which MTs probe the cytoplasm by rapid polymerization and depolymerization in order to trap KTs, can result in erroneous arrangements. Among those mono-, syn- and merotelic attachments can be distinguished (Cimini and Degrassi, 2005). Syntelic attachments (both sister KTs are attached to one spindle pole) and monotelic attachments (one sister KT is attached to both spindle poles) leave individual KTs unattached and tension between sister KTs cannot be generated. Both scenarios are detected by a surveillance mechanism, known as the spindle assembly checkpoint (SAC). The SAC delays anaphase onset, thereby allows time to correct these mistakes and to achieve proper amphitelic attachment for each chromosome. Only when all chromosomes have properly bi-oriented at the metaphase plate of the mitotic spindle, the SAC becomes satisfied and anaphase commences. Merotelic attachments (bipolar attachment with additional monotelic attachment of one of the two KT) are difficult to detect and therefore pose a serious thread to aneuploidy.

2.4.3. Regulation of metaphase to anaphase transition

The metaphase to anaphase transition is a 'point of no return': Cohesion between sister chromatids is dissolved and chromosomes segregate to future daughter cells. A precise execution of the metaphase to anaphase transition is one of the crucial steps in accurate chromosome segregation since any mistake during this process

could lead to aneuploidy or its serious consequences.

Premature initiation of anaphase is prevented by the SAC, which inhibits the anaphase-promoting complex or cyclosome APC/C (Fig. 4). The APC/C is a multi-subunit RING-finger E3 ubiquitin ligase that targets key mitotic regulators for destruction by the proteasome. By using either Cdc20 or Cdh1 as activator proteins, which recognize sequence specific degrons (the most prominent being the D-Box and KEN-Box) in target proteins, the APC/C selects substrates for ubiquitylation (Glotzer et al., 1991; Pfleger et al., 2000).

Any misattached chromosome is recognized by the SAC and leads to the generation of a diffusible 'wait-anaphase' signal at the corresponding KT. This signal is represented by a multi-subunit complex, the mitotic checkpoint complex (MCC), eventually leading to sequestration of Cdc20, an essential activator of the APC/C (Nasmyth, 2005). Only when the last chromosome has properly attached to MTs from opposite poles and aligned at the metaphase plate, the checkpoint-dependent inhibition of the APC/C is relieved and anaphase is initiated. In conjugation with its accessory protein Cdc20, the APC/C mediates, among others, the ubiquitylation of the anaphase inhibitor securin and cyclin B1, leading to their degradation by the ubiquitin-proteasome system (UPS) and activation of separase. This giant and essential protease cleaves the Scc1 subunit of the cohesin complex and sister chromatids spring apart (Uhlmann, 2003). Cyclin B1 degradation and inactivation of the master regulatory kinase Cdk1 coordinates anaphase with the subsequent exit from mitosis.
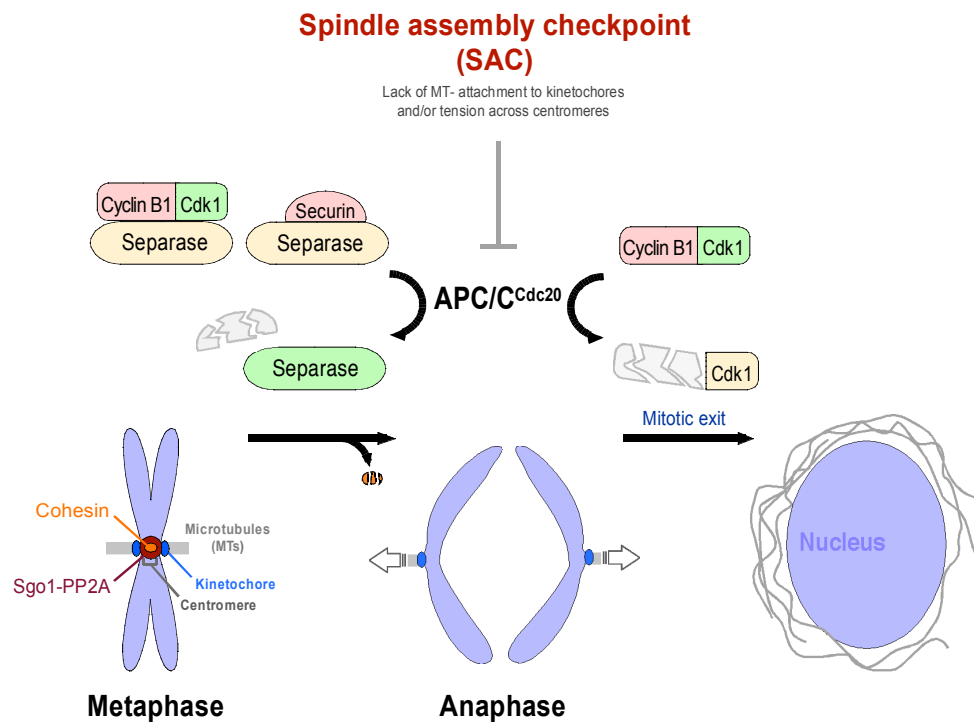
Figure 4. Regulatory network of mitotic sister chromatid separation. The spindle assembly checkpoint (SAC) displays a signaling cascade emanating from erroneously attached kinetochores. The SAC inhibits the APC/C^Cdc20 until all chromosomes have achieved correct bipolar attachment to the MTs of the mitotic spindle. When the SAC is satisfied, the de-repressed APC/C^Cdc20 mediates the proteolytic degradation of the two separase inhibitors securin and cyclin B1. Consequently, separase-dependent cleavage of the Scc1 subunit of remaining centromeric cohesin triggers sister chromatid separation in anaphase. Cyclin B1 degradation also leads to Cdk1 inactivation, thereby coordinating anaphase with subsequent exit from mitosis. Figure modified from Stemmann.

2.4.4. Separase – a giant cysteine endopeptidase

The activation of separase, which is followed by the proteolytic cleavage of chromosomal cohesin, serves as the universal trigger of eukaryotic anaphase. Separase is located in the cytoplasm of all eukaryotes and belongs to the family of cysteine endopeptidases. Despite low conservation of their primary structures, separases from different species seem to have conserved tertiary structures according to bioinformatic investigations (Jager et al., 2004). The active site of the large protease (typically 160 - 250 kDa) is located near the C-terminus and contains an invariable catalytic dyad consisting of a histidine and a cysteine residue (Uhlmann et al., 2000).

Unconventional regulation of separase

To ensure the timely separation of sister chromatids, separase activity must be highly controlled. Securin, the first identified inhibitor of separase (Zou et al., 1999), accumulates in G1 phase and blocks separase until metaphase to anaphase transition, when it is degraded in an APC/C dependent manner. Securin also exerts a positive effect on separase since securin knock-out cells exhibit reduced level and activity of separase (Jallepalli et al., 2001). According to the current view the positive effect is due to securin, assisting the correct folding of the giant separase. Surprisingly, securin does not seem to be essential in vertebrates, since human HCT116 cells lacking securin exhibit chromosome missegregation only transiently, soon regaining a stable karyotype (Pfleghaar et al., 2005). Moreover, viability and mild phenotype of securin knock-out mice are indicative of additional regulation of separase (Mei et al., 2001). Preliminary data from the Stemmann lab indicate that securin and separase influence each other in a mutually positive manner. Compared to free securin, separase associated securin is stabilized. In addition, securin interacts cotranslationally with the N-terminal half of separase. Consistent with the model separase requires the assistance of securin to reach its natively folded state. Thus, the synthesis and the inhibition of this essential but potentially dangerous protease are intimately and elegantly coupled (Böttger and Hellmuth, personal communication).

As an additional level of regulation, separase is excluded from the nucleus, presumably to prevent cohesin cleavage in interphase (Sun et al., 2006). Furthermore, a securin-independent, negative regulation of separase in mitosis was discovered in *Xenopus* cell free extracts. Here, a constitutive activation of Cdk1 by non-degradable cyclin B1 (cyclinB1ΔN) blocks anaphase onset (Stemmann et al.*,* 2001). Cyclin B1ΔN is APC/C resistant, since it lacks 90 amino acids at the N-terminus including the D-Box (destruction-box). Subsequent studies indicated that under these conditions Cdk1 first phosphorylates and then binds and inhibits separase. The phosphorylation of separase by cyclin B1-Cdk1 complex in mitosis is thought to induce a conformational change in separase that allows inhibitory binding of the kinase complex to the protease (Boos et al., 2008). When the phosphorylation of Ser1126 or within a domain referred to as CLD (Cdc6-like domain) is prevented by mutation of separase, cohesin cleavage and sister chromatid separation are no longer blocked by high Cdk1 activity. Indeed, it was later shown that mitotic cells,

which lack both securin and Cdk1-dependent inhibition of separase, suffer from premature loss of cohesion while loss of just one regulation is tolerated (Huang et al., 2008 and 2009). Several *in vivo* studies have emphasized the crucial importance of cyclin B1-Cdk1 complex for the regulation of vertebrate separase and demonstrate that in contrast to securin, cyclin B1-Cdk1-mediated separase inhibition is essential for the viability of mammals (Holland and Taylor, 2006; Huang et al., 2008; Huang et al., 2005). According to these findings, a transgenic stable cell line, referred to as SA-cells, was generated from Hek 293 Flp-In cells (Boos et al., 2008; Holland and Taylor et al., 2006). Upon tetracycline (Tet) induction, cells overexpress a hyperactive, Cdk1-resistant separase carrying a Ser1126Ala mutation. This phosphorylation-site mutant separase (SA-separase) has profound effects on the cell cycle profile exhibiting premature sister chromatid separation followed by SAC dependent accumulation in metaphase (Boos et al., 2008; Holland and Taylor, 2006).

Metazoan separase is additionally regulated by auto-cleavage and association with PP2A, which occur in a mutually exclusive manner and seem to have antagonistic roles (Holland et al., 2007; Zou et al., 2002). This is illustrated by the fact that overexpression of a non-cleavable separase mutant, which leads to premature separation of sister chromatids, recruits more PP2A than wild-type separase and is fully rescued by simultaneously preventing PP2A binding to separase (Holland et al., 2007). Separase auto-cleavage negatively regulates PP2A association, however, the biological significance of both these regulations remains largely enigmatic.

Unconventional functions of separase

Interestingly, the inhibition in the separase-Cdk1 complex is mutual, i.e. vertebrate separase acts as an inhibitor of Cdk1, a biochemical activity, which, importantly, does not require proteolytic activity. Consistently, Gorr et al. (2006) demonstrated that this Cdk-inhibitory function is necessary for cytokinesis at the end of vertebrate female meiosis I.

Abundant experimental data indicate that separase has additional functions that extend beyond cleavage of cohesin and inhibition of Cdk1 at the end of meiosis I: 1) In *S. cerevisiae*, it was demonstrated that the kinetochore-associated protein Slk19 is a *bona fide* proteolytic substrate of separase (Sullivan et al., 2001). Slk19 has a non-essential role in mitotic exit, however, its cleavage does not affect exit from mitosis. Furthermore, no Slk19 homologues have been identified in higher eukaryotes yet.

2) In budding yeast, securin is phosphorylated by Cdk1, which inhibits its ubiquitination by the APC. However, securin phosphorylation is retracted by the phosphatase Cdc14. Since separase is known to activate Cdc14 independent of cohesin cleavage (Stegmeier et al., 2002), it is supposed that a positive feedback loop increases the abruptness of anaphase (Holt et al., 2008). 3) In mammalian cells, the separase-securin complex is found to be associated with membranes, thereby modulating membrane traffic and protein secretion (Bacac et al., 2011). 4) There is evidence in budding yeast that separase stabilizes the mitotic spindle (Uhlmann et al., 2000) and there is some debate whether separase might also be important for spindle elongation in anaphase (Jensen et al., 2001; Severin et al., 2001). 5) *C. elegans* embryos that lack separase are osmo-sensitive indicating that separase might play a role in the formation of a proper eggshell (Siomos et al., 2001). 6) Another study on worms demonstrated a role of separase in the establishment of cell polarity as exemplified by the defective anterior-posterior body axis formation in separase RNAi embryos (Rappleye et al., 2002). It was speculated that this might be due to a defect in the microtubule-dependent association of the paternal pronucleus or centrosome with the cell cortex. 7) Vertebrate separase but not its proteolytic activity is needed for the extrusion of the first polar body – a special form of cytokinesis and visible hallmark of successful completion of female meiosis I (Gorr et al., 2006; Kudo et al., 2006). Most likely, separase fulfills this unanticipated function by binding and inhibition of Cdk1-cyclin B1 (Gorr et al., 2006). 8) Rec8, the meiotic counterpart of Scc1, is cleaved by separase during meiosis. While phosphorylation merely promotes the separase dependent cleavage of Scc1, it is an essential prerequisite for the recognition and proteolysis of Rec8 by separase in anaphase I of meiosis (Hauf et al., 2005; Kudo et al., 2009). 9) Interestingly, a recent study by Tsou and Stearns (2006) suggests that separase might play an important role in the disengagement of centrioles at the end of mitosis.

All these data imply that separase has additional downstream substrates. The example of Slk19 suggests that these putative targets of separase might also be cleaved. Besides autocleavage of Metazoan separase, no proteolytic substrates of separase other than cohesin (and Slk19 in *S. cerevisiae*) have been found to date.

2.5. Specialties of meiosis

Germ cells are formed by a special kind of cell division called meiosis, in which two consecutive rounds of chromosome segregation, without an intermediate S phase, give rise to four haploid gametes from a single diploid cell. In preparation for meiosis, homologous chromosomes pair (synapse) and form cross-overs by recombination, which are later resolved into chiasmata. These chiasmata and cohesion of chromosome arms are what keeps homologous chromosomes paired, while sister chromatids are held together by centromeric cohesion. Hence, the removal of cohesin from chromosome arms and centromeres, respectively, triggers the separation of homologs in meiosis I and of sister chromatids in meiosis II.

Like Sgo1 in mitotic prophase, Sgo2 is essential for the protection of centromeric cohesin during meiosis I. A significant difference is that in meiosis both steps of cohesin removal are triggered by separase-dependent cleavage of cohesin. As the cohesin subunit Rec8, the meiotic counterpart of Scc1, requires phosphorylation for recognition and processing by separase, Sgo2 likely protects it from cleavage by mediating PP2A-dependent dephosphorylation (Kitajima et al., 2004; Kudo et al., 2009; Riedel et al., 2006; Rivera & Losada, 2006). How Sgo-PP2A is inactivated after meiosis I to allow subsequent sister chromatid separation in meiosis II is largely unknown.

2.6. The centrosome

In animal cells, the centrosome belongs to the main microtubule-organizing centre (MTOC), a structure, from which mitotic spindle MTs emerge. First discovered in 1883 by Edouard van Beneden, centrosomes were named and described as the 'special organ of cell division' by Theodor Boveri in 1888. In many cells centrosomes are required to organize the dynamic arrays of MTs throughout the cell cycle. During interphase of the cell cycle, MTs determine cell shape, polarity and motility, whereas during M phase, they form the bipolar spindle required for chromosome segregation (Rieder et al., 2001). It should be pointed out, however, that spindle formation in cells of higher plants and oocytes of some animals do not exhibit centrosomes (Gadde & Heald, 2004).

Supernumerous centrosomes in cells create the potential for either multipolar divisions or bipolar divisions with merotelic attachments that can lead to aneuploidy, cell death or cancer (Ganem et al., 2009; Nigg, 2002). To ensure the presence of two centrosomes required for proper mitotic spindle formation, the centrosome has to be duplicated once and only once per cell cycle (Mazia, 1987). Duplication of centrioles begins near the G1/S boundary and is completed in G2 phase (Doxsey et al., 2005).

2.6.1. Centrosome structure

A canonical centrosome consists of a pair of orthogonally arranged centrioles embedded in an amorphous protein matrix known as pericentriolar material (PCM) (Fig. 5). Visualized by electron microscopy as a fibrous lattice, the PCM contains over 100 different proteins such as γ-tubulin, which is required for MT nucleation (Dictenberg et al., 1998). Centrioles, the core centrosomal components, are tiny, barrel-shaped structures consisting of nine MT-triplets in a ring-shaped arrangement. In human cells, a mature centriole is about 300-700 nm in length and 250 nm in diameter.

Due to generational differences, each member within one centriole pair features structural and functional asymmetry. The older and fully mature mother centriole is characterized by two sets of appendages at its distal end (distal- and subdistal appendages). The subdistal appendages are required for MT anchoring and depend on proteins including pericentrin, ninein, dynactin and centriolin (reviewed in Bornens, 2002). During G1, the daughter centriole lacks centriolar appendages but acquires appendages proteins at G2/M and defined appendages in G1 phase of the next cell cycle. Furthermore, the mother centriole exhibits another distinct function in non-proliferating cells as basal body that seed the growth of cilia, having crucial roles in development and disease.
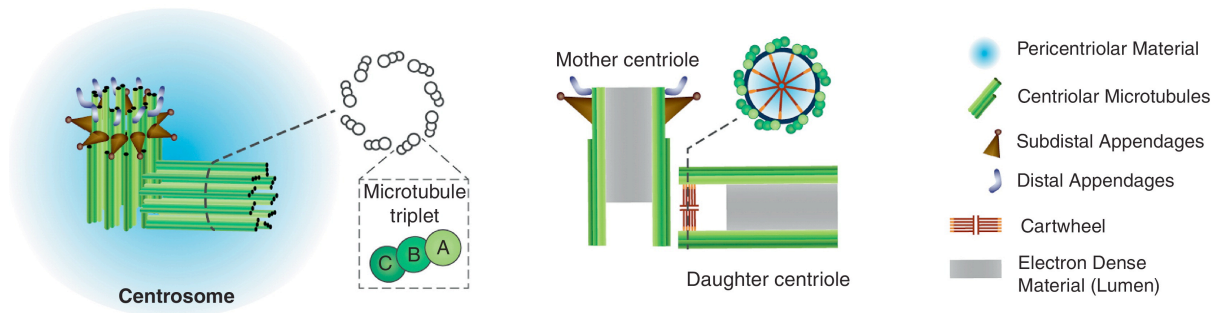
Figure 5. Canonical structure of a vertebrate centrosome. The centrosome is the major microtubule-organizing center (MTOC) of most animal cells. The core structure of a centrosome (depicted in green on the left) is made of two MT-based cylinders of defined length (300-700 nm) and diameter (250 nm), the centrioles. A centrosome consists of a mature mother centriole and an immature daughter centriole, which are orthogonally arranged to each other and embedded in an electron-dense matrix, the pericentriolar material (PCM, in blue). Each human centriole is composed of nine MT-triplets (A-, B-, C-tubules) in a ring-shaped arrangement (see centriole cross-sections). The initial structure from which the daughter centriole is formed is a nine-fold symmetric scaffold, the cartwheel (see longitudinal section of a centrosome on the right). The mother centriole is distinguished by two sets of nine appendages at its distal end, subdistal and distal appendages. Figure taken from Brito et al. (2012).

2.6.2. The canonical centrosome duplication cycle

The formation of new centrioles is a crucial process and of particular importance for the duplication of the whole centrosome. In proliferating cells, the number of centrioles is normally controlled through a canonical duplication cycle in coordination with the chromosome cycle. Consistently, four consecutive steps in the centrosome cycle have been defined through electron microscopy (Fig. 6): Centriole disengagement (late mitosis/early G1 phase), centriole duplication (S phase), centrosome maturation (G2 phase) and centrosome separation (M phase) (Nigg, 2007). During prophase, centrosomes are typically associated with the nuclear envelope and migrate to opposite poles of the cell. Upon nuclear envelope breakdown, each spindle pole is characterized by the presence of one centrosome comprising two tightly associated centrioles. Each centrosome nucleates MTs to form the mitotic spindle. After cell division each daughter cell receives one centrosome with a pair of centrioles. At the end of mitosis/early G1, the two centrioles loose their tight orthogonal engagement and remain only loosely joined. Loss of this tight association between daughter and mother centriole is termed 'centriole disengagement' and involves separase and Plk1 activity (Tsou and Stearns, 2006;

Tsou et al., 2009). The event of centriole disengagement is proposed to license the two centrioles for a new round of duplication, i.e. the outgrowth of a new centriole perpendicular to each pre-existing one (Tsou and Stearns, 2006).

During G1, the two disengaged centrioles that were mother and daughter centrioles in the previous cell cycle are able to nucleate MTs (Piel et al. 2000). During centriole duplication in S phase, the newly forming daughter centrioles are unable to recruit PCM or act as MTOCs. Primarily in early mitosis, Plk1 activity is essential to convert the daughter centrioles to a functional MTOC (Wang et al., 2011). Centrin, a small calcium binding protein is one of the first proteins that localizes at distal sites of newly forming centrioles, thereby conferring structural integrity (Beisson and Wright, 2003; Bettencourt-Dias and Glover, 2007; Salisbury et al., 2002). Until late G2, the two new procentrioles elongate until they reach full length and remain tightly associated in an orthogonal arrangement referred to as 'engaged centrioles'. The engagement of two centrioles prevents further re-duplication.

In G2 phase, the two centrosomes are still physically linked by meshed fibers composed of rootletin and other components (Bahe et al., 2005). These fibers are tethered at the ends of the two parental (mother- and grandmother) centrioles by a large protein called C-Nap1. Upon phosphorylation of C-Nap1 by the mitotic kinase Nek2 (Mayor et al., 2000) cohesion between centrosomes is finally fully lost in early mitosis. As a result, the two centrosomes separate and start to generate the mitotic spindle. Upon cell division, each daughter cell receives one centrosome, which has to be duplicated once in the following cell cycle. As a consequence of the centrosome duplication cycle, a dividing cell in M phase contains three generations of centrioles: A grandmother/daughter pair of centrioles and a mother/daughter pair.

The relationship between the licensing step of centriole disengagement and centriole duplication potential is only poorly understood. Studying centriole disengagement and centriole growth after addition of purified centrosomes to *Xenopus* egg extract, experiments from Tsou and Stearns (2006) proposed a role of separase in centriole disengagement. Their data show that centriole disengagement is blocked by addition of non-degradable forms of either securin or cyclin B1. Since both treatments inhibit separase, these experiments indirectly suggested a role of separase in centriole disengagement. However, a direct proof for a function of separase in centriole disengagement is lacking. If separase acts direct on centrosomes, then identification

of a separase substrate during centriole disengagement would be of great interest to cell cycle research.
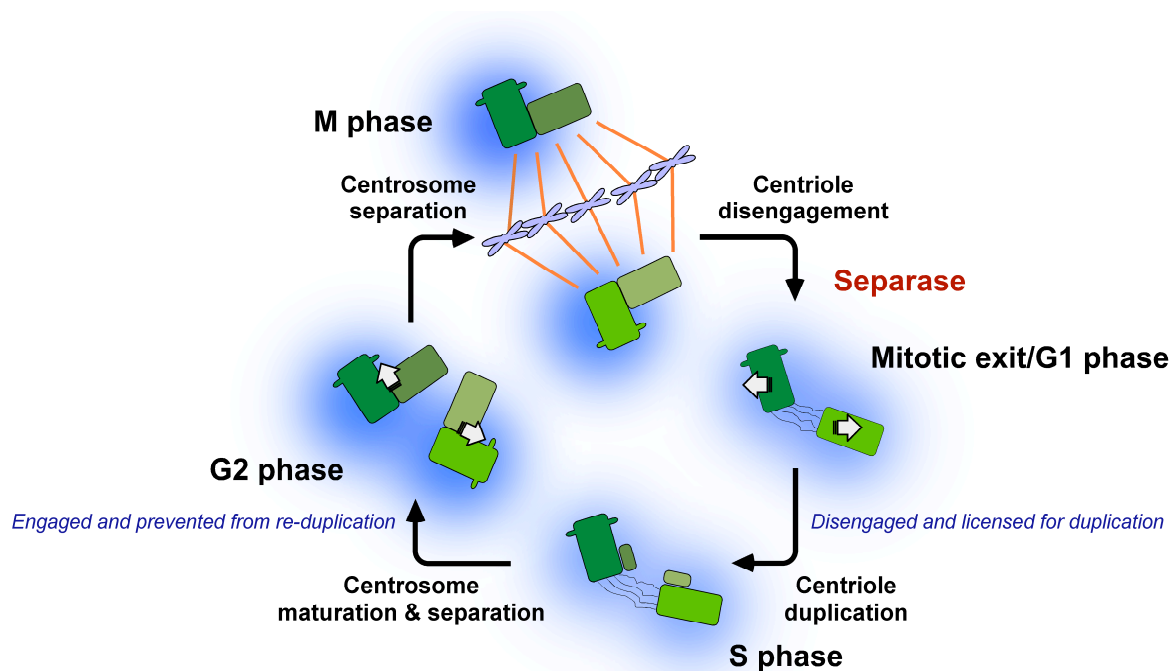
Figure 6: The canonical centrosome duplication cycle. Four consecutive steps in the centrosome cycle have been defined through electron microscopy: Centrosome segregation (M phase), centriole disengagement (late mitosis/early G1 phase), centriole duplication (S phase), and centrosome maturation (G2 phase). The schematic representation of the centriole duplication cycle shows differently colored centrioles (green), indicating origin and age of each individual centriole, which are embedded in the PCM (blue). Centrosome maturation is characterized by growth of the daughter centriole and by the recruitment of additional PCM proteins. At the beginning of mitosis, each spindle pole is characterized by a centrosome, comprising two centrioles. At the end of mitosis/early G1, the two centrioles loose their tight perpendicular arrangement, a process called centriole disengagement. It requires separase activity and is a prerequisite for centriole duplication. Each of the two preexisting centrioles duplicate in the following S phase. Daugther centrioles start to grow and elongate orthogonally from the preexisting mother centrioles until the have reached full length in G2 phase. After proper centriole duplication, there are three generations of centrioles in one cell: One grandmother and one mother, each paired with a daughter. At the beginning of mitosis, the two centrosomes separate from each other to form a bipolar spindle. During cell division, each daughter cell receives one centrosome.

2.6.3. Formation of centrioles

Genetic and RNAi screens in *C. elegans* identified five proteins required for proper centriole formation, that is ZYG-1, SAS-4, SAS-5, SPD-2 and SAS-6 which are also present and similarly essential in eukaryotic centriole formation (Delattre et al., 2004; Dammermann et al., 2004; Kemp et al., 2004; Leidel and Gönczy, 2003; Pelletier et

al., 2004). However, the core machinery for centriole biogenesis only consists of a few proteins, among them polo-like kinase 4 (reviewed by Azimzadeh and Marshall, 2010) and the coiled coil protein Sas-6 (Leidel et al., 2005). Protein levels and activity of Plk4 and Sas-6 are critical for centriole assembly since overexpression of either Plk4 or Sas-6 in humans leads to the formation of multiple new centrioles ('flower-like structure') adjacent to the existing mother centriole (Habedanck et al., 2005; Strnad et al., 2007).

The initial formation of procentrioles is characterized by the appearance of a cartwheel-like structure with nine-fold symmetry. Recent data elucidated the structural basis of the highly conserved nine-fold radial symmetry of centrioles dependent on SAS-6 oligomerization (Kitagawa et al., 2011; van Breugel et al., 2011). Remarkably, electron microscopy revealed that SAS-6 formed rod-shaped homodimers that interact via their N-terminal domains to generate oligomers. Solely Sas-6 oligomerization forms a cartwheel-like structure *in vitro*, the scaffold for centriole assembly. Consequently, at least two control mechanisms operate to restrict centriole formation to only once per cell cycle, Plk4 and Sas-6.

Centriole elongation and proper maturation proceed throughout S and G2 phase, a process dependent on several proteins, including SAS-4, POC5, OFD1 and CP110 (reviewed by Nigg and Stearns, 2011).

In summary, several molecular players of centriole biogenesis have been identified and centriole structure is well defined by EM. Nevertheless, the molecular mechanisms centriole assembly and regulations thereof remain poorly understood.

2.6.4. Role of shugoshin at centrosomes

Mammalian Sgo1 and Sgo2 are renowned for protecting centromeric cohesin during early mitosis and throughout meiosis I, respectively (Lee et al. 2008, Llano et al., 2008; Tang et al., 2004; McGuinness et al., 2005). Of human Sgo1 several splice variants were detected (McGuinness et al., 2005; Wang et al., 2006). The two main isoforms, Sgo1-A1 (527 aa) and the small Sgo1-C2 (292 aa), exhibit entirely different subcellular localization patterns. While Sgo1-A1 localizes to centromeres until anaphase, Sgo1-C2 (sSgo1) is primarily found at centrosomes instead of centromeres (Wang et al., 2006 and 2008). Sgo1-A1 is comprised of exons 1 to 8 whereas Sgo1-C2 lacks 268 amino acids encoded by exon 6 but contains 40 amino acids at the C-terminus encoded by exon 9. Accordingly, Dai and colleagues

proposed that the sequence encoded by exon 6, which is present in Sgo1-A1 but not -C2, contains a centromere localization signal (Wang et al., 2008). Additional functional analysis indicated that Sgo1 depletion by RNAi results in the formation of multipolar spindles, which is suppressed by ectopic expression of Sgo1-C2 (Wang et al., 2008). Based on these findings the short Sgo1 variant was proposed to function specifically in maintenance of centriole cohesion (Wang et al., 2008).

2.6.5. Spindle assembly and faithful chromosome segregation in the absence of centrosomes?

During mitosis or meiosis, reliable chromosome segregation depends on the correct assembly of MTs into a bipolar spindle. During spindle assembly, cells nucleate MT from various sources, including centrosomes, chromosomes (Heald et al., 1996; Maiato et al., 2004), and the spindle microtubules (Mahoney et al., 2006). The view that spindle formation requires centrosomes exhibits no generality as cells of higher plants do not require centrosomes for spindle formation (Gadde & Heald, 2004). Consistently, centrosomes are absent during female meiosis in many organisms including nematodes, fruit flies, *Xenopus,* mice and humans and many others have no centrosomes present (Manandhar et al., 2005).

The formation of a functional bipolar spindle without centrosomes depends on the GTP-bound form of the small G protein Ran promoting MT nucleation in the vicinity of chromosomes (Bastiaens et al., 2006; Caudron et al., 2005). Experiments in *Xenopus* egg extract showed that the presence of a sufficiently high concentration of Ran-GTP caused MT nucleation and led to the organization of spindle-like structures in the absence of either chromosomes or centrosomes (Carazo-Salas et al., 1999; Ohba et al., 1999).

In mouse embryos, remarkably, centrioles continue to be absent during the first cleavages (Szöllösi et al., 1972) and reappear only at the 64-cell stage as judged by EM (Gueth-Hallonet et al., 1993). Imposing analyses from the Ellenberg lab showed that centrosomal-independent spindle assembly proceeds by self-organization of numerous MTOCs in live maturing mouse oocytes. Using 4D confocal microscopy, this research group demonstrated that most of the MTOCs are formed *de novo* in prophase from interphase-like MT networks and that after NEBD a Ran-dependent, massive increase in MT nucleation contributes to MTOC clustering and chromosome biorientation (Schuh and Ellenberg, 2007).

However, a natural or continuous absence of centrosomes in proliferating Metazoan tissue has not been reported yet. Numerous experimental studies have inactivated centrosomes in Metazoan cells by either electroporation of specific antibodies (Bobinnec et al., 1998), addition of MT poisons (Keryer et al., 1984) or laser irradiation (Berns and Richardson, 1977). Interestingly, acentriolar cells frequently proceed into mitosis, assemble a normal mitotic spindle and reform centrioles. Likewise, when centrosomes have been ablated in transformed cells by needle microsurgery or laser treatment, mitosis proceeds normally with formation of a regular bipolar spindle followed by cytokinesis and progression into G1 (Hinchcliffe et al., 2001; Khodjakov et al., 2000). Complete ablation of one of the two centrosomes in HeLa cells at metaphase gives rise to one centrosome containing and one acentrosomal daughter cell. The latter continues with the cell cycle and undergoes *de novo* centriole re-formation (La Terra et al., 2005). Impressive laser ablation studies from Khodjakov and colleagues demonstrate that procentriole formation is initiated within the PCM meshwork and that the mother centriole limits the number of newly forming centrioles indirectly by restricting PCM size rather than directly by providing a template for new centriole assembly (Loncarek et al., 2008). In contrast to transformed cells, it was shown that non-transformed mammalian cells arrest in G1 phase in the absence of centrioles and do not form centrosomes *de novo* (Hinchcliffe et al., 2001; Khodjakov and Rieder, 2001).

Interestingly, *Drosophila* mutants lacking Sas-4 loose centrioles during embryogenesis but – apart from a delayed spindle assembly – develop largely normally (Basto et al., 2006). These mutant flies die shortly after birth due to the absence of cilia in specific sensory neurons rather than suffering from difficulties within mitotic cell divisions. This fact, together with the finding that a *Drosophila* cell line, which constitutively lacks centrioles divides quite normally and does not recruit PCM proteins to from a centrosome-like structure at the spindle poles corroborates the dispensability of centrioles for mitotic divisions in *Drosophila* (Debec et al., 1982; Moutinho-Pereira et al., 2009). While centrioles are dispensable for accurate spindle assembly in humans, they seem to be more crucial for proper spindle positioning and tissue development since defects in spindle orientation can cause a cystic kidney disease, called nephronophthisis (Simons and Walz, 2006).

The importance of the *de novo* pathway in proliferating cells remains unclear. However, only transformed cells escape the G1 arrest in the absence of centrosomes

and are able to amplify multiple centrioles *de novo*, which results in random centrosome amplification, multipolar spindles and aneuploidy.

2.6.6. Cilia formation

Centrioles have supposably emerged for the primary purpose to seed the growth of cilia and flagella, important sensory and motile organelles, which are present in almost all cells of the human body (reviewed by Marshall and Nonaka, 2006). The majority of cells produce a single immotile cilium, called the primary cilium that serves as sensory organelle and transduces chemical and mechanical signals (Praetrius and Spring, 2005). Retinal, auditory or olfactory cells have sensory cilia essential for communicating sensory stimuli to the nervous system. In mammals, cells in the oviduct or airways present numerous motile cilia on their cell surface beating in coordinated waves (multiciliated cells). For example, the beating of myriad cilia covering the oviduct moves the fertilized female egg from the ovary to the uterus. Motile cilia present on epithelial cells of human lungs and trachea are essential to sweep mucus and dirt out of the airways (Ibanez-Tallon et al., 2003).

There are different mechanisms of ciliogenesis, which enable the production of various types of cilia and flagella (Carvalho-Santos et al., 2011). In quiescent or differentiated cells, a primary cilium is extended from a basal body analogous to the centrioles. Here, the mother centriole turns into a basal body whose distal appendages are required for docking to the plasma membrane. In multi-ciliated cells, hundreds of centrioles are produced and duplicated by using a pre-existing centriole as a template. However, the majority of centrioles in these cells are generated through the acentriolar (*de novo*) pathway, in which procentrioles form around a non-microtubule based structure, the deuterosome. Following their assembly in the cytoplasm they move to the cell surface where they form the ciliary axoneme (Dirksen, 1991; Hagiwara et al., 2004). The control of 'only one' centriole forming per mother is abrogated in these cells, as 200-300 cilia are formed per cell (Vladar and Stearns, 2007). In contrast to the canonical duplication cycle in actively dividing cells, the generation of more than two centrioles from the existing mother centriole and further nucleation of multiple centrioles characterize deuterosome-dependent centriole formation in ciliating cells (Carvalho-Santos et al., 2011). Even though ciliogenesis and centrosome duplication have distinctive features, they produce seemingly identical structures, i.e. centrioles.

2.6.7. Centrosome function in disease and cancer

Aberrations in centriole number, structure and function are implicated in several diseases including ciliopathies, male sterility, primary microcephaly and cancer. Of more the more than 100 proteins, which localize to either centrioles or the PCM, many are associated with disease or cancer (reviewed by Nigg and Raff, 2009).

The presence of extra centrosomes might be associated with genomic instability and abberant cell divisions and, as such, represent a hallmark of many tumors. First indications for a role of centrosomes in tumorigenesis originate from knockdown experiments of the tumor suppressor p53, which caused centrosome amplification (Fukasawa, 2007). Lately, a mechanistic link was drawn between extra centrosomes and chromosomal instability (Ganem et al., 2009; Silkworth et al., 2009). Chromosomally unstable cells with multiple centrosomes are able to undergo bipolar mitotic divisions due to centrosome clustering at each pole. However, the transient formation of multipolar spindles increases the incidence of merotelic attachments, which are hardly recognized by the SAC and, thus, cause chromosome missegregagtion and aneuploidy. It is therefore hypothesized that tumorigenesis caused by chromosome instability is a consequence of supernumerary centrosomes. Therefore, proteins required for clustering of multiple centrosomes display putative targets for selective cancer treatment strategies.

Commonly, one can distinguish between structural and numerical centrosome defects (reviewed by Bettencourt-Dias et al., 2011). Structural aberrations are a consequence of mutated centrosomal proteins, which cause alterations in centrosome size and MT nucleation. Centrosome amplification or overduplication is a consequence of a numerical defect and can be triggered by overexpression of Plk4, a kinase required for centriole formation. Moreover, mutation in the tumor suppressor BRCA1 (breast and ovarian cancer susceptibility protein 1) causes centrosome amplification, multipolar spindle formation, thus contributes to aneuploidy as observed in breast tumors (Deng et al., 2001; Starita et al., 2004; Xu et al., 1999). BRCA1 usually functions in the nucleus by stimulating repair of damaged DNA but it is localized also at the centrosomes, where it regulates centrosome duplication and MT nucleation (Brodie and Henderson, 2012).

Concerning centrosome-associated diseases of brain development, the most investigated and studied neurodevelopmental disorder is autosomal recessive primary microcephaly, which is characterized by reduced brain size. Interestingly, all

seven genes implicated in microcephaly encode ubiquitously expressed proteins that localize to centrosomes and are involved either in centriole duplication, maturation or spindle positioning. These include microcephalin, Cdk5Rap2, ASPM, CPAP, STIL, Cep152 and WDR62 (Cox et al., 2006; Megraw et al., 2011). Diseases caused by defects of the motile cilia, like *situ inversus*, are called primary ciliary dyskinesia (PCD). With regard to immotile cilia diseases, there exist a variety of syndromes called ciliopathies in which gene mutations cause a failure of primary cilia assembly and function or of the transport of signaling molecules. These include, for example, disorders such as polycystic kidney disease (PKD), nephronophthisis, retinitis pigmentosa and Joubert and Meckel syndrome (reviewed by Bettencourt-Dias et al., 2011).

2.7. *Xenopus laevis* as a model system

While yeast is ideal for studying the genetics of the cell cycle, the biochemistry of the cell cycle is most easily analyzed in the egg extract of the African clawed frog, *Xenopus laevis*. These frogs are easy to breed and have been kept in laboratories since the 1940´s, originally to test for pregnancy. Injection of human chorionic gonadotropin (hCG, the same hormone as in the urine of pregnant women) into the lymph sac of a female frog triggers spawing on the next day. With over 1 mm in diameter, *Xenopus* eggs carry large stockpiles of proteins needed for cell division and contain 100.000 times more cytoplasm than an average cell in the human body. Due to their enormous size, it is relatively easy to inject test substances. Mature eggs from many vertebrates including humans arrest in metaphase of meiosis II until fertilization. This metaphase II arrest is achieved by the presences of a cytostatic factor (CSF) identified as XErp1 (*Xenopus* Erp1) in *Xenopus* and represents an inhibitor of APC/C^{Cdc20} (Schmidt et al., 2005 and 2006).

Alternatively, freshly laid eggs can be crushed by centrifugation after removal of the jelly coat by mild reduction. These extracts are still arrested in metaphase II and are thus referred to as CSF-extracts. Importantly, upon addition of Ca^{2+}, which mimics fertilization, XErp1 is degraded in a phosphorylation-dependent manner and the extract progresses from metaphase II into interphase (Rauh et al., 2005). The *Xenopus* cell-free extract can be used to recapitulate many events of the cell cycle and, thus, provides a great opportunity to investigate the involvement of specific

proteins during mitotic or meiotic processes. Major advantages of the extract are its synchrony regarding cell cycle state and its amenability to biochemical manipulations such as addition of mRNA or immuno-depletion of proteins, for example. Besides, an anaphase-like extract can be prepared from CSF-extract. To this end non-degradable cyclin B1 (Δ90 cyclin B1) has to be added prior to Ca^{2+} addition. At this stage, the APC/C becomes active but meiotic exit is nevertheless blocked due to constitutive Cdk1-cyclinB1 activity. Whether or not Cdk1-cyclinB1 inhibits also separase under these conditions depends on the concentration of Δ90 cyclin B1, which is why low and high Δ90 extracts (80 nM or >120 nM) are distinguished (Stemmann et al., 2001).

2.8. Aim of this work

At the end of mitosis, the two centrioles of each centrosome loosen their tight perpendicular arrangement. This so-called centriole disengagement constitutes an essential licensing step for later centriole duplication in S phase, thereby ensuring that centrosomes are duplicated once, and only once, per cell cycle (Wong and Stearns, 2003). The molecular mechanisms of centriole engagement/disengagement and the regulations thereof remain poorly understood. Studying the centrosome cycle is of great importance for basic and clinical research since supernumerous centrosomes contribute to the development of cancer (Ganem et al., 2009).

Separase triggers sister chromatid separation in eukaryotic anaphase by endoproteolytic cleavage of the Scc1 subunit of chromosomally bound cohesin. An unanticipated, additional role of separase in centriole disengagement was proposed by Tsou and Stearns (2006). However, their study provided only indirect evidence for the involvement of separase. Moreover, it left unanswered whether the proteolytic activity of separase was required for centriole disengagement and – if yes – what the downstream centrosomal substrate might be. Preliminary data from the Stemmann lab (Schöckel, 2009) suggested that the proteolytic (and not the Cdk1-inhibitory) function of separase is indeed required for centriole disengagement. Therefore, the ultimate goal of this work was to search for the substrate. Several experiments were planned in this direction:

1) Ectopic expression of hyperactive separase triggered not only premature sister chromatid separation but also precocious centriole disengagement (L. Schöckel,

Master thesis). Using this assay, the only known substrate of separase was to be tested. More specifically, the effects of transient overexpression of non-cleavable Scc1 *versus* wild-type Scc1 were to be investigated.

2) If there was any hint that cohesin plays a role in centriole engagement, then it should be tested whether centriole disengagement can be artificially triggered. To this end, an Scc1 variant engineered to be cleaved by a site-specific protease other than separase was generated. Centrosomes of cells that express the engineered instead of endogenous cohesin were to be interrogated for disengagement upon exposure to the corresponding protease.

3) If Scc1 was indeed part of the molecular glue between engaged centrioles, the next question would be whether this involves the whole cohesin complex? Insertion of artificial cleavage sites into another subunit followed by its ectopic cleavage was to address this issue.

4) A further aim was to check whether additional players or mechanisms are involved in the regulation of centriole disengagement? The prophase pathway is involved in the protease independent removal of chromosomal cohesin. It requires Wapl and kinase activity of Plk1 and is counteracted by Sgo1. Accordingly, it should be examined if Sgo1 and its antagonists played a role during centriole disengagement.

3. RESULTS

3.1. Studying centriole disengagement in *Xenopus* cell-free extracts

Centriole disengagement can be studied in *Xenopus* egg extracts and, interestingly, is blocked by non-degradable forms of the anaphase inhibitor securin or cyclin B1 (Tsou and Stearns, 2006). Since both proteins inhibit separase´s proteolytic activity (Stemmann et al., 2001; Zou et al., 1999), a role of this protease in centriole disengagement has been proposed (Tsou and Stearns, 2006). However, the involvement of separase in the centrosome cycle has not been studied directly in this *in vitro* system.

In order to distinguish between engaged and disengaged centrioles, antibodies against the two human centriolar proteins centrin 2 and C-Nap1 were raised in rabbit and guinea pig, respectively. Then, centrosomes, which were predicted to be either engaged or disengaged based on the cell cycle stage at the time of their isolation, were immunostained for centrin 2 and C-NAP1 and analyzed by immunofluorescence microscopy (IF). While the distal centriolar marker centrin 2 always gave rise to two clearly separated signals, the proximal marker C-NAP1 was resolved into two populations only when the centrioles had lost their tight perpendicular association. Thus, a centrin 2:C-NAP1 signal ratio of 2:1 *versus* 2:2 indicates centriole engagement *versus* disengagement (Fig. 7a).

3.1.1. Inhibitors of separase blocked centriole disengagement in *Xenopus* egg extract

With these tools in hands, the *in vitro* centriole disengagement assay of Tsou and Stearns (2006) could be revisited. First, it was tested whether centriole disengagement indeed requires separase activity, as reported by these authors. To this end, isolated, engaged centrosomes were added to meiotically arrested *Xenopus* egg extract (CSF-extract), which was supplemented with N-terminally truncated (ΔN), stabilized forms of recombinant securin or cyclin B1. The CSF-extract was then released into interphase by mimicking fertilization with Ca^{2+}. Finally, centrosomes were re-isolated from the extract, immunostained for centrin 2 and C-NAP1 and

analyzed by IF (Fig. 7a). Indeed, non-degradable forms of securin and cyclin B1, inhibited centriole disengagement in a dose-dependent manner (Fig. 7b).
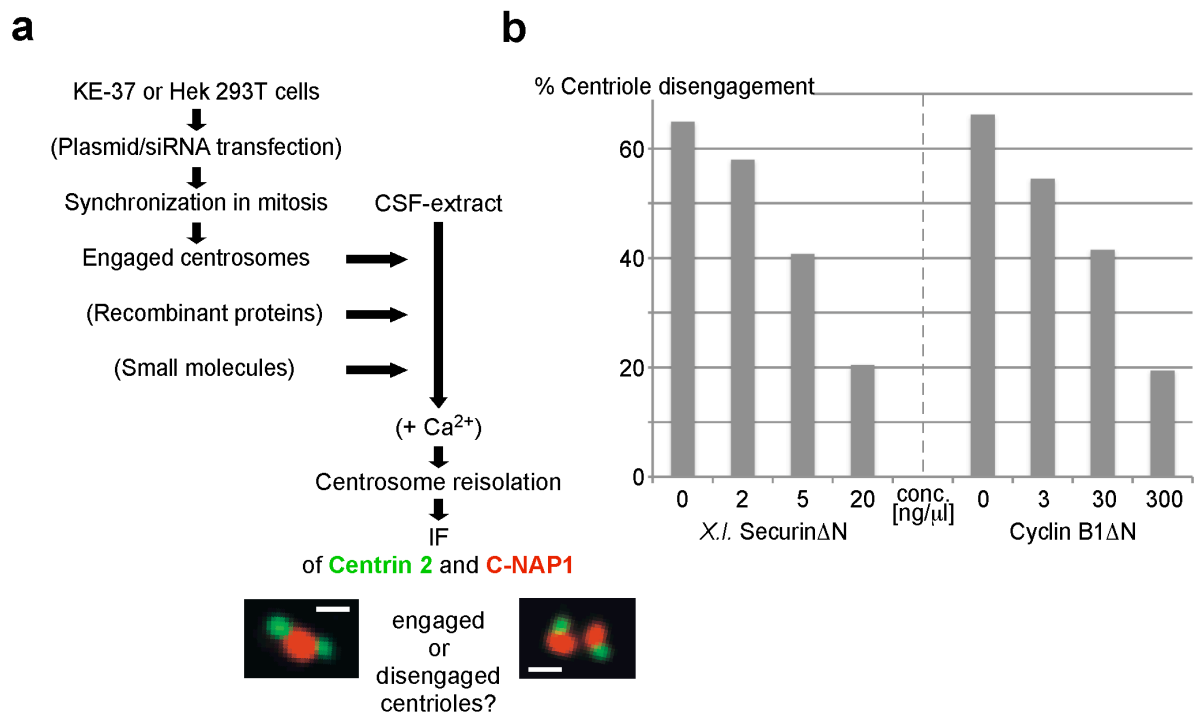
Figure 7. Inhibitors of separase block centriole disengagement in *Xenopus* egg extract. **(a)** Flow chart of the *in vitro* centriole disengagement assay as used in figures 7b, 8b, 15, 18b. Optional steps are in brackets. Scale bars in immunofluorescence microscopy (IF) images represent 0.5 µm. **(b)** CSF-extract was supplemented first with reference buffer, *Xenopus laevis* securinΔN, or human cyclin B1ΔN and then with isolated human centrosomes. Forty minutes after Ca^{2+} addition, centrosomes were re-isolated and analyzed by IF. Between 100 and 160 centrosomes each were analyzed. Centriole disengagement was calculated by correcting for the 23% of disengaged centrioles present in the starting centrosome preparation. (Master thesis; Schöckel, 2009).

3.1.2. Separase´s proteolytic activity is needed for centriole disengagement

Tsou and Stearns did not clarify, which of the two known biochemical activities of separase, the proteolytical or the Cdk1-inhibitory, might be required for centriole disengagement. Therefore, rescuing experiments with recombinant separase variants were conducted. Capitalizing on the fact that *Xenopus* securin is a poor inhibitor of human separase (Schöckel, 2009), recombinant, securin-free forms of wild type (WT) or protease-dead (PD; Cys-2029-Ser) human separase (Fig. 8a) were added to egg extracts, in which endogenous separase was inhibited by non-degradable *Xenopus* securinΔN. WT- but not PD-separase was able to re-install centriole disengagement under these otherwise restrictive conditions (Fig. 8b). A Ser-

1126-Ala (SA) mutation in human separase prevents Cdk1-cyclin B1 binding and, hence, mutual inhibition of protease and kinase (Gorr et al., 2005). This SA-separase restored centriole disengagement in cyclin B1ΔN supplemented extracts but not when combined with a Cys-2029-Ser mutation (Fig. 8a, b). Together, these experiments provide direct proof that the proteolytic, and not the Cdk1-inhibitory, activity of separase is needed for centriole disengagement in *Xenopus* egg extract.
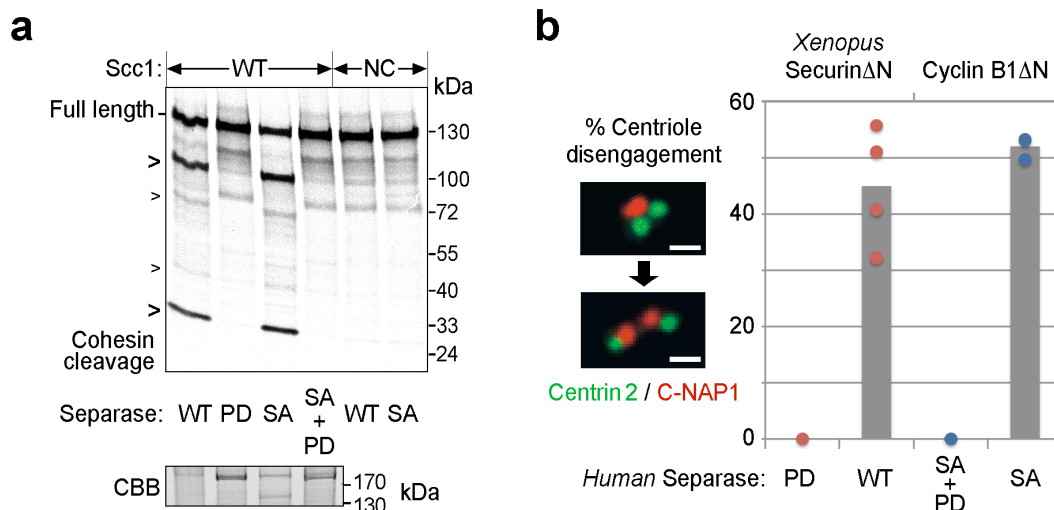
Figure 8. Centriole disengagement requires proteolytically active separase. **(a)** Characterization of recombinant, securin-less human separases. Wild type (WT), protease-dead (PD), Cdk1 binding deficient, phosphorylation site mutant (SA), and double mutant (SA+PD) separase were characterized by SDS-PAGE/Coomassie staining (CBB) and for their ability to cleave ^{35}S-labeled WT-Scc1 or a non-cleavable (NC) variant thereof. Arrowheads label cleaved Scc1 fragments. Figure taken from Schöckel, 2009. **(b)** Centriole disengagement was blocked by addition of *Xenopus laevis* securinΔN (43 ng/µl) or human cyclin B1ΔN (300 ng/µl) to CSF extract (compare to Fig. 7b). Then, engaged centrioles and securin-free human separase (see a) were added and the egg extract was released from the CSF arrest into interphase. Finally, centrosomes were re-isolated and analyzed by immunofluorescence microscopy (IF). Centriole disengagement specifically induced by the proteolytic activity of separase was calculated by subtraction of the background (20-40%), i.e. centriole disengagement in the presence of PD or SA+PD separase. Note that depending on arrest efficiency and individual preparation 15-35% of centrosomes appeared disengaged even without addition of any proteins. Shown are averages (grey bars) of 4 (left) and 3 (right) independent experiments (dots). At least 60 centrosomes per sample were analyzed.

The purification and characterization of recombinant proteins, e.g. securinΔN, cyclin B1ΔN, human separase as well as the conducted experiments were described in Schöckel (2009).

3.2. Removal of cohesin coordinates the disengagement of centrioles with the separation of chromatids

3.2.1. Cohesin is associated with purified centrosomes

After preparative centrosome isolation from Hek 293T or KE-37 cells by sequential sucrose gradient centrifugation, a Western blot analysis was carried out to assay each fraction for the presence of centrosomes. As centrosomal marker protein served γ-tubulin, which localizes to the pericentriolar matrix (PCM) of centrosomes (Dictenberg et al., 1998). Interestingly, the cohesin subunits Scc1 and Smc1 co-purified with γ-tubulin raising the possibility that cohesin might also be a centrosomal component (Fig. 9a). Consistent with this possibility, Scc1-eGFP was associated with centrosomes as judged by IF (Fig. 9b). Nevertheless, a possible contamination of the centrosome preparation with chromatin cannot be excluded (see Fig. 25, EM-structure of purified centrosomes).
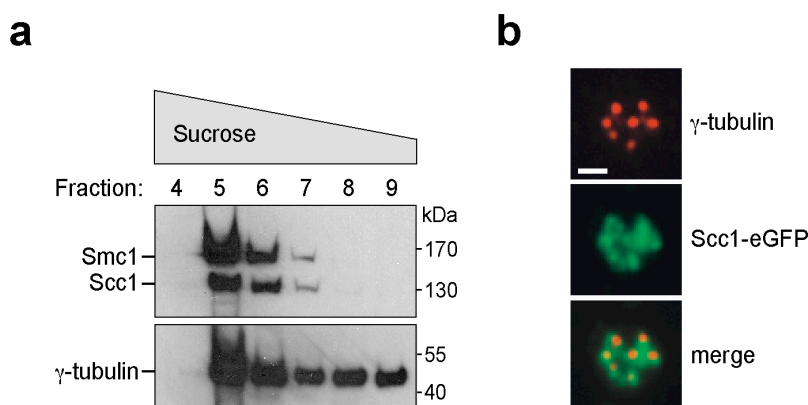
Figure 9. Cohesin is associated with purified centrosomes. **(a)** Fractions of the last step of a centrosome purification from metaphase-arrested KE-37 cells were analyzed by immunoblotting. Figure taken from Schöckel, 2009. **(b)** Centrosomes isolated from metaphase-arrested, Scc1-GFP overexpressing Hek 293T cells were co- immunostained for γ-tubulin (mouse) and GFP (rabbit) and analyzed by fluorescence microscopy. Scale bar represents 1 μm.

3.2.2. Centriole disengagement is promoted by separase and inhibited by non-cleavable Scc1

What is the proteolytic target of separase? Might even cohesin be the sought-after substrate of separase in centriole disengagement? Consistent with this idea, cohesin

(Fig. 9a, b), separase and presumed (self-) cleavage products thereof can be found in association with centrosomes (Beauchene at al., 2010; Gregson et al., 2001, Guan et al., 2008; Kong et al., 2009; Nakamura et al., 2009; Warren et al., 2000). Furthermore, knockdown of Scc1 by RNAi results in the formation of multipolar spindles and splitting of centrioles (Beauchene at al., 2010; Losada et al., 2005; Nakamura et al., 2009). This observation is contradicted, however, by a report of separase-resistant, non-cleavable (NC) Scc1 blocking chromosome segregation, albeit not centriole disengagement (Tsou et al., 2009).

Various engineered subunits of cohesin were used to resolve this controversy and rigorously assess the putative involvement of cohesin in the centrosome cycle. First, the effect of separase resistant Scc1, in which the two separase cleavage sites are mutated, was investigated. By inducible overexpression of Cdk1-resistant SA-separase in a stable Hek 293 cell line, premature separation of sister chromatids can be triggered in prometaphase-arrested cells (Boos et al., 2008; Holland et al., 2006). In these so-called SA-cells, WT- or NC-Scc1 was constitutively overexpressed by transient transfection. Thirty-six hours later, cells were treated with nocodazole and tetracycline (Tet) to synchronize them in mitosis and induce SA-separase expression, respectively. An additional twelve hours thereafter, the status of transgene expression, sister chromatid cohesion and centriole engagement were assessed in parallel. The ectopic Scc1 alleles were equally expressed and WT- but not NC-Scc1 declined on chromatin upon induction of the deregulated separase (Fig. 10a). As expected, NC-Scc1 largely suppressed premature separation of sister chromatids while WT-Scc1 could not (Fig. 10b). IF-analysis of isolated, immunostained centrosomes revealed that precocious centriole disengagement also occurred in Tet-treated SA-cells and, remarkably, was prevented by NC- but not WT-Scc1 (Fig. 10c). Together, these findings not only provide independent *in vivo* evidence for a role of separase in the licensing step of centrosome duplication and, in this respect, confirm alternative approaches (Thein et al., 2007; Tsou et al., 2009). They also imply that cohesin might indeed be the sought-after separase substrate at centrosomes.
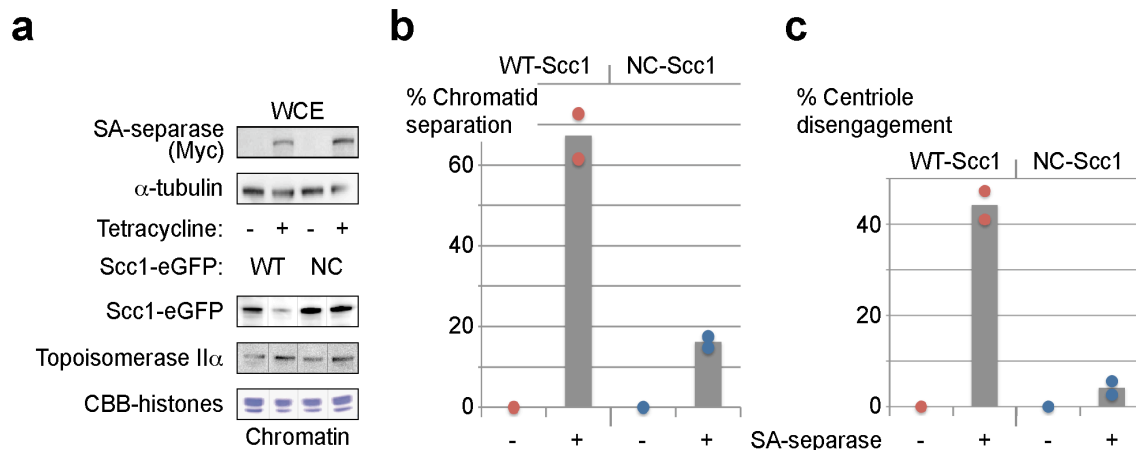
Figure 10. Separase resistant Scc1 blocks separation of sister chromatids and centrioles. **(a)** Whole cell extracts (WCE, upper panels) and isolated chromatin (lower panels) from thymidine-nocodazole synchronized SA-cells expressing GFP-tagged WT-Scc1 or a separase resistant cohesin mutant (NC) were characterized by Western blot analysis or SDS-PAGE/Coomassie staining (CBB). Note that the lanes shown in the lower panels, although not directly juxtaposed, nevertheless are from the same gel. The experiment was carried out by M. Möckel **(b)** Separase-induced chromosome splitting was determined from spreads by subtraction of the background (5-10%), i.e. percentage of cells with one-chromatid-chromosomes in the absence of Tet (negative controls). Shown are averages (grey bars) of two independent experiments. 100 cells were analyzed in each sample. **(c)** Centriole disengagement is induced by activation of separase in prometaphase and is blocked by NC-Scc1. Centrosomes were spun from lysates of siRNA and nocodazole treated SA-cells directly onto coverslips and analyzed by IF. The percentage of separase induced centriole disengagement was determined by subtraction of the background (25%), i.e. centriole disengagement in the absence of Tet (negative control). Shown are averages (grey bars) of two independent experiments (colored dots) representing a total of 150 centrosomes per column.

3.2.3. Artificial cleavage of Scc1 triggers centriole disengagement *in vitro*

NC-Scc1 did not co-immunoprecipitate with separase arguing against the possibility that it might act as a competitive inhibitor of the protease (Möckel, 2010). Nevertheless, it could not be fully excluded that NC-Scc1 might act as a dominant negative inhibitor in the cellular context and prevents separase from cleaving the real centrosomal target. To unequivocally test if cohesin was indeed keeping centrioles tightly paired, the first cleavage site in Scc1 was converted by mutation from a recognition site for separase into one for 3C protease of human rhinovirus (henceforth called HRV protease; Cordingley et al., 1990). The second cleavage site was left unchanged to ensure that the resulting HRV-Scc1 could still be cleaved by separase and, hence, was less cytotoxic than NC-Scc1. *In vitro,* separase cleaved

WT- and HRV-Scc1, while HRV protease cleaved only HRV-Scc1, as expected (Fig. 11a). In a co-immunoprecipitation experiment HRV-Scc1 interacted with Smc1 and -3 like WT-Scc1 indicating that HRV-Scc1 retained functionality (Fig. 11b). Next, endogenous Scc1 was replaced with HRV-Scc1 and then it was tested, whether centriole disengagement could artificially be triggered by HRV protease treatment. To this end, stable Hek 293T cell lines were created that inducible expressed WT- or HRV-Scc1 from an episomal vector upon Tet addition (Fig. 11c) (Bornkamm et al., 2005). Induced cells were transfected with siRNA targeting the 3'UTR of endogenous *SCC1* mRNA. This treatment not only depleted endogenous Scc1 but also increased the amount of recombinant Scc1 indicating that cells try to keep a constant level of total Scc1 (Fig. 11d). Following Scc1 depletion and synchronization in prometaphase, corresponding cell lysates were incubated with HRV protease before centrosomes were finally isolated and examined by IF. Remarkably, HRV protease treatment caused up to 40% centriole disengagement when endogenous Scc1 had previously been replaced by HRV-Scc1 (Fig. 11e). Consistently, HRV protease-induced centriole disengagement was accompanied by cleavage of HRV- but not WT-Scc1 (Fig. 11f). Through artifical cleavage of an engineered Scc1 by a site-specific protease other than separase centriole disengagement was triggered *in vitro* indicating that Scc1 plays a role in keeping centrioles together.
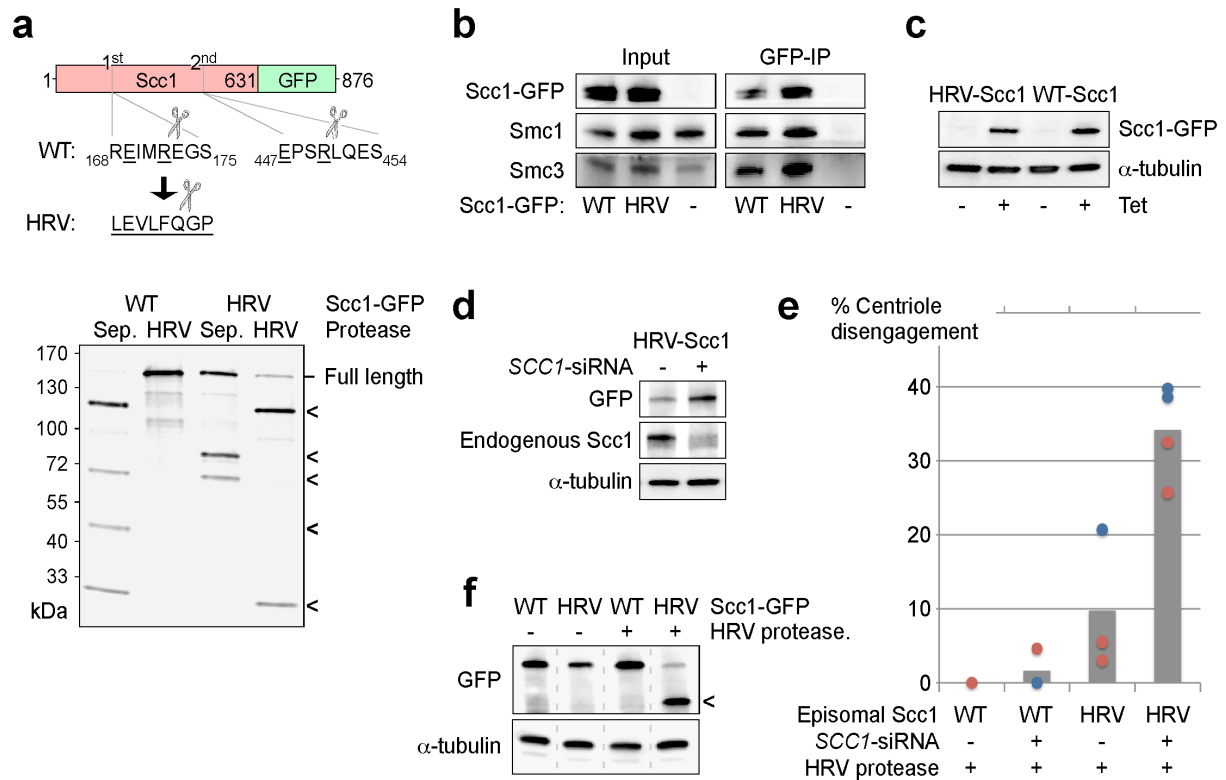
Figure 11. Cleavage of an engineered Scc1 triggers centriole disengagement *in vitro.* **(a)** The first separase cleavage site in Scc1 was replaced by one for human rhinovirus (HRV) 3C protease (see cartoon). ^{35}S-labelled WT- and HRV-Scc1 were incubated with separase (Sep.) or HRV protease and analyzed by SDS-PAGE/autoradiography. Arrowheads label major Scc1 cleavage fragments. Note that HRV-Scc1 can still be cleaved by separase at the second cleavage site. **(b)** HRV-Scc1 is fully competent to interact with other cohesin subunits as judged by IP-Western analysis of transiently transfected Hek 293T cells. GFP- expressing cells served as negative control (-). **(c)** Episomally encoded WT- and HRV-Scc1 are inducibly and equally expressed in Hek 293T cells as judged by immunoblotting. **(d)** Transfection of a 3'UTR directed siRNA results in depletion of endogenous- and increase of transgenic Scc1 as exemplified by Western analysis of the stable HRV-Scc1 cell line. **(e)** Episomal cell lines expressing WT- or HRV-Scc1 were transfected with *SCC1* siRNA or mock treated as indicated. Four days later, cells were treated for 12 hours with nocodazole and then harvested. Lysates were combined with bacterially expressed HRV protease prior to spinning of centrosomes onto coverslips. Given are the percentages of centriole disengagement after subtraction of the background, i.e. disengagement in the corresponding negative controls (WT-Scc1 samples; -siRNA: 18-26%, +siRNA: 14-17% = negative controls). Experiments were normalized to WT-Scc1 with or without siRNA (blue and red circles, respectively). Shown are averages (grey bars) of 3 to 4 independent experiments. Between 30 and 200 centrosomes per sample were analyzed. **(f)** Western blot analysis of HRV protease treated lysates (see **e**) revealed specific cleavage of HRV-Scc1 (arrowhead). Note that the shown lanes, although not directly juxtaposed, nevertheless origin from the same gel.

3.2.4. Artificial cleavage of Scc1 triggers centriole disengagement *in vivo*

To see whether separase could be functionally replaced also *in vivo*, endogenous Scc1 was exchanged for eGFP-tagged WT- or HRV-Scc1 as before. However, HRV protease (or, as a negative control, eGFP) was then expressed by transient transfection of the cells with corresponding plasmids. Finally, cells were arrested in mitosis and lysed to directly isolate centrosomes and assess centriole engagement by IF (see Fig. 12a for workflow overview). Importantly, centriole disengagement was specifically induced by HRV protease in HRV-Scc1 expressing cells and again enhanced, when endogenous Scc1 had been depleted by RNAi (Fig. 12a).

The *in situ* analysis of the centriole engagement status in intact, mitotically arrested cells was hampered by weak centrosomal signals for C-NAP1 (Faragher and Fry, 2003). As the signal greatly increases upon isolation of centrosomes from the same cells (data not shown), loss of centrosome-associated factors during the purification process probably grants better access of the antibody, thereby increasing sensitivity. For the robust imaging of C-NAP1 in cells two alternative strategies were employed. In a first approach the cells were released from prometaphase into G1 phase, i.e. into a cell cycle stage, in which centrosomes exhibit an intensive IF signal for C-Nap1. To eliminate effects of separase activation during this transition, non-degradable securin was co-expressed along with HRV protease (see Fig. 12b for workflow overview). Quantitative analysis of the *in situ*-stained centrosomes confirmed the above result, i.e. that HRV protease efficiently triggered disengagement of centrioles in HRV-Scc1- but not WT-Scc1 expressing cells. Thus, the *in vivo* experiments faithfully recapitulated and, thereby, confirmed the *in vitro* analysis.
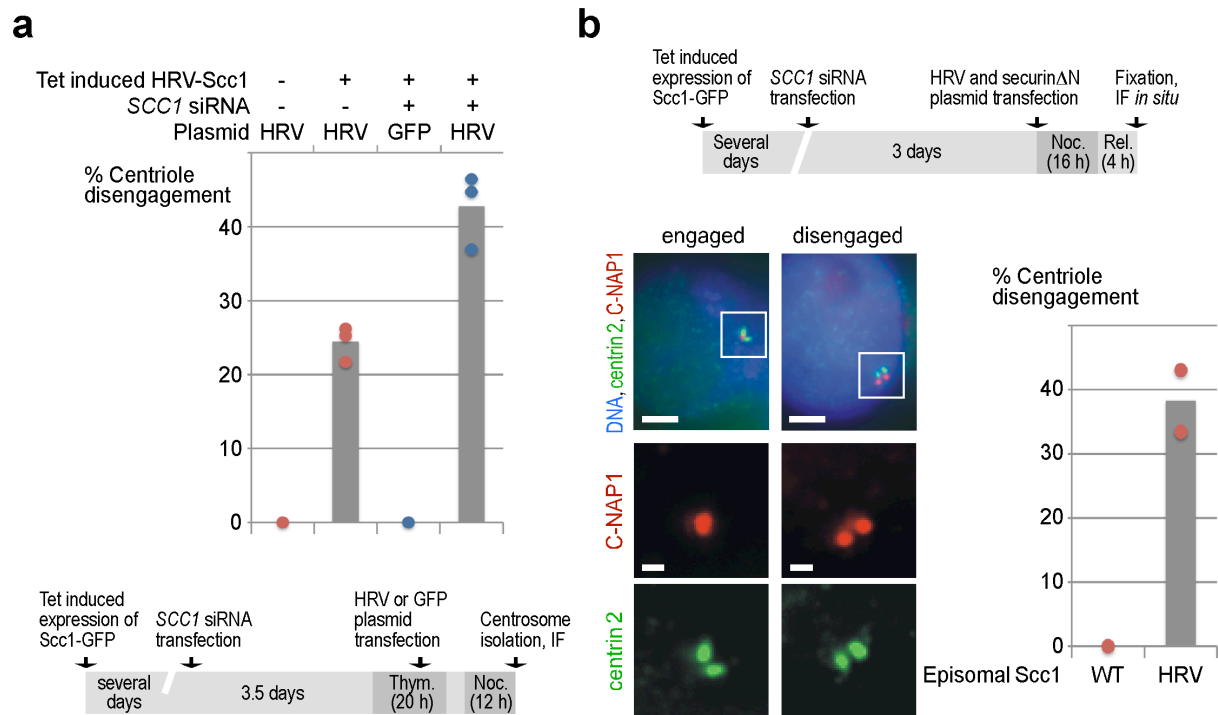
Figure 12. Cleavage of an engineered Scc1 triggers centriole disengagement *in vivo.* **(a)** Expression of HRV protease triggered centriole disengagement in Hek 293T cells, in which endogenous Scc1 had been replaced by HRV-Scc1. Episomal cell lines were induced with Tet and transfected with *SCC1* siRNA and/or HRV expression plasmids as indicated at the top. In parallel (see time line at bottom), cells were thymidine-nocodazole synchronized prior to centrosome isolation and IF. Given are the percentages of centriole disengagement after subtraction of the background (23-39%), i.e. disengagement in the corresponding negative controls (-Tet or GFP instead of HRV protease, color coded). Averages (grey bars) of three independent experiments (dots) are shown, representing at least 370 centrosomes per column. **(b)** Tet-induced episomal cell lines were treated with *SCC1* siRNA. Three days later, cells were additionally transfected with HRV protease- and securinΔN expression plasmids in nocodazole-containing medium (see time line at top). After release (Rel.) into G1 phase, cells were fixed, stained for centrin 2, C-Nap1 and DNA and centriole disengagement status was assessed *in situ*. Insets from the top images (scale bars = 1 µm) are shown magnified below (scale bars = 250 nm). Between 100 and 400 centrosomes per sample were counted. Shown are averages (grey bars) of 2 independent experiments (colored dots). The background (46.5% disengaged centrioles in WT-Scc1 samples = negative controls) was subtracted to specifically quantify HRV protease-induced centriole disengagement in HRV-Scc1-expressing cells.

In a second approach cells were not released from mitosis but instead pre-extracted with a special buffer (Gregson et al., 2001) to demask C-Nap1 for better antibody access and IF-signal. Cells grown on coverslips are easily dislodged and lost by washing when in mitosis and, hence, rounded up. Therefore, the pre-extraction and immunostaining were carried out in suspension. Only thereafter, cells were carefully centrifuged onto coverslips and analyzed by IF-microscopy. In this way, the centriole

engagement status could indeed be monitored in fixed mitotic cells (Fig. 13). As centrosomes are not located in one layer, stacks were analyzed. When super-imposed, the images illustrate a 4:4 signal ratio of centrin 2 *versus* C-Nap1 and indicate the typical SA-separase induced centriole disengagement pattern (Fig. 13a, b). In the presence of nocodazole, centrosomes separation is inhibited, which is the reason for this ratio, thus indicative for centriole disengagement. Consistent with previous experiments, over-expression of de-regulated, hyperactive SA-separase induced premature centriole disengagement (Fig. 13c) also according to this form of analysis (Fig. 10c). Taken together, these data provide the strongest evidence yet for a crucial role of Scc1 as part of the molecular glue between engaged centrioles.
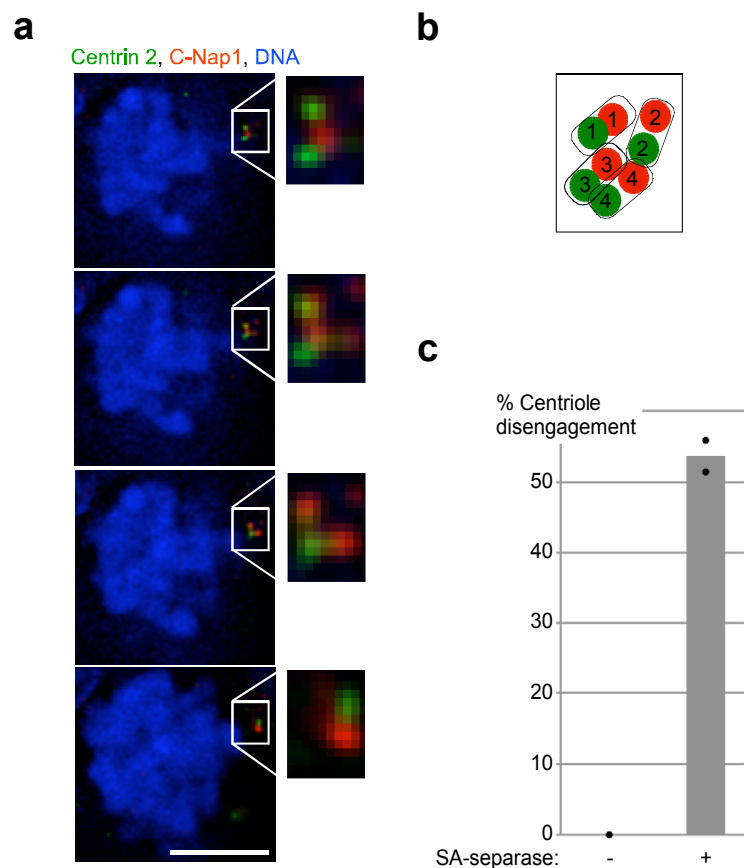
Figure 13. Separase-induced centriole disengagement in prometaphase. **(a)** Centriole disengagement was monitored in mitotic SA-cells. After 16h of Tet-induction, nocodazole arrested cells were harvested and pre-extracted with CSK-buffer (Gregson et al., 2001) to improve the subsequent detection of C-Nap1. Pre-extraction and staining for centrin 2, C-Nap1 and DNA was carried out in suspension, prior to spinning cells onto coverslips. Images were taken on a DMI 6000 inverted microscope (Leica) and processed with deconvolution software. Insets from the images are shown magnified on the right. Note that stacks were collected, as centrosomes are not located in one layer. The four images are represent one stack and illustrate, when super-imposed a 4:4 signal ratios of centrin 2 *versus* C-Nap1. In

the presence of nocodazole, centrosome separation is inhibited, which is the reason for this ratio, thus indicating centriole disengagement (scale bar 200 nm). **(b)** Cartoon representing the projection of the four images from one stack shown in b. SA-separase induced centriole disengagement reveals a 4:4 ratio of centrin 2 (green) and C-Nap1 (red) **(c)** Quantification of SA-separase induced centriole disengagement in mitotic cells. Between 100 and 200 centrosomes per sample were analyzed. Shown are average (grey bars) of two independent experiments (black dots) after subtraction of the background (22%), i.e., centriole disengagement in the absence of Tet (negative control).

3.2.5. Ectopic cleavage of the cohesin ring within Smc3 triggers centriole disengagement

Does Scc1 mediate centriole engagement as part of the cohesin ring complex and, if yes, does cohesin provide a topological or a physical linkage between centrioles? Inspired by an elegant study, which addressed these questions in connection with the role of yeast cohesin in sister chromatid cohesion (Gruber et al., 2003), a human Smc3 was engineered that could be artificially cleaved by tobacco etch virus (TEV) protease. To this end, three consecutive TEV cleavage sites each were inserted at opposing positions of minimal coiled coil probability into both antiparallel strands of Smc3 (Fig. 14a). The resulting TEV-Smc3 was not only efficiently and specifically cleaved by TEV protease *in vitro* but, indicative of preserved activity, it also interacted like WT-Smc3 with Smc1 and Scc1 in co-immunoprecipitation experiments (Fig. 14a, b). Hek 293T cells were co-transfected with siRNA targeting the 3'UTR of endogenous *SMC3* mRNA and expression plasmids for recombinant TEV- or WT-Smc3. Cells were then synchronized by consecutive treatments with thymidine and nocodazole and finally harvested. Corresponding lysates were treated with recombinant TEV protease and then used for immunoblotting and isolation of centrosomes. As predicted, TEV protease treatment cleaved TEV-Smc3 but not WT-Smc3 (Fig. 14c). At the same time, it also triggered disengagement of TEV-Smc3 centrioles but did so appreciably only when endogenous Smc3 had been depleted (Fig. 14c, bottom).
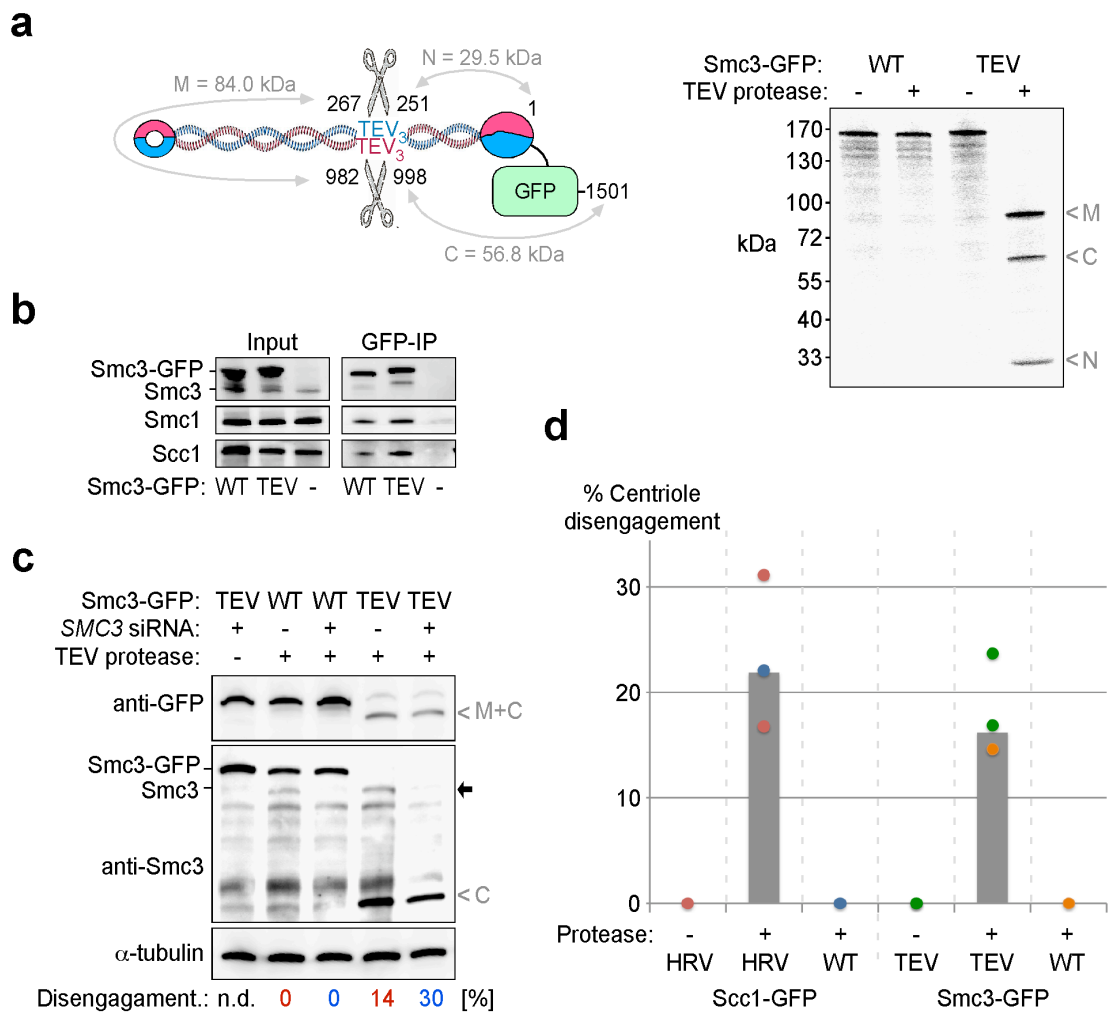
Figure 14. Artificial proteolysis of the cohesin ring within Smc3 triggers centriole disengagement. **(a)** TEV protease cleavable human Smc3 (TEV-Smc3) was generated by integration of three consecutive sites (TEV$_3$) into two opposing positions of minimal coiled coil probabilities within the Smc3 arm (see cartoon). Treatment of ^{35}S-labelled TEV-Smc3 but not WT-Smc3 with TEV protease resulted in three fragments, marked N, M, and C for N-terminal, middle, and C-terminal, respectively, as judged by SDS-PAGE/autoradiography. **(b)** TEV-Smc3 retains full competence to interact with other cohesin subunits as judged by IP-Western analysis of transiently transfected Hek 293T cells. GFP-expressing cells served as negative control (-). **(c)** Hek 293T cells were co-transfected with WT- or TEV-Smc3 expression plasmids and *SMC3* or *GL2* siRNA, as indicated. Two days later and 12 hours after nocodazole addition, lysates were prepared, incubated with TEV protease and analyzed by Western blot and IF of pelleted centrosomes. Grey arrowheads and a black arrow label cleavage fragments of TEV-Smc3 and endogenous Smc3, respectively. Percentages of centriole disengagement are indicated at the bottom. The background (21 and 25% disengaged centrioles in WT-Smc3 with and without siRNA, respectively = negative control) was subtracted from the corresponding TEV-Smc3 samples to quantify TEV protease induced centriole disengagement (color coding). 200 centrosomes each were analyzed. n.d., not determined. **(d)** Hek 293T cells were transfected with expression plasmids encoding WT- or HRV-Scc1 or WT- or TEV-Smc3 as indicated. In case of Smc3, a corresponding siRNA was co-transfected, which targets the 3'UTR of the endogenous mRNA. Following thymidine-nocodazole synchronization, centrosomes were isolated and incubated either alone or

together with recombinant, pure TEV or HRV protease. Finally, centrosomes were re-isolated and analyzed by IF microscopy. Given are averages (grey bars) of three independent experiments. Color-coding of dots identifies the corresponding background (27-30%) used for normalization. Between 400 and 700 centrosomes were analyzed in each sample.

Can centrioles even be disengaged in a purified system? To address this issue, centrosomes were first isolated from cells, in which endogenous Scc1 or Smc3 had been replaced by their engineered forms. Only then they were treated with the corresponding protease. Indeed, HRV and TEV protease induced centriole disengagement in HRV-Scc1- and TEV-Smc3 containing centrosome preparations, respectively (Fig. 14d). While highly specific, centriole disengagement in this purified system was nevertheless inefficient, indicating a supporting activity in mitotic cell lysates lost during the centrosome isolation procedure. This assumption is further supported by the fact that the highest centriole disengagement rates of around 40% were observed upon incubation of corresponding centrosomes in a mixture of highly concentrated CSF-extract with HRV or TEV protease (Fig. 15).
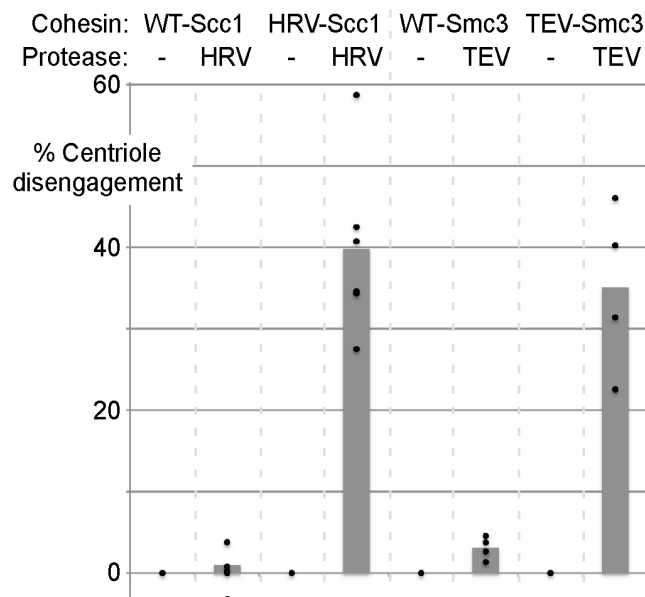
Figure 15. Hek 293T cells were transfected with expression plasmids encoding WT- or HRV-Scc1 or WT- or TEV-Smc3 as indicated. In case of Smc3, a corresponding siRNA was co-transfected, which targets the 3'UTR of the endogenous mRNA. Following thymidine-nocodazole synchronization, centrosomes were isolated and incubated either alone or together with TEV- or HRV-protease in CSF-extract. Finally, centrosomes were re-isolated and analyzed by IF. Given are averages (grey bars) from four (Smc3) or six (Scc1) experiments. Between 50 and 250 centrosomes were analyzed in each sample. The background (23% disengaged centrioles even in samples without protease) was subtracted to quantify TEV and HRV protease induced centriole disengagement.

This fact, together with the finding that Smc1 localizes to centrosomes (Fig. 24; Fig. 25, Wong and Blobel, 2008), militates in favor that the same tripartite Scc1-Smc1-Smc3 ring, which keeps sister chromatids paired, also mediates centriole engagement.

3.3. The prophase pathway promotes centriole disengagement

The bulk of cohesin is removed from chromosome arms by the phosphorylation-dependent prophase pathway early in vertebrate mitosis, while centromeric cohesin is protected by Sgo1-PP2A until separase becomes active in anaphase. Might the prophase pathway also displace a subpopulation of centrosomal cohesin in preparation for later centriole disengagement? If so, then impairment with the prophase pathway should obstruct centriole disengagement, while abrogation of Sgo1 function should result in premature centriole disengagement even in the absence of active separase.

3.3.1. Plk1 and Wapl promote centriole disengagement *in vivo*

A recent study demonstrated a role in centriole disengagement also for polo like kinase 1 (Plk1) (Loncarek et al., 2010; Tsou et al., 2009). Consistently, BI2536, a specific Plk1 inhibitor (Lenart et al., 2007), suppressed not only premature separation of sister chromatids but also precocious centriole disengagement in prometaphase-arrested, Tet-induced SA-cells (Fig. 16a-c). Two functions of Plk1 may contribute to this phenotype: Plk1 helps to remove the bulk of cohesin from chromosomes as part of the prophase pathway (Sumara et al., 2002). In addition, it phosphorylates Scc1, thereby turning cohesin into a better substrate for separase (Hauf et al., 2005).
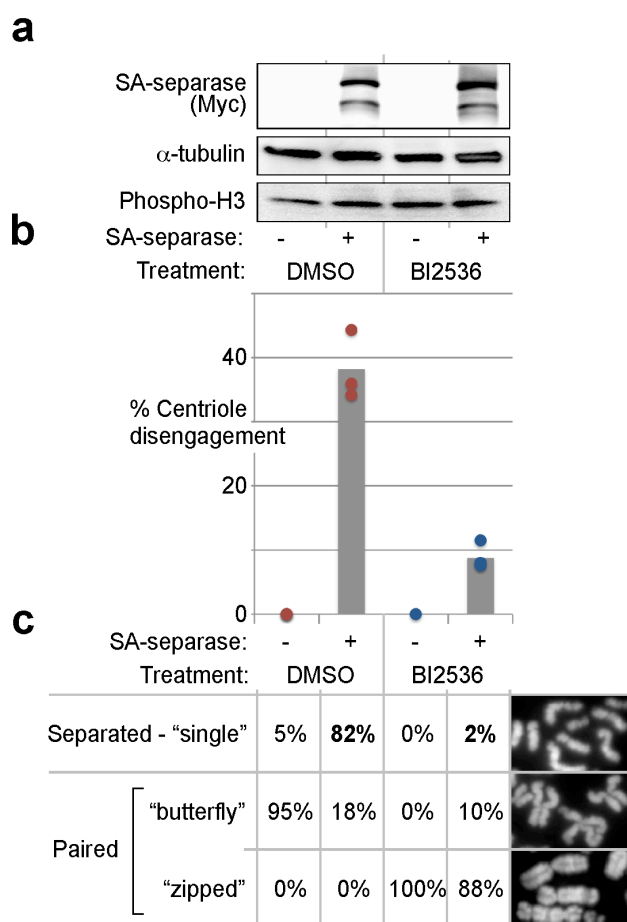
Figure 16. Plk1 (Polo like kinase 1) activity is required for centriole disengagement *in vivo*. **(a)** Western blot analysis of Tet- induced expression of Myc$_6$-tagged SA-separase in a stable Hek 293 line. Cells had been treated with nocodazole and BI2536 or DMSO. Because Plk1 inhibition delays mitotic entry, samples were ensured to be all in mitosis by immunoblot analysis of serine 10 phosphorylation of histone H3, a mitosis specific posttranslational modification. **(b)** Centrosomes of the cells in (a) were spun from lysates directly onto coverslips and analyzed by IF microscopy. The percentage of SA-separase induced centriole disengagement was determined by subtraction of the background (negative control), i.e. centriole disengagement in the absence of Tet (16-22%). Shown are averages (grey bars) of three independent experiments (dots). Between 100 and 300 centrosomes were analyzed per sample. **(c)** In one experiment (red dot in b), the sister chromatid separation status was also determined by fluorescence microscopy of spread, Hoechst 33342 stained chromosomes (n = 100 per column).

The opening of cohesin in prophase but not the cleavage of Scc1 in anaphase requires the cohesin-associated factor Wapl (Gandhi et al., 2006; Kueng et al., 2006). Thus, if Plk1 promoted centriole disengagement as part of the prophase pathway, then interfering with Wapl function by siRNA mediated depletion should also inhibit centriole disengagement. To address this issue, SA-cells were transfected with a *WAPL* siRNA (Kueng et al., 2006) prior to nocodazole treatment

and separate overexpression. Indeed, this knockdown partially inhibited unscheduled separation of sister chromatids and disengagement of centrioles relative to the mock treated (GL2) control (Fig. 17a, b). However, the rescuing effects of Wapl depletion were small in comparison to Plk1 inhibition, even on chromosomal level. This is likely due to the facts that separase can also cleave arm cohesin when the prophase pathway fails (Gimenez-Abian et al., 2004) and that the SA-cell system capitalizes on effects induced by deregulated separase.
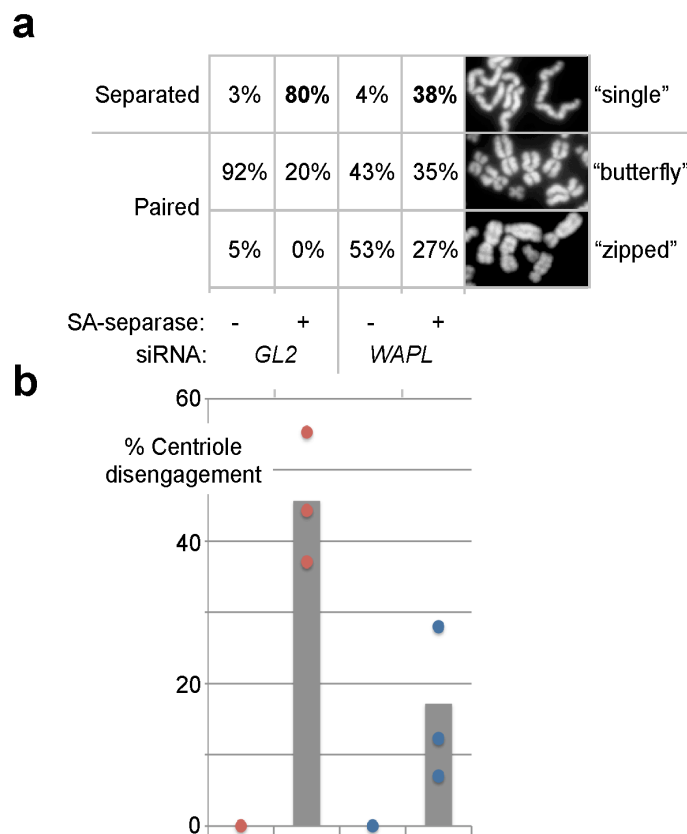
Figure 17. Centriole disengagement requires the prophase pathway. **(a)** Wapl depletion partially rescues premature sister chromatid separation in nocodazole treated SA-cells as judged by chromosome spreading. Shown are averages of three independent experiments representing a total of 160 - 200 cells per column. **(b)** Wapl depletion partially rescues premature centriole disengagement. Centrosomes from *WAPL* siRNA treated SA-cells were isolated and processed for IF microscopy. Separase-induced centriole disengagement was determined as described in 10c. Shown are averages (grey bars) of three independent experiments (dots) representing a total of 400 centrosomes per column. Color-coding of circles identifies the corresponding background used for normalization (15-27% for *GL2* siRNA without Tet and 21-28% for *WAPL* siRNA without Tet).

Does Plk1 promote separase-dependent cleavage of centrosomal cohesin like it does in case of chromosomal cohesin? A comparison of separase- *versus* HRV

protease induced centriole disengagement could address this question because, in contrast to the former, the latter cleavage reaction is independent of Scc1 phosphorylation (Fig. 18a). To minimize the effect of the prophase pathway, WT- or HRV-Scc1 containing centrosomes were isolated from thymidine/nocodazole-synchronized cells, in which prophase-sensitive cohesin should have been largely displaced. These centrosomes were then incubated in CSF extract, in which Plk1 had been inhibited by BI2536 addition or left active. Finally, separase or HRV protease was added and centriole disengagement assessed shortly thereafter. While Plk1 inhibition had only a minor effect on the disengagement of HRV-Scc1 containing centrioles by HRV protease, it blocked centriole disengagement by separase almost completely (Fig. 18b). This difference is most likely due to rapid dephosphorylation of Scc1 in extracts lacking Plk1 function. This *in vitro* experiment therefore suggests that Plk1 has the prophase-independent, additional function of phosphorylating centrosomal cohesin, thereby stimulating its cleavage by separase in anaphase.
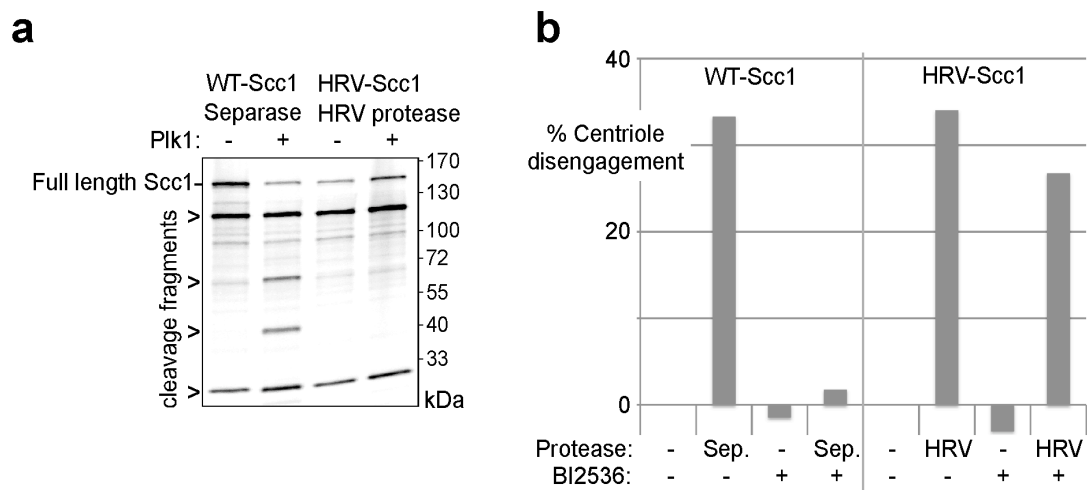
Figure 18. Plk1 activity triggers separase induced centriole disengagement. **(a)** Cleavage of HRV-Scc1 by HRV protease is unaffected by Plk1, whereas cleavage of WT-Scc1 by separase is stimulated by Plk1-dependent phosphorylation. ^{35}S-labeled WT- or HRV-Scc1 were incubated with active separase or HRV protease in the presence or absence of Plk1. Cleavage reactions were resolved by SDS-Page and analyzed by autoradiography. **(b)** Plk1 stimulates separase-dependent centriole disengagement. WT- or HRV-Scc1 containing centrosomes were incubated in CSF-extract in the presence or absence of active separase (Sep.), HRV protease, or BI2536 (200 nM), as indicated, re-isolated and imaged by IF microscopy. For each condition, 100-200 centrosomes were analyzed. The percentage of centriole disengagement in the absence of protease and Plk1 inhibitor (20 and 24% for WT- and HRV-Scc1, respectively) was used for background subtraction. This correction also explains the slightly negative values in absence of Plk1- and protease function. The slight inhibitory effect of BI2536 on HRV samples indicates that the prophase pathway aids disengagement of a small fraction of G2 centrosomes.

3.3.2. Shugoshin 1 (Sgo1) inhibits centriole disengagement *in vivo*

To study also the involvement of the prophase pathway in centriole disengagement in the absence of separase activity, U2OS cells were deprived of the mitotic cohesin protector shugoshin 1 (Sgo1), thereby rendering susceptible to the prophase pathway even centromeric cohesin (McGuinness et al., 2005; Salic et al., 2004; Tang et al., 2004). Following siRNA transfection and cell synchronization in prometaphase, chromosomes and centrosomes were isolated and analyzed by IF microscopy. As predicted, loss of Sgo1 function resulted in loss of sister chromatid cohesion as well as loss of centriole engagement (Fig. 19 a-c). Consistently, a short Sgo1 isoform (sSgo1 or Sgo1-C2) previously reported to function in centriole engagement is also targeted by the utilized siRNA (Wang et al., 2008 and data not shown). Thus, the licensing step of centrosome duplication is facilitated by the prophase pathway and separase and counteracted, respectively, by Sgo1 and known inhibitors of anaphase, i.e. securin and Cdk1-cyclin B1.
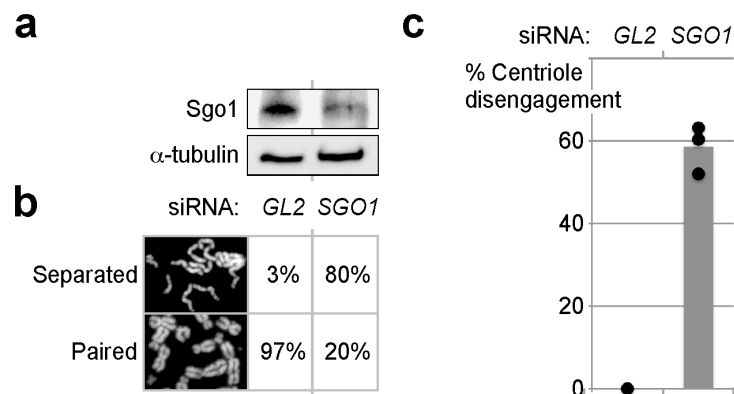
Figure 19. Sgo1 (Shugoshin 1) activity is required for centriole disengagement *in vivo*. **(a)** Immunoblot documenting the siRNA dependent depletion of Sgo1 from thymidine-nocodazole synchronized U2OS cells. **(b)** Sgo1 depletion induces premature separation of sister chromatids as judged by chromosome spreading. Averages of three independent experiments representing a total of 437 U2OS cells are given. **(c)** Sgo1 depletion induces premature centriole disengagement in U2OS cells. Centriole disengagement specifically induced by loss of Sgo1 function was determined essentially as described above. Shown is the average (grey bar) of three independent experiments (dots) representing a total of 422 centrosomes per column.

3.4. Mutual exclusive localization and function of shugoshin isoforms to centromeres *versus* centrosomes

Alternative splicing gives rise to different isoforms of mammalian Sgo1 (Mc Guinness et al., 2005; Wang et al., 2006). For human Sgo1 several isoforms have been described, which differ mostly in the presence or absence of exon 6 and exon 9, respectively (Wang et al., 2008). The canonical Sgo1-A1 (527 amino acids) localizes to centromeres, where it protects cohesin. In contrast, Sgo1-C2 (292 amino acids) has been reported to associate with centrosomes and to function in the engagement of centrioles. Ectopic expression of this short isoform preserved premature centriole disengagement, which otherwise occurred upon siRNA-mediated depletion of Sgo1 (Wang et al., 2008). Compared to Sgo1-A1, the short Sgo1-C2 lacks 268 amino acids encoded by exon 6 but contains additional 40 amino acids at its C-terminal end, which are encoded by exon 9. Wang and colleagues suggested that the alternative localization and function of Sgo1-C2 are determined by the absence of exon 6. However, recent localization experiments indicated that the peptide encoded by exon 9 might be responsible. For example, while transiently overexpressed in HeLa cells, the usual centromeric localization of Sgo2 was abrogated when it was fused via its C-terminus to the exon 9 encoded Sgo1-peptide. This defect was not due to C-terminal tagging *per se*, as a Sgo2-eGFP fusion localized normally to centromeres (B. Mayer, personal communication). This observation and others begged the question whether exon 9 rather than exon 6 might determine the localization of Sgo1 isoforms. Further questions remained to be answered since Wang and co-workers did not clarify whether Sgo1-A1 is able to rescue centriole disengagement. Therefore, additional Sgo1 splice variants besides Sgo1-A1 and Sgo1-C2 have to be investigated. For example, Sgo1-A2 (561 amino acids), which include both, exon 6 and the small exon 9. To investigate this discrepancy in more detail, the depletion-rescue experiment was repeated and extended.

3.4.1. Localization of various Sgo1 isoforms

Mainly characterized by the presence or absence of the amino acids encoded by exon 6 or exon 9, several Sgo1 variants were investigated for their subcellular localization. To this end, stable Hek 293 cell lines were generated, which inducibly

overexpress various N-terminally Myc$_6$-tagged Sgo1 variants (Sgo1-A1, -A2, -C2) including PP2A binding deficient Sgo´s (Sgo1-A1NI, -A2NI, -C2NI). In addition, stable celll lines expressing chimeras of either Myc$_6$-Sgo2- or Myc$_6$- or eGFP- fused to exon 9 of Sgo1 were created (Fig. 20a for schematic representation). Sgo transgenes carried silent mutations in regions where *SGO1* siRNA targeted the corresponding Sgo1 mRNA and, thus, were resistant to siRNA mediated kockdown (McGuinness et al., 2005). Transgene expression was verified by Western blot and localization of various Sgo1 isoforms was investigated by fluorescence microscopy (Fig. 20b, 21). Transgene expression slightly varied in stable cells but was roughly equal to endogenous Sgo1 protein level (Fig. 20c). The expression of Sgo2-Exon 9 could not be detected by Western blot analysis after 48h of induction. This could be due to blotting problems or lower expression level, which might be caused by its larger size or rapid degradation.

To determine the localization of various isoforms by IF-microscopy, centrin 2 was used as centrosomal marker. The results from Wang et al. (2008) could be confirmed as the small splice variant Sgo1-C2 was solely found at centrosomes and was excluded from mitotic chromosomes, while *vice versa* the long Sgo1-A1 exclusively localized to centromeres and not centrosomes in stable cells (Fig. 21). Surprisingly, Sgo1-A2 was excluded from mitotic chromosomes and instead found to localize to centrosomes. The fact that Sgo1-A2 harbors both, exon 6 and exon 9, argues against the hypothesis from the Dai laboratory, as they claimed that exon 6 mediates centromeric localization (Fig. 21).
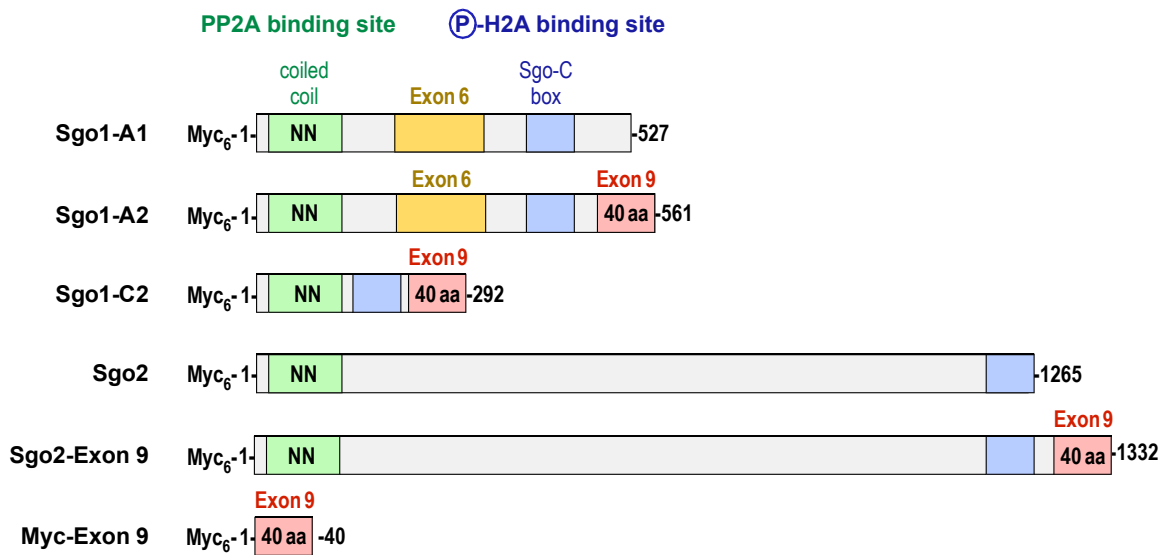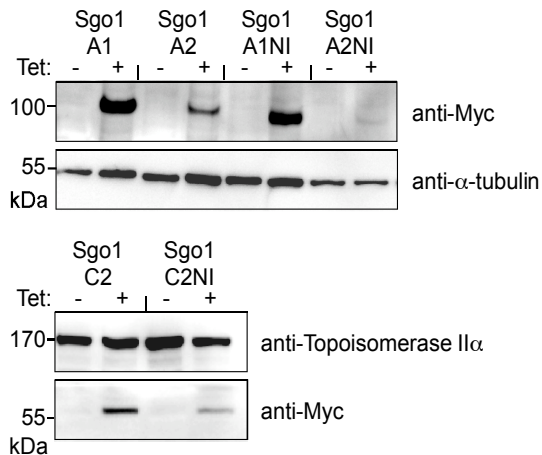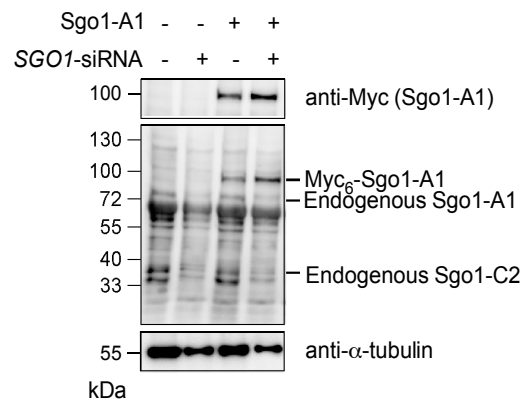
Figure 20. Generation of stable Hek 293 cells expressing different shugoshin splice variants and chimeras thereof. **(a)** Schematic representation of N-terminally Myc$_6$-tagged shugoshin variants. Note that the homology between Sgo1 and Sgo2 is restricted to a N-terminal coiled coil domain and a conserved C-terminal basic region referred to as Sgo-C box. The double Asn motif (NN) is required for PP2A binding (Tang et al., 2006) whereas the Sgo-C box mediates binding to phosphorylated Histone H2A (Kawashima et al., 2010). PP2A binding deficient Sgo1 variants were generated by introduction of a N61I point mutation (e.g. Sgo1-A1NI, -A2NI, -C2NI). Chimeras of either Myc$_6$-Sgo2 or Myc$_6$ fused to exon 9 of Sgo1 were created as control. **(b)** Transgene expression in stable cell lines was induced with Tet and verified by Western blot analysis. α-tubulin and topoisomerase IIa served as loading control. **(c)** Upon induction, Hek 293 cells expressed transgenic Myc$_6$-tagged Sgo1-A1 variants, at levels comparable to endogenous Sgo1. Note that transfection of *SGO1* siRNA resulted not only in depletion of endogenous Sgo1 isoforms but at the same time in an increase of the transgenic variant.

Taken together, these localization studie indicate that the large peptide encoded by exon 6 does not dictate the centromeric localization of Sgo1 and rather support the proposed hypothesis that the small peptide encoded by exon 9 fulfills this role. Consistently, centromeric localization of Sgo2 was abrogated in stable cells expressing Sgo2-Exon 9 (fusion of full-length Sgo2 with the C-terminus of Sgo1-A2 including the amino acids encoded by exon 9) and confirmed previous results. Remarkably, expression of the relevant exon in fusion with Sgo2 or the Myc- or GFP-tag only, directed both proteins to centrosomes (Fig. 21; Karalus, 2012). Expression of Sgo2-Exon 9 transgene could only be verified by Western blot analysis when over-expressed for one week (Karalus, 2012). Moreover, immunoflourescence microscopic analysis revealed specific centrosomal signals for Myc_6-Sgo2-Exon 9, arguing that is is expressed, albeit at comparably low level (Fig. 21). Nevertheless, this data reinforce the claim that the tiny peptide encoded by exon 9 dictates Sgo1's localization to centrosomes rather than the much larger peptide encoded by exon 6 as suggested by Wang et al. (2008).

3.4.2. Localization of a PP2A binding deficient Sgo1

Sgo1-A1 is known to recruit PP2A to centromeres where it is thought to keep cohesin dephosphorylated, thereby protecting phosphorylation dependent removal of cohesin and premature separation of sister chromatids (Kitajima et al., 2006; Riedel et al., 2006; Tang et al., 2006). In 2006, Tang and colleagues investigated the PP2A binding deficient version of Sgo1 carrying a N61I point mutation and demonstrated that it no longer localized to centromeres. Inconsistent with their data, induced transgenic Hek 293 cells that carried the same point mutation (Sgo1-A1NI) exhibited a centromeric Sgo1 localization signal when investigated in this study (Fig. 21). Thus, PP2A binding seems to be either unnecessary for proper centromeric localization of Sgo1 or this point mutation does not completely abrogate the Sgo1-PP2A interaction. To address the role of PP2A in regulating Sgo1´s localization at centrosomes, stable cell lines that inducibly express PP2A deficient forms of Sgo1 were investigated. These mutants carried the same point mutation as described by Tang et al. (2006). IF-analysis showed that Sgo1-C2NI and -A2NI, like their canonical counterparts, were excluded from mitotic chromatin and only detectable at centrosomes (data not shown).
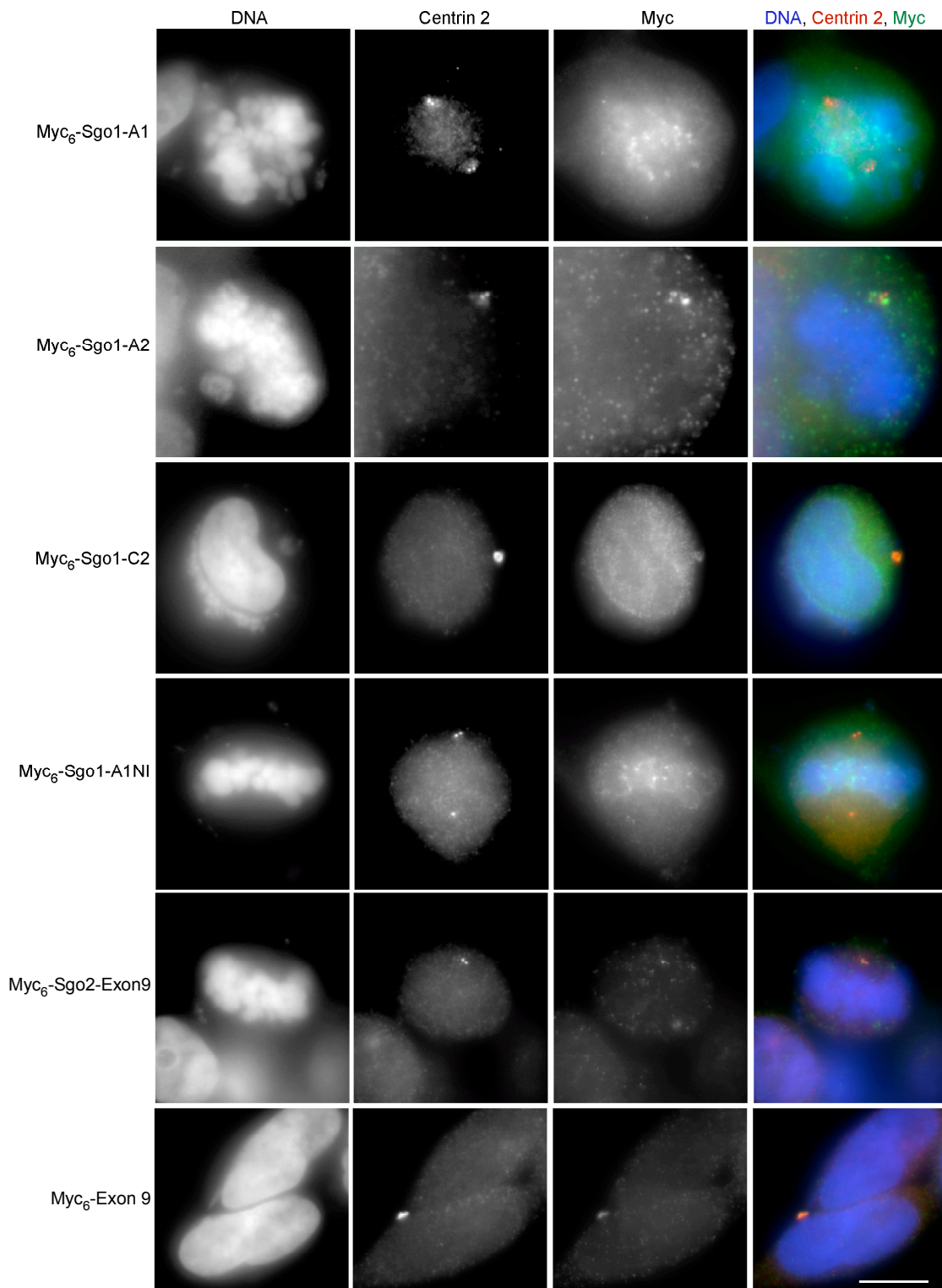
Figure 21. Localization of Myc$_6$-tagged shugoshin isoforms and chimeras thereof. **(a)** Tet-induced stable Hek 293 cells were grown on coverslips, fixed with ice-cold methanol and processed for IF microscopy. Immunostaining was carried out with antibodies against centrin 2 and Myc. Hoechst 33342 was used to stain DNA (scale bar = 10 µm). Note that Sgo1-A1 and Sgo1-A1NI localized only to the centromeric region whereas Sgo1-A2 and Sgo1-C2 were present only at centrosomes. Expression of Myc$_6$-tagged chimeras showed that the exon 9-encoded peptide directs Sgo2 and even Myc$_6$ to centrosomes.

3.4.3. Mutually exclusive function of Sgo1 isoforms at centromeres *versus* centrosomes

As the above findings suggest that the presence or absence of exon 9 determines Sgo1´s localization, the next question was whether localization correlates with function. Therefore, the different Sgo isoforms were compared in their ability to preserve sister chromatid cohesion and centriole engagement (see top of Fig. 22 for the workflow). To prevent SAC-dependent mitotic arrest in response to Sgo1 depletion and consequent premature loss of sister chromatid cohesion, the cell cycle was arrest, first with thymidine in S-phase and subsequent by taxol in prometaphase. After 40 h of Tet-induced expression of the respective Sgo1 isoform and 26 h after siRNA-mediated knockdown, cells were harvested. Transgene expression was verified by Western blot analysis (Fig. 20b). As previously shown (Fig. 19), Sgo1 depletion causes premature centriole disengagement and precocious separation of chromatids (data not shown). Analyzing chromosome spreads assessed effects on chromosomal cohesion whereas IF of centrosomes using centrin 2 and C-Nap1 as marker antigens enabled to assess the engagement status of centrioles. Remarkably, each transgenic Sgo1 isoform could functionally replace endogenous Sgo1 only in one of its two functions. Accordingly, Sgo1-A1 only suppressed premature separation of sister chromatids, while Sgo-A2 and Sgo-C2 exclusively prevented precocious disengagement of centrioles (Fig. 22a, b). Since the only amino acids that are shared by Sgo1-A2 and -C2 but absent from Sgo1-A1 are those encoded by exon 9 (Fig. 20a), the very C-terminal 40 amino acids must be required for the centrosomal function of Sgo1.

Also the PP2A binding deficient version, Sgo-A1NI, showed a slight rescuing effect in sister chromatid cohesion (Fig. 22a). This marginal effect is probably due to residual PP2A binding to transgenic Sgo1-A1NI as confirmed by IP experiments (data not shown). Similarly, the PP2A binding deficient mutants Sgo1-A2NI and Sgo1-C2NI also rescued centriole disengagement like their canonical counterparts (Fig. 22b). Therefore, PP2A in complex with Sgo1 seems to be not only necessary for the protection of centromeric cohesin but also for physically shielding centrosomal cohesin.

Remarkably, Sgo2-Exon 9 not only localized to centrosomes it also replaced Sgo1´s function in protecting centrosomal cohesin. Sgo2-Exon 9 exhibited an equal rescue efficiency of centriole disengagement as Sgo1-A2 and -C2 (Fig. 22b). This effect is

not due to overexpression of Sgo2 *per se*, as wild-type Sgo2 only localizes to centromeres and not centrosomes when transiently overexpressed in Hek 293T cells (Karalus, 2012). Likewise, the exon 9 dependent targeting of just any protein to centrosomes is not sufficient to protect centrosomal cohesin, since Myc$_6$-Exon 9 and GFP-Exon 9, showed a centrosomal localization but did not rescue centriole disengagement (Fig. 22a, b; Karalus, 2012). This demonstrates that targeting *per se* is necessary but not sufficient for the protection of centrosomal cohesin. Moreover, since Sgo2-Exon 9 is not drastically overexpessed in analyzed stable cells and endogenous Sgo2 is not able to rescue the Sgo1 depletion phenotype of centriole disengagement militates in favor for the small C-terminal peptide acting as a centrosomal localization signal (CLS). These data demonstrate that the exon 9 dependent localization of Sgo1 variants closely correlates with their function. Based on the above findings, it can be further postulated that the presence or absence of the 40 amino acids encoded by exon 9 determines whether Sgo1 shields centrosomal or centromeric cohesin, respectively.

a

b
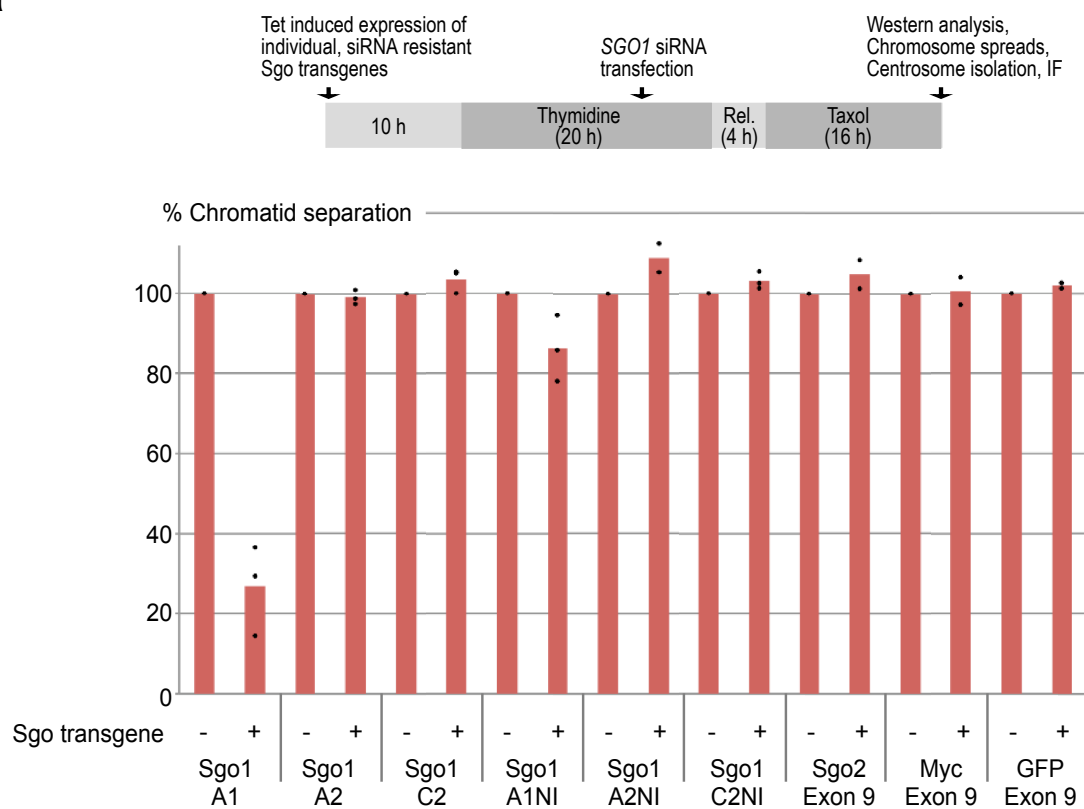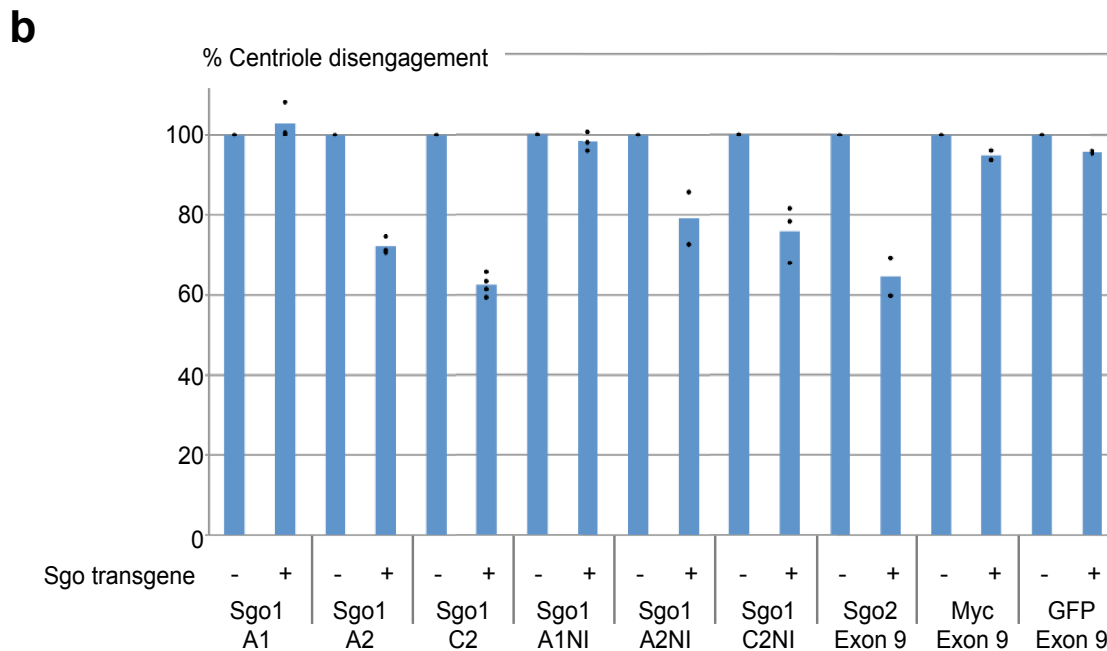
Figure 22. Exon 9 is required for the centrosomal function of Sgo1. **(a)** Stable cell lines were induced with Tet and transfected with *SGO1* siRNA as indicated at the top. In parallel (see time line on top), cells were synchronized in prometaphase prior to spreading of chromosomes, isolation of centrosomes and IF microscopy. Analysis of chromosome spreads illustrates that only the expression of the Sgo-A1 transgene rescued premature sister chromatid separation. Shown are averages (red bars) of 2 to 4 independent experiments (dots) representing in total 100 - 200 cells per column. **(b)** Premature centriole disengagement induced by *SGO1* siRNA treatment was specifically rescued by expression of exon 9 containing *SGO1* transgenes, i.e., Sgo1-A2, -C2, -A2NI, -C2NI and Sgo2-Exon 9. Shown are averages (blue bars) of 2 to 4 independent experiments (dots) representing in total 100 - 200 centrosomes per column. To quantify the relative values of the two Sgo functions, in sister chromatid separation and centriole disengagement, the uninduced control was always set 100% and the Tet induced samples were quantified relative the this control.

3.4.4. Mutation of three conserved amino acids within the peptide encoded by exon 9 reconstitutes centromeric localization

Alternative splicing patterns are highly divergent in various organisms. Therefore sequences related to human exon 9 have so far only been found in primates like orangutans, gibbons and rhesus macaques. The exon 9 encoded C-terminal peptide encomprises only 40 amino acids. Yet, its absense or presence might still have a great effect on Sgo1´s overall biochemical behavior. To largely rule out this possibility and to identify functionally relevant residues within the exon 9 encoded peptide, two point mutations were generated (Fig. 23a). The exchange of an ILY motif for AAA

caused especially strong effects and, thus, was characterized in more detail. To this end, a stable Hek 293 cell line was generated that inducibly over-expresses the mutated Sgo1-A2^{AAA} isoform, which is siRNA resistant and encodes a N-terminal Myc$_6$-tag. First, localization of Sgo1-A2^{AAA} was investigated by IF-microscopy. Astonishingly, this Sgo1-A2 variant was found to localize to the centromere of mitotic chromosomes instead of centrosomes (Fig. 23c). While Sgo1-A2 is excluded from mitotic chromatin, Sgo1 A2^{AAA} showed distinct signals at the centromere. Sgo1-A2^{AAA} was further characterized by the ability to rescue premature sister chromatid separation or centriole disengagement induced by Sgo1 depletion. Transgene expression was analyzed by Western blot analysis (Fig. 23b). As control served Sgo1-A1 and Sgo1-A2 and depletion-rescue experiments were conducted as previously described (Fig. 22a). Interestingly, localization closely correlated with function. The analysis of chromosome spreads revealed that Sgo1-A2^{AAA} rescued sister chromatid separation, similarly to Sgo1-A1. Sgo1-A2^{AAA} did not guard centriole engagement anymore but now shielded sister chromatid cohesion (Fig. 23d). These data substantiate the role of exon 9 encoded peptide acting as a CLS since mutation of just three consecutive amino acids within the corresponding peptide abrogated both the pro-centrosomal as well as the anti-centromeric targeting effect, which tightly correlated with Sgo1 function.

a

Sgo1-A1 : -RRSKK**SMKQIQ**-527

Sgo1-A2 : -RRSKK RALEVSPAKEAIF**ILY**YVREFVSRFPDCRKCKLETHI CLR-561   Exon 9

Sgo1-A2^AAA : -RRSKK RALEVSPAKEAIF**AAA**YVREFVSRFPDCRKCKLETHIC LR-561

b

c

d
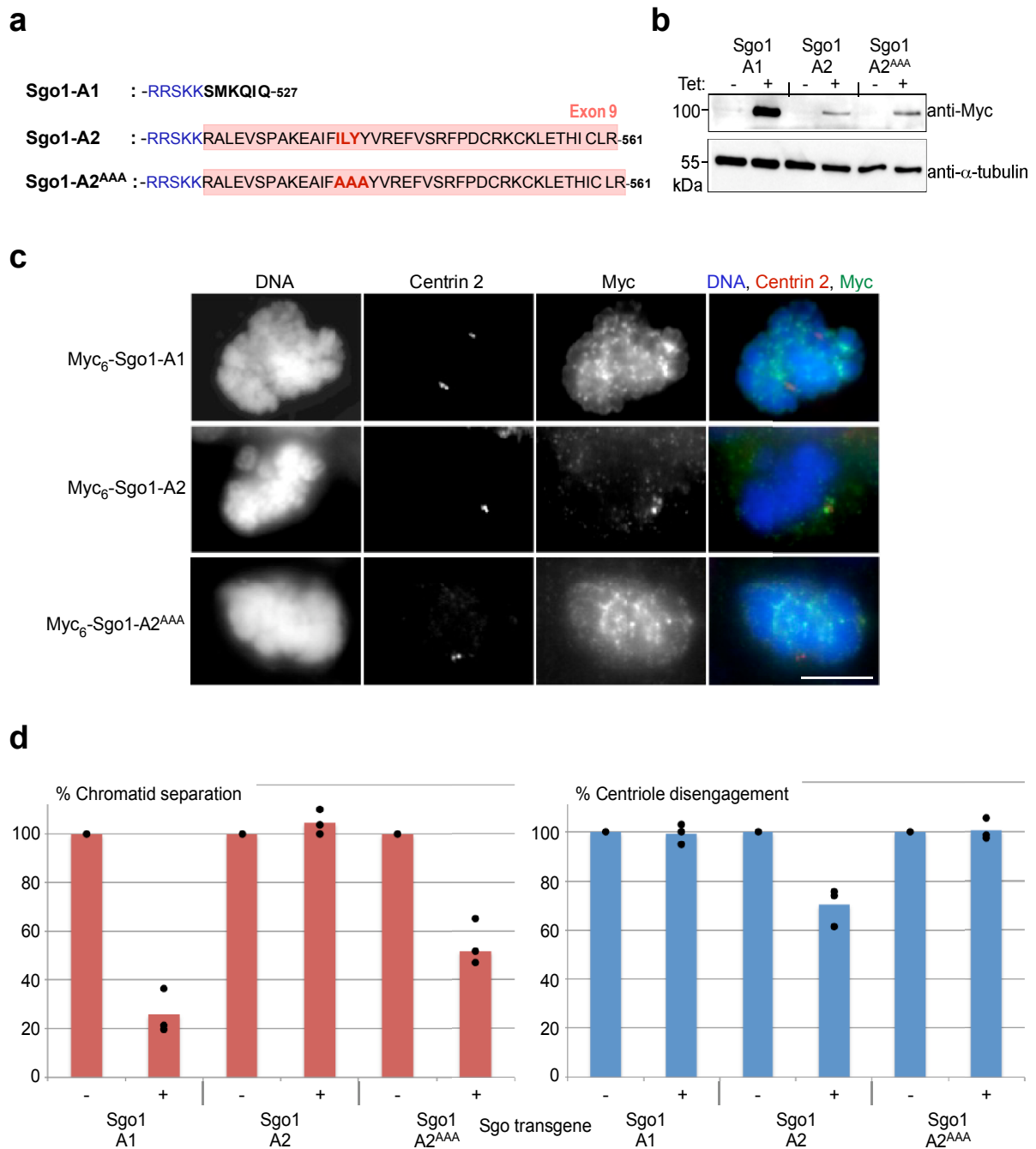
Figure 23. Mutation of just three consecutive amino acids within the corresponding peptide of exon 9 reprograms Sgo1 to localize and functions at centromeres instead of centrosomes **(a)** Schematic representation of the C-terminal ends of Sgo-A1, Sgo1-A2 and Sgo2-A2^AAA. The ILY motif in Sgo1-A2 was exchanged to AAA in Sgo2-A2^AAA.**(b)** Transgene expression in stable cell lines was induced with Tet and verified by Western blot analysis. As loading control served a-tubulin. **(c)** Tet-induced stable Hek 293 cells expressing either Sgo1-A1, -A2 or -A2^AAA (N-terminally Myc$_6$-tagged and siRNA resistant) were grown on coverslips, fixed with ice-cold methanol and processed for IF microscopy. Immunostaining was carried out with antibodies against Centrin 2 and Myc. Hoechst 33342 was used as DNA stain (scale bar = 10 μm). **(d)** Stable cell lines were induced with Tet, transfected with *SGO1* siRNA and depletion-rescue experiments were conducted as previously described (Fig. 22a). Analysis of chromosome spreads illustrates that not only Sgo-A1 but also the expression of Sgo1-A2^AAA preserved sister chromatid cohesion. Shown are averages (red bars) of three independent

experiments (dots) representing in total 100 spreads per column. Premature centriole disengagement was rescued only by the expression of Sgo1-A2. Shown are averages (blue bars) of three independent experiments (dots) representing in total 100 centrosomes per column. To quantify the relative values of the two Sgo functions, in sister chromatid separation and centriole disengagement, the uninduced control was always set 100% and the Tet induced samples were examined relative the this control.

3.5. Localization of cohesin at centrosomes

Where exactly is cohesin located at centrosomes? To follow this question, synchronized U2OS cells were depleted of endogenous Smc1 by siRNA or left untreated. After 48h, cells were pre-extracted as described (Wang et al., 2008), fixed with formaldehyde and immunostained for endogenous C-Nap1 and Smc1, respectively. The successful knockdown was verified by Western blot analysis (Fig. 24a). IF microscopy of Smc1-depleted cells revealed enlarged nuclei or increased chromosome numbers. Most likely, the SAC becomes active in cells lacking cohesin. SAC-mediated arrest is not permanent and cells can eventually escape mitotic arrest in a process termed mitotic slippage and finally become tetraploid. The fluorescence intensity of Smc1 obviously decreased upon Smc1 knockdown (Fig. 24b) demonstrating that the antibody is specific and suitable for further analysis by electron microscopy (EM).

To assess their putative suitability for immuno-EM, purified centrosomes were analyzed by transmission electron microscopy in terms of purity and preservation of ultrastructure. To this end, centrosomes were fixed, embedded in Epon and finally subjected to ultrathin sectioning and electron microscopy (PD Dr. S. Geimer, Cell Biology, University of Bayreuth). Centrosomes were detected within several sections and featured a well-preserved centriole structure (Fig. 25a). Cross-sections of centrioles revealed the typically cylindrical pattern of nine MT-triplets in a ring-shaped arrangement. Notably, MT-triplets (A-, B-, C-tubules) were readily dicernable. Since the electron micrographs displayed centrosomes with an intact ultrastructure, the centrosome purification protocol was adequate and compatible with further analysis by immuno-EM. In collaboration with PD Dr. S. Geimer, immuno-gold EM was applied to fine-map the localization of endogenous Smc1 on isolated centrosomes. For that purpose, purified centrosomes were centrifuged onto coverslips, fixed, labeled with anti-Smc1 antibody, then exposed to an anti-mouse secondary antibody

conjugated to 6 nm gold and finally embedded in Epon.

a

b
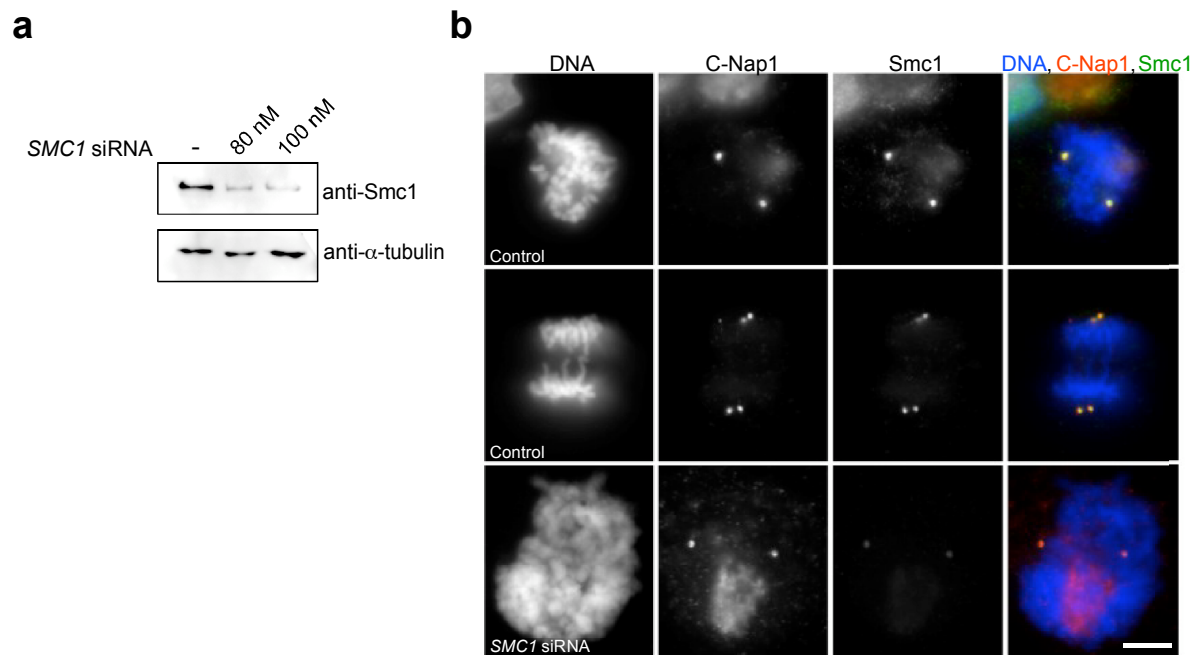
Figure 24. The cohesin subunit Smc1 localizes to centrosomes. **(a)** Immunoblot documenting the siRNA dependent depletion of Smc1 in U2OS cells. **(b)** The centrosomal, Smc1 dependent fluorescence intensity decreases upon treatment with *SMC1* siRNA. Synchronized U2OS cells were transfected with *SMC1* siRNA (100nM) or left untreated (control), grown on coverslips, pre-extracted (Gregson et al., 2001) and fixed with 3.7% formaldehyde. The IF-staining was carried out with antibodies against C-Nap1 and Smc1. DNA was visualized with Hoechst-33342 (scale bar = 10 µm).

Electron micrographs illustrated positive signals for centrosomal Smc1 as judged by the signals of the 6 nm gold particles. For demonstration purposes, two consecutive sections of one and the same centrosome are depicted (Fig. 25b, c). The centriole in the longitudinal cut featured Smc1 staining along MT-triplets and also around the proximal end of the MT-triplets (red dots). The cross-section of the other centriole exhibits Smc1 signals at the proximal part of the MT-triplets. Both centrioles are connected via fibrous material, where Smc1 was detected as well. After superimposition of gold particles from three serial sections (8 sections in total), Smc1 could be found at the proximal ends of both centrioles as well as in the space between them (Fig. 25d). This localization is consistent with cohesin being a centriolar protein.
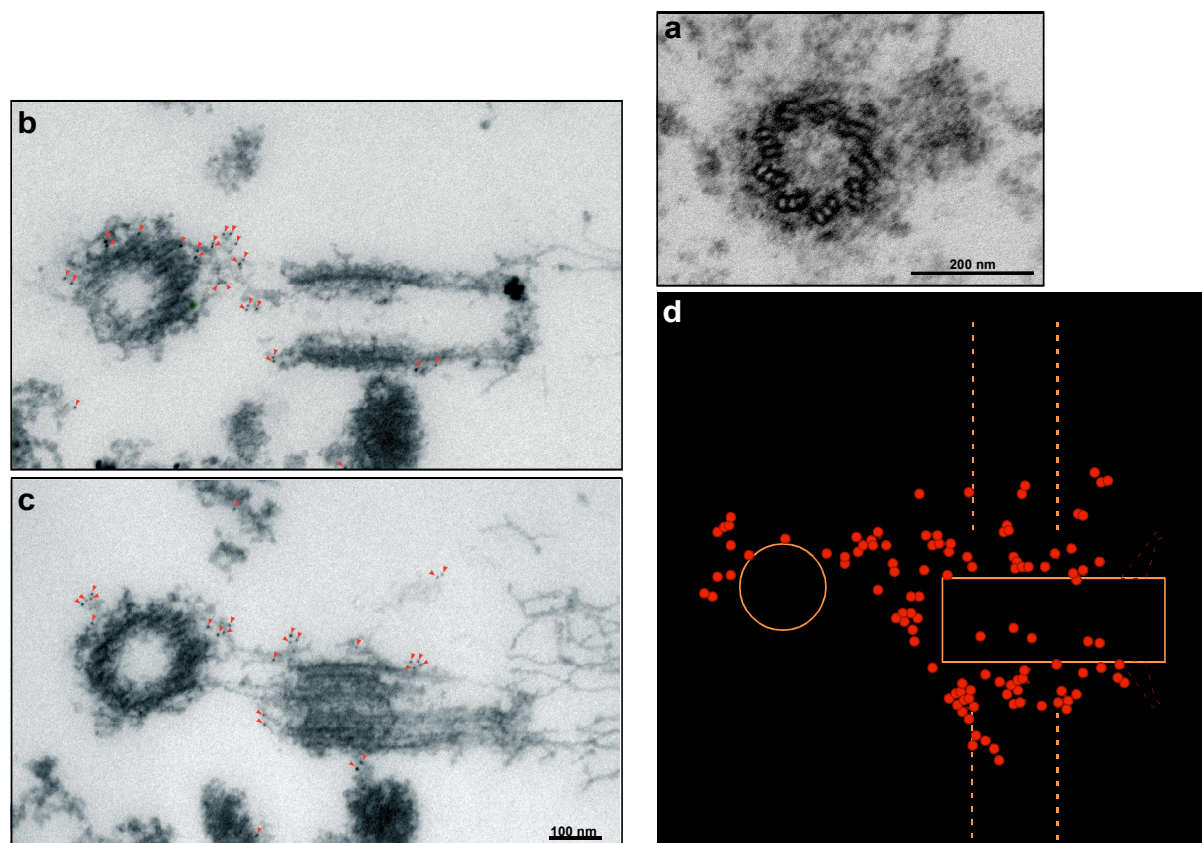
Figure 25. Smc1 localizes to the proximal part of centrioles. **(a)** Electron micrograph of a purified centrosome illustrating the cross-section of one centriole. The typical structure of nine intact MT-triplets verifies a preserved cylindrical ultrastructure. In the longitudinal cut a second centriole, most probably the outgrowing daughter, becomes visible. **(b and c)** Serial cross sections through the proximal part of one centriole and a longitudinal cut of the orthogonally positioned, second centriole. Due to its lack of subdistal appendages, this longitudinal cut most probably illustrates the daughter centriole. Smc1 is concentrated at the proximal end and along microtubule fibrils as judged by the signals of the 6 nm gold particles (red dots). **(d)** Graphical illustration of the statistical analysis of the Smc1 staining from the sections depicted in b and c plus additional ones. Three series of sections (8 in total) were arranged that one centriole (amber rectangle) was at the same relative position. Then, Smc1 signals were super-imposed onto these series. Depicted are the cross-section (amber circle) and the longitudinal cut (amber rectangle) of the centrioles from the consecutive section in the left. Dashed amber lines illustrate the position of the analyzed centrioles from other sections, which were arranged at the same relative position. Superimposition of the gold-labeled signals (red dots) from three serial sections (8 sections in total) suggest that cohesin concentrates around the proximal ends of both centrioles. In addition, Smc1 was found enriched in the space between both centrioles (Images courtesy of PD Dr. S. Geimer).

4. DISCUSSION

Supernumerary centrosomes might be associated with genomic instability and abberant cell divisions and, as such, represent a hallmark of many tumors (Ganem et al., 2009). Therefore, a strict control of centrosome and centriole number is crucial for accurate chromosome segregation. The regulatory machinery of the cell cycle must control not only a chromosome cycle but also a centrosome cycle, whereas the integration of both cycles is pivotal for genome stability (Mazia, 1987). In order to keep centrosome and centriole number constant over successive cell divisions, the centrosome cycle is governed by two distinct rules: cell cycle control and copy number control (Nigg, 2007). The latter enforces the formation of only one procentriole next to a pre-existing parental centriole. Mechanisms, which limit centrosome duplication to once per cell, are still poorly understood. However, a fundamental step is the disengagement of centrioles at the end of mitosis, a prerequisite for subsequent centriole duplication in S phase (Tsou and Stearns, 2006; Wong and Stearns, 2003). The finding that separase and Plk1 activity are required for centriole disengagement offers an appealing explanation for the coupling of centriole duplication to the traverse of the cell cycle (Tsou and Stearns, 2006; Tsou et al., 2009). Centriole disengagement is tightly coordinated with sister chromatid separation, which is even more corroborated by the data presented herein. Within this work, the molecular basis and regulation of centriole disengagement was addressed. Previous studies had already raised the intriguing possibility that engagement of centrioles is controlled in a manner that parallels sister chromatid cohesion with newly duplicated structures held together by cohesin and released by the combined activity of Plk1 and separase (Beauchene et al., 2010; Nakamura et al., 2009; Tsou et al., 2009). Herewith, this attractive model was further elaborated in indicating that cohesin is required for centriole engagement as it is for sister chromatid cohesion. The cohesin complex has previously been shown by several independent studies to localize to centrosomes and has recently been implicated in the structural integrity of centrosomes (Gregson et al., 2001; Guan et al., 2008; Kong et al., 2009; Nakamura et al., 2009). But until now, the precise function of cohesin´s localization to centrosomes remained elusive and there has been no robust evidence supporting cohesin as a centriole engagement factor so far.

4.1. Centriole disengagement requires the proteolytic activity of separase

First experiments confirm the hypothesis put forward by Tsou and Stearns (2006) that separase triggers centriole disengagement in *Xenopus* egg extract. However, the involvement of separase in their *in vitro* system was not assessed directly. Within this work, various mutants of recombinant human separase were compared in their ability to rescue centriole disengagement in *Xenopus* egg extracts, in which endogenous separase was constitutively inhibited. It could be shown that recombinant separase added *in trans* overcomes the inhibitory effect of non-degradable securin and cyclin B1 on centriole disengagement providing strong evidence for a direct involvement of separase in centriole disengagement. By comparing protease-dead (PD) with Cdk1-binding deficient (SA) variants, the function of separase in centriole disengagement was unambiguously attributed to the proteolytic activity while the Cdk1-inhibitory activity was clearly dispensable (Fig. 7b), thus confirming previous results (Tsou et al., 2009).

With this perception, a thrilling quest for a putative substrate of separase followed. Since cohesin was the most studied and appealing substrate that is proteolytically cleaved by separase at chromosomes, further experiments were designed to address whether cohesin is the sought after substrate of separase at centrosomes. In accordance with this attractive hypothesis, cohesin, separase and presumed (self-) cleavage products thereof can be found in association with centrosomes (Beauchene at al., 2010; Gregson et al., 2001, Guan et al., 2008; Kong et al., 2009; Nakamura et al., 2009). Furthermore, knockdown of Scc1 by RNAi results in the formation of multipolar spindles and centriole disengagement (Beauchene et al., 2010; Losada et al., 2005; Nakamura et al., 2009).

4.2. Cohesin as a centriole engagement factor

Further experiments represent that centriole disengagement can be prematurely triggered in prometaphase-arrested cells by either expression of recombinant SA-separase or siRNA mediated depletion of the cohesin protector Sgo1.

Cells with inducible expression of a hyperactive SA-separase were used and illustrated that centriole disengagement is blocked upon transient expression of NC-Scc1. However, in a set of experiments according to the Nasmyth approach (Gruber et al., 2003), centriole disengagement was prematurely promoted in cells expressing

cohesin subunits engineered to contain artificial protease cleavage sites together with the corresponding protease. Interestingly, artificial endoproteolysis of cohesin triggers centriole disengagement irrespective of position, i.e. whether cleavage occurs in Scc1 or Smc3. Therefore, it is tempting to speculate that, reminiscent of its behaviour in sister chromatid cohesion, the tripartite Scc1-Smc1-Smc3-ring provides topological rather than physical linkage between centrioles.

These findings could lead to the assumption that cleavage of chromosomal cohesin creates a diffusible cohesin fragment or subcomplex, which would then induce centriole disengagement *in trans.* However, this hypothesis can be excluded since artificial cleavage of Smc3 occurs under rather non-physiological conditions. The resulting unnatural protein fragments and -termini would likely lack biological function and, thus affirming that centrosomal cohesin is cleaved. A further aspect militating against secondary implications by chromosomes is the fact that 99% of chromosomal cohesin already resides in the cytoplasm due to its displacement by the prophase pathway when centriole disengagement takes place at the end of mitosis. However, it cannot be excluded that the employed centrosomes are contaminated with residual DNA fragments despite extensive DNase treatment. Both chromosomally bound and soluble cohesin was largely removed during the isolation of centrosomes and, hence, absent from most of our *in vitro* assays (data not shown).

A dosage effect might explain why the inhibitory effect of non-cleavable Scc1 (NC-Scc1) on centriole disengagement was missed in a previous study (Tsou et al., 2009). In contrast to our transiently transfected cells, the long-existing stable line (Hauf et al., 2001) used by Tsou and colleagues might be selected for very low level expression of the highly toxic NC-Scc1. By using correlative timelapse IF microscopy, Tsou and colleagues focused their analysis on the most severely affected population of NC-Scc1 cells (5% of the total) in which sister chormatid separation failed. In the nine cells that were examined, centriole disengagement was not affected and occured quite normally, explaining their claim that cohesin is not involved in the engagment of centrioles (Tsou et al., 2009). Due to its primarily nuclear localization, NC-Scc1 might affect chromosome segregation more than centriole disengagement under such conditions. On the other hand, endogenous Scc1 was still present when NC-Scc1 was expressed under the control of a tetracycline-regulated promotor in these cells, thereby allowing partial incorporation of separase-cleavable WT-Scc1 in the cohesin complex and finally centriole disengagement.

4.3. The prophase pathway promotes centriole disengagement

A recent study demonstrated a role in centriole disengagement for Plk1, whose activity was mapped to late G2 or early mitosis prior to securin destruction and separase activation in anaphase (Tsou et al., 2009). Combined downregulation of both, separase and Plk1, had synergistic effects and resulted in a tight block of centriole disengagement in late telophase. Therefore, this combines the action of Plk1 and separase activity during early and late mitosis, respectively. Consistently, BI2536, a small chemical inhibitor of Plk1, suppressed both premature disengagement of centrioles and precocious separation of sister chromatids in the background of hyperactive separase (Fig. 16). On the chromosomal level, Scc1 phosphorylation by Plk1 is fully dispensable for dissociation of cohesin in early mitosis but enhances its cleavage by separase (Hauf et al., 2005; Hornig and Uhlmann, 2004), which is consistent with the data presented herein (Fig. 18a). Instead, phosphorylation of Scc3 is needed for cohesin removal during prophase but is not required for efficient sister chromatid separation in anaphase (Hauf et al., 2005) indicating that separase activity is sufficient to remove all cohesin from chromosome arms and centromeres. In contrast, centriole disengagement triggered either by induction of separase in SA-cells or by recombinant active separase added *in trans* to *Xenopus* egg extract supplemented with centrosomes was inhibited by increasing amounts of Plk1 inhibitor BI2536 (Fig. 16 and 18). This effect is most likely due to rapid dephosphorylation of Scc1 and, hence, indicates a second and different role of Plk1 in centriole disengagement. Within this context, Plk1 could promote separase-independent removal of cohesin in prophase and have a prophase-independent, additional function of stimulating separase-specific cleavage of centrosomal cohesin in late mitosis.

Remarkably, depletion of Wapl, a protein that contributes to the dissociation of chromosomal cohesin during prophase, antagonized both premature disengagement of centrioles and precocious separation of sister chromatids in the background of active separase (Fig. 17). However, rescue effects of Wapl depletion were small compared to Plk1 inhibition. Apart from possible limitations in knock-down efficiency, this effect is most likely due to the facts that separase is capable of cleaving arm cohesin when the prophase pathway failed (Gimenez-Abian et al., 2004), and that the SA-cells used in this assay take advantage of the hyperactive separase to cleave cohesin. Consequently, this also argues in favor of a role of Plk1 activity in positively

influencing separase activity. Since effects on both chromosomes and centrosomes were observed by either Plk1 inhibition or Wapl depletion, the existence of two populations of cohesin at centrosomes as observed at chromosomes is likely: One of them sensitive to phosphorylation and thus removed in early mitosis, and the other one protected from phosphorylation, thus persisting until separase activation in anaphase onset.

In agreement with this assumption, depletion of the mitotic cohesin protector Sgo1 resulted in loss of centriole engagement as well as sister chromatid cohesion (Fig. 19). This finding is consistent with previous data reporting that the small Sgo1-C2 localizes to centrosomes and functions in maintaining cohesion between centrioles (Wang et al., 2008). Interestingly, mutation of putative phosphorylation sites for Plk1 within Sgo1-C2 diminished its centrosomal localization arguing for the importance of Plk1 function at centrosomes (Wang et al., 2008). Moreover, the appearance of multiple spindle pole bodies (SPB) in *sgo1* mutant yeast cells in meiosis I suggests that Sgo1 also modulates the maintenance of SPB in yeast (Macy et al., 2009). At chromosomes, Sgo1 counteracts Plk1 function at centromeres by recruiting PP2A and, hence, protecting cohesin from removal by the prophase pathway. Favoring the model of a prophase-like removal of cohesin from centrosomes, a centrosomal localization of PP2A subunit B56a has previously been reported (Flegg et al., 2010; Sontag et al., 1995). Remarkably, the same subunit has been reported to interact with Sgo1 at centromeres (Kitajima et al., 2006; Riedel et al., 2006; Tang et al., 2006) and, interestingly, to associate with human separase (Holland et al., 2007). According to this, it is tempting to speculate that centrosomal Sgo1 is associated with PP2A and protects cohesin from cleavage by separase at centrosomes, most probably by keeping cohesin dephosphoryled as it is known for the chromosomal Sgo1-PP2A complex (Kitajima et al., 2006). Indeed, evidence in that direction was observed (see below).

4.4. The dual use of cohesin ensures the coordination of two cycles

The data presented herein contribute to a better understanding of how the chromosome cycle is synchronized with the centrosome cycle: Concomitantly to their generation in S phase, sister chromatids are paired by cohesin, which entraps both DNA double strands in its middle (Gruber et al., 2003; Haering et al., 2008; Uhlmann and Nasmyth, 1998). At the same time, the newly arising daughter centriole becomes tightly coupled to its mother centriole. Remarkably, this pairing is again mediated by the cohesin ring, which possibly provides a topological linkage once more. Usage of the same "glue" guarantees its later removal from chromosomes and centrosomes by the same activities.

Together with previously published data, the results presented in this thesis allow to put forward the following model of how the chromosome cycle is coordinated with the centrosome cycle (Fig. 26). Like chromosomal cohesin, centrosomal cohesin may also consist of two discernable populations. While the prophase pathway removes the first population of cohesin, the second is protected by Sgo1 and only destroyed by separase in late mitosis or early G1-phase. The resulting centriole disengagement licenses centrosomes for later duplication and, intriguingly, occurs at a time when DNA replication is licensed as well.
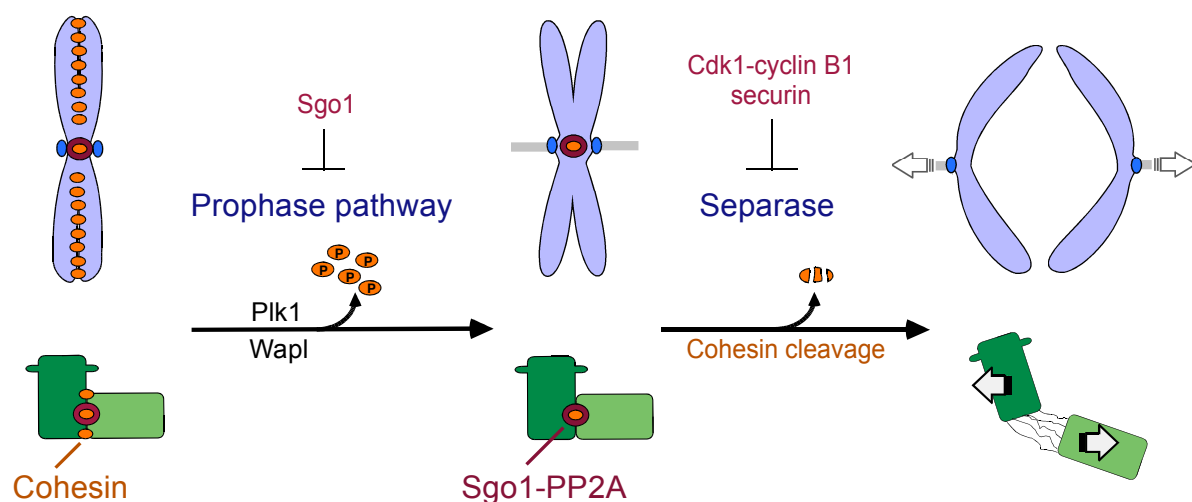
Figure 26. The dual use of cohesin ensures coordination of the chromosome- and the centrosome cycle. The model proposes that centrioles (green), like sister chromatids (light blue), are held together by two pools of cohesin (amber ovals), i.e. a prophase-responsive fraction and one protected by Sgo1 (dark red). Consequently, centriole disengagement and sister chromatid separation occur in a highly similar fashion, with separase removing the remaining cohesin by proteolytic cleavage of Scc1.

4.5. How are the centrosome cycle and the chromosome cycle coordinated?

It is a general principle that replication of DNA is highly controlled and restricted to occur only once per cell cycle. The same is true for centrosomes. Once centrioles have duplicated in S phase, they cannot duplicate again until the next S phase (Wong and Stearns, 2003). It has been reported that, during G1 phase, Cdk2-cyclinE regulates the initiation and progression of both, DNA replication and centrosome duplication (Hinchchliffe et al., 1999; Matsumoto and Maller, 2004; Meraldi et al., 1999; Sluder and Nordberg, 2004). A centrosomal localization signal (CLS) has also been reported for cyclin E, comprising a 20 aa domain necessary not only for its centrosomal localization but also for Mcm5 recruitment to centrosomes (Ferguson and Maller, 2008), arguing in favor of the coupling of DNA replication with centrosome duplication.

However, coupling of both cycles is disturbed in p53 mutant cell lines, which possess a defective G1/S checkpoint and undergo multiple rounds of centrosome duplication when an early S phase arrest is established with drugs like hydroxyurea (HU) or aphidicolin (Cunha-Ferreira et al., 2009; Hermerly et al., 2009). To check whether this effect is not only restricted to p53^{-/-} cells, p53 could be knocked down in Hek 293T cells, which are not transformed by p53 mutation. This should facilitate centriole disengagement followed by over-duplication of centrosomes.

4.5.1. How is cohesin loaded onto centrosomes?

It is tempting to speculate that these parallels between the chromosome- and the centrosome cycle go even further and include similar mechanisms of cohesin loading and establishment. As described in the introductory paragraph, cohesin is recruited to chromosomes via Scc2 and -4 as well as the preRCs at origins of replication. The origin recognition complex (ORC) and the minichromosome maintenance complex (MCM) are two pivotal factors of the preRC (Blow and Dutta, 2005). It is intriguing that they or at least subcomplexes of them localize to centrosomes as well (Ferguson and Maller, 2008; Ferguson et al., 2010; Prasanth et al., 2004; Stuermer et al., 2007). Orc1-5 were found at centrosomes while Orc1 and -2 are required to regulate centrosome duplication (Prasanth et al., 2004; Hemerly et al., 2009). Moreover, Mcm2-7 were found to localize to centrosomes, while Mcm2 and -5 were shown to control centriole number (reviewed by Knockleby and Lee, 2010). Interestingly,

overexpression of Orc1 or Mcm5 prevents overduplication of centrosomes in p53$^{-/-}$ cells arrested in S phase (Ferguson and Maller, 2008; Hermerly et al., 2009). At a molecular level this observation might be explained by an ORC- and MCM-dependent hyper-recruitment of cohesin to centrosomes, which would counteract the unscheduled disengagement of centrioles. Assuming that the same loading cascade is operative at centrosomes, then the centriole disengagement phenotype caused by loss of ORC or MCM function might explain the failure of proper cohesin recruitment to centrosomes.

The hypothesis, that cohesin is recruited via preRCs and Scc2/4 to centrosomes, brings up numerous predictions which can be addressed, for example, in *Xenopus* egg extracts. Centrosome duplication, i.e the outgrowth of new centrioles on pre-existing ones, can be easily studied when these extracts are released from metaphase into interphase (Tsou and Stearns, 2006). To this end, the immunodepletion of cohesin from these extracts has to be established first. Following addition of sperm nuclei, which harbor one centrosome that serves as a template for centriole assembly, it will be checked whether newly forming centrioles fail to engage with the pre-existing ones when centrosomes are duplicated in cohesin-less oocyte extract. This can be assessed on the one hand by measuring the distance of the two centrosomal centrin 2 signals by IF microscopy. One the other hand a specific *Xenopus* C-Nap1 antibody in combination with centrin 2 antibody will clarify this issue by measuring the C-Nap1:centrin 2 ratio. If the distance between centrioles is indeed increased in the cohesin-free sample relative to the mock-depleted control then peptide antibodies against Orc1, Mcm5 and Scc2/4 will be raised and tested for the requirement of the corresponding antigens for the establishment of centriole disengagement in analogous immunodepletion experiments.

There are several indications from the literature that the same factors that license or inhibit DNA replication regulate the duplication of centrioles. One such factor is geminin, which is known to prevent DNA re-duplication by blocking Cdt1-MCM interaction (Ballabeni et al., 2004; Tada et al., 2001; Wohlschlegel et al., 2000). Indeed, geminin is found to localize at centrosomes in all cell cycle phases except G1 (Lu et al., 2009). Kockdown of geminin results in centrosome over-duplication whereas its overexpression blocks centrosome over-duplication in p53 mutant cells arrested in S phase (Tachibana et al., 2005). This effect seems counterintuitive since

the same phenotypes that were described for overexpression and knockdown of geminin were observed for the knockdown and overexpression of MCM and ORC, respectively. However, is has been shown that geminin also has a positive role in stabilizing Cdt1 (Narasimhachar and Coue, 2009). Nevertheless, the functions of ORC, MCM and geminin in regulating centrosome duplication seem to be different from these in controlling DNA replication and, thus, need to be addressed in the future.

4.5.2. What is held together by centrosomal cohesin?

How does cohesin keep centrioles engaged? Due to limiting dimensions, it is physically impossible that one cohesin ring with 50 nm in diameter embraces two centrioles with a size of about 400 x 250 nm each. Cohesin may rather turn the PCM into a rigid gel or crosslink proteins within the PCM, thereby keeping centrioles tightly paired in an indirect manner. The field now largely agrees that DNA is no constituent of centrosomes, but there are indications from the literature that RNA is associated with centrosomes from *Spisula* oocytes (Alliegro et al., 2006) raising the question whether RNA is also present at centrosomes of vertebrates where cohesin can form rings.

Quite recently, Matsuo and co-workers identified kendrin as a novel substrate of separase at centrosomes where it is thought to keep centrioles engaged (Matsuo et al., 2012). Since kendrin is a giant coiled-coil protein and located in the PCM, it is conceivable that separase has to cleave two substrates to allow centriole disengagement. Cohesin might crosslink kendrin, thereby protecting premature centriole disengagemant. However, the contribution of those two substrates in centriole engagement has to be assessed and raises new thrilling issues: How do kendrin and cohesin interact? Does the artificial cleavage of both proteins have additive effects in the disengagement process? To address the latter, transgenic cell lines have to be created that inducibly express TEV cleavable kendrin in combination with HRV cleavable Scc1. Ectopic cleavage by either one or both site-specific proteases will shed more light on this issue.

Besides kendrin, it is conceivable that cohesin has further centrosomal interaction partners. To address this thrilling quest one could perform cohesin immunoprecipitation (IP) experiments in *Xenopus* cell-free extracts on the one hand. These extracts lack centrosomes but intriguingly one single *Xenopus* egg innately

harbors a myriad of centrosomal proteins sufficient to assemble about 2000 centrosomes (Gard et al., 1990). Eventually, any protein that specifically interacts with cohesin will be identified by mass spectrometry (MS) and further characterized. On the other hand, the quest for a centrosomal substrate of cohesin can be mastered by a further unbiased biochemical approach. The interaction of thousands of proteins within the centrosome seems incompatible with the specific co-purification of just one or a few proteins with cohesin under native conditions. To this end, stable cell lines that inducibly express His-tagged Scc1 or Smc3 need to be generated. Centrosomes from these cells have to be crosslinked with DTSSP (3,3´-Dithiobis [sulfosuccinimidylpropionate]), a bifunctional, amine-reactive agent, whose central disulfide bond can be readily cleaved with reducing agents (Lambert et al., 2011). Crosslinking is necessary due to the transient interaction of thousands of proteins within the centrosome making an ordinary IP too unspecific. Then, centrosomes need to be disassembled in non-reducing buffer containing 6 M guanidine hydrochloride and His-tagged cohesin subunits have to be purified by affinity chromatography under denaturing conditions. After reversion of the DTSSP-mediated crosslinks by reduction, samples will be resolved by SDS-PAGE and subsequent MS will identify proteins that are specifically associated with Scc1 and/or Smc3. The ultimate goal then is to test by IF-microscopy whether siRNA-mediated depletion of putative cohesin substrates results in premature disengagement of centrioles.

4.6. An alternatively spliced exon reprograms Sgo1 to protect centrosomal instead of centromeric cohesin

Sister chromatid separation is a crucial step of the chromosome cycle and achieved by sequential removal of cohesin, first from chromosome arms by the prophase pathway and then from the centromere by separase-dependent cleavage in anaphase (Waizenegger et al., 2000). During prophase, centromeric cohesion of sister chromatids is protected by the evolutionarily conserved protein shugoshin (Sgo), which recruits PP2A, thereby counteracting phosphorylation of cohesin (Kitajima et al., 2004; McGuinness et al., 2005; Riedel et al., 2006; Tang et al., 2006). In mammals, Sgo1 and Sgo2 shield centromeric cohesin during early mitosis and meiosis I, respectively (Lee et al., 2008; McGuinness et al., 2005; Tang et al., 2004). However, in humans alternative splicing gives rise to several isoforms of human

Sgo1 (McGuinness et al., 2005; Wang et al., 2006). The two most prominent isoforms are the longer Sgo-A1 and the smaller Sgo1-C2. Depletion of all of them by RNAi results not only in premature sister chromatid separation but also in precocious centriole disengagement (Fig. 19). Thus, centromeric and centrosomal cohesin complexes might be protected by different Sgo1 variants. Wang and colleagues (2008) provided further insights into the molecular mechanism of Sgo1 regulation and demonstrated that both isoforms exhibit an entirely different subcellular localization pattern and vary in their function (Wang et al., 2006; Wang et al., 2008). While they hypothesized that this is due to the presence or absence of the relatively large peptide encoded by exon 6, the data presented herein elucidated that, in fact, the tiny exon 9 encoded peptide is the crucial factor that designates Sgo1´s localization and function.

During this work, several Sgo1 variants, mainly characterized by the presence or absence of exon 6 or exon 9, were investigated in terms of their subcellular localization and their ability to prevent precocious sister chromatid separation and centriole disengagement when all endogenous isoforms of Sgo1 were depleted by siRNA. Rescue experiments with stable transgenic cell lines demonstrated that all exon9-containing Sgo1 variants exclusively localized at centrosomes where they function in shielding centrosomal cohesin. Yet, chromosomal cohesin was only protected by exon 9-less Sgo1 isoforms. Remarkably, expression of the relevant peptide in fusion with Sgo2 artificially directed Sgo2 to centrosomes where it suppressed the premature centriole disengagement caused by Sgo1 depletion. To exclude that Sgo2 protects centrosomal cohesin *per se*, analogous control experiments need to be done with stable transgenic cell lines expressing WT-Sgo2. However, it could be shown that WT-Sgo2 does not localize to centrosomes when transiently overexpressed in Hek 293T cells (Karalus, 2012). Moreover, endogenous Sgo2 is not able to rescue centriole disengagement, which argues in favor of the small C-terminal peptide acting as a centrosomal localization signal. Accordingly, the fusion of the relevant peptide with eGFP or Myc also directed both proteins to centrosomes, yet only the Sgo2-based chimera was able to now protect centriole engagement. It is most likely that Sgo2 in fusion with exon 9 can protect centrosomal cohesin and not GFP fused to exon 9 because the former and not the latter can recruit PP2A. To unambiguously address this question, depletion-rescue experiments

have to be conducted with transgenic cells expressing a PP2A binding deficient Sgo2 fused to the peptide encoded by exon 9.

In summary, all these findings demonstrate that 1) the centrosomal localization signal of Sgo1 is transferable, and 2) targeting *per se* is necessary but not sufficient for protection of centrosomal cohesin.

Alternative splicing patterns are highly divergent in various organisms. Therefore sequences related to human exon 9 have so far only been found in primates like orangutans, gibbons and rhesus macaques. However, the strongest argument substantiating the role of exon 9 as a crucial factor of Sgo1´s localization and function are the findings that mutation of just three consecutive amino acids within the corresponding peptide inactivated both the pro-centrosomal as well as the anti-centromeric targeting effect (Fig. 23c). Importantly, the data presented herein show that localization closely correlated with function as revealed by depletion-rescue experiments with stable transgenic cell lines. While Sgo1 mutated in the exon 9 coding peptide was not able to protect centrosomal cohesin anymore, it instead shielded chromosomal cohesin (Fig. 23d). Thus, Sgo1 function seems to be determined by its exon 9-dependent localization. Taken together, these data provide the strongest evidence yet for a crucial role of the small peptide encoded by exon 9 in Sgo1´s localization and function.

4.6.1. What is the operating principle of the small peptide encoded by exon 9

What is the mechanism that inhibits Sgo1´s centromeric targeting? With regard to bioinformatical research, potential nuclear localization signals (NLS) have been predicted in Sgo1 (cNLS Mapper, Kosugi et al., 2009). On the one hand, a putative NLS has been presumed in the large peptide of exon 6, (present in Sgo1-A1 and -A2) and on the other hand, in the basic motif of the Sgo C-Box (present in all Sgo isoforms). It has been proposed that the conserved Sgo C-Box at the C-terminus of Sgo1 and -2 is required for proper centromeric localization mediated through binding to Bub1 phosphorylated histone 2A (H2A) (Kawashima et al., 2010). Sgo1´s centromeric localization is abrogated completely when a single but highly conserved lysine residue within the Sgo C-Box (K491I mutation in humans or K298I in *S. pombe*) is mutated (Kawashima et al., 2010). Therefore, the small C-terminal peptide of exon 9 needs to fulfill two main functions. First, it is obliged to suppress the

recruitment to centromeres in a dominant negative manner and, second, it must serve as a centrosomal localization signal.

How could the small peptide encoded by exon 9 prevent centromeric targeting through the Sgo-C-Box? There are three possibilities that come to mind. First, the corresponding peptide might mask a putative NLS in the C-Box of Sgo1, thereby indirectly inhibiting Sgo1´s centromeric localization by preventing its entry into the nucleus. This indirect mechanism would only work when there is no nuclear envelope, thus, Sgo1 would gain access to the chromosomes during mitosis. Therefore, a second possibility could be that the small peptide represents a nuclear export signal (NES) that targets Sgo1 for export from the cell nucleus to the cytoplasm. The facts that the Sgo C-Box is the only sequence stretch reasonably conserved between Sgo1 and Sgo2, and that the fusion of exon 9 to Sgo2 abrogates the centromeric localization of Sgo2 raises the third and most conceivable option that the small peptide might sterically block the C-Box of Sgo1 from recruitment to centromeres. Consistently, transient overexpression of Sgo1-C2 does not interfere with the localization of endogenous Sgo1 to centromeres (B. Mayer, personal communication) leading to the suggestion that the C-terminal peptide of exon 9 probably acts *in cis* and that no heterodimers of different Sgo1 variants are formed. The hypothesis that exon 9 actively suppresses heterodimerization can be ascertained by differentially tagged Sgo1 in co-IP experiments.

Taken together, it is assumed that the exon 9 coding peptide operates in an intramolecular fashion in sterically blocking the C-Box of Sgo1, which is depicted in the model below (Fig. 27). It is also supposable that exon 9 acts as a molecular mimicry and competes with phosphorylated H2A for binding to the Sgo1-C-Box, thereby inhibiting centromeric localization. If this is true, then a phospho-site mutant will locate to centromeres. Consistent with this model is the assumption that the exon 9 coding peptide recruits a hitherto unknown factor, which would then mask the Sgo C-box. However, no interaction partners were found with co-IP experiments after incubation of bacterially expressed MBP-exon 9 in human cell lysates (B. Mayer, personal communication). Therefore, a possible interaction might arise from a more complex structure composed of the small C-terminal peptide and elements of the 'core Sgo1'. To further clarify whether the small C-terminal peptide of Sgo1 blocks the Sgo C-Box by an intramolecular interaction, its putative interplay with 'core Sgo1' fragments has to be assessed by yeast-2-hybrid (Y2H) and Far Western analyses.

Concerning the Y2H assay, putative interactions of the tiny peptide with the Sgo C-Box or full length Sgo1 were investigated (D. Karalus, Master thesis). Several combinations were tested, though a possible interaction between full-length Sgo1 and the small peptide of exon 9 was visible. However, the results obtained from the Y2H assay have to be confirmed.

Centromeric localization of both, Sgo1 and Sgo2 during early mitosis significantly depends on the mitotic kinase Bub1 (Huang et al., 2007; Kitajima et al., 2005; Tang et al., 2004). Depletion of Bub1 results in hyper-cohesion along chromosome arms while centromeric cohesion is lost (Kitajima et al., 2005; Tang et al., 2004). Based on these data, another possibility could be that Sgo1 is recruited to chromosomes through other crucial factors before later confining to centromeres. Interestingly, centrosomal Sgo1 isoforms are not only absent from centromeres but also excluded from the whole mitotic chromatin (Fig. 21). A possible scenario could be generally that Sgo1´s intramolecular folding, which is mediated by the peptide encoded by exon 9, blocks a putative site needed for primary targeting to chromosomes. The insertion of a triple mutation in the conserved residues in the small C-terminal peptide of Sgo1-A2 might prevent folding, thereby allowing targeting to the chromatin and subsequent centromeric localization (Fig. 23). Furthermore, posttranslational modifications such as phosphorylation of the C-terminus might favour an accurate intramolecular folding. Kinase-specific phosphorylation sites have been predicted in front of the Sgo C-Box. A mutation of these serine residues to alanine followed by transient expression in Hek 293T cells and IF-microscopy might elucidate this matter. A phosphorylation-site mutant will localize to centromeres if this hypothesis is correct.

4.6.2. What is the mechanism of targeting Sgo1 to centrosomes?

Besides inhibiting Sgo1´s centromeric localization, the exon 9 coding peptide plays a crucial role in centrosome targeting and serves as centrosomal localization signal (CLS) of Sgo1. Several CLS are known, which seem to be conserved in closely related proteins like cyclins (Ferguson and Maller, 2008; Matsumoto and Maller 2004; Pascreau et al., 2010) or Polo-like kinases (Jiang et al., 2006). Accordingly, CLS´s have been reported in cyclin E (Matsumoto and Maller 2004), cyclin A2 (Pascreau et al., 2010), and BRCA2 (Nakanishi et al., 2007). Experiments within this work demonstrated that the CLS of Sgo1 is transferable (Fig. 21b). Yet, ClustalW protein sequence alignment revealed no similar targeting element in the C-terminal part of

centrosomal Sgo1. The tiny peptide also lacks a PACT domain, a conserved centrosomal targeting motif required for recruiting pericentrin and AKAP450 to centrosomes (Gillingham and Munro, 2000). Interestingly, no motifs related to a CLS have been found in the C-terminal part of centrosomal Sgo1, suggesting that a novel CLS is located in exon 9. Many proteins are recruited to centrosomes by the action of the dynein-dynactin complex (Quintyne and Schroer, 2002). Whether Sgo1´s are recruited to centrosomes by the same complex remains a question to be answered in future.

As mentioned before, the peptide encoded by exon 9 probably harbors an internal NES as the region selected for mutation contains several hydrophobic amino acids. Therefore, the switch of a centrosomal to a centromeric localization of Sgo1-A2^{AAA} caused by this triple mutation could be due to the destruction of a putative NES. A typical NES motif consists of hydrophobic amino acids like leucine or isoleucine arranged in a special pattern. According to Güttler et al. (2010), a classical NES is leucine-rich and possesses a typical consensus pattern of ϕ x_{2-3} ϕ x_{2-3} ϕ x ϕ (ϕ = L, I, V, F, M; x = any aa). The mutated region of the conserved ILY motif in Sgo1-A2^{AAA} seems to fulfill the above criteria, yet none of the described NES patterns could be reconciled with the small C-terminal peptide. Also bioinformatical analyses with NES prediction programs brought no clear evidence for a supposable NES pattern. Nevertheless, these programs, even when experimentally determined, cannot predict all NES. In general, the NES mediates binding to the major nuclear export receptor, CRM1 (chromosome region maintenance protein 1)/exportin-1, and facilitates the nuclear-cytoplasmic shuttling of proteins. CRM-1 mediated export can be prevented by treatment with fungicide leptomycin B (LMB). By covalently binding to a cysteine residue of CRM1, LMB specifically inhibits CRM1 function (Kudo et al., 1999). Interestingly, Forgues et al. (2003) observed that CRM1 localizes to centrosomes and that CRM1 inhibition by LMB or CRM1 sequestration by a hepatitis B viral protein (HBx) contributes to the formation of multiple centrosomes. It was also found that several centrosomal proteins such as pericentrin, γ-tubulin or BRCA1 are shuttled to centrosomes by CRM1 independent of the nuclear export pathway (Brodie and Henderson, 2012; Liu et al., 2009). If the various centrosomal Sgo1 isoforms harbor a putative NES motif, which is recognized by CRM1, then ectopic expression of fluorophore-labeled Sgo1-A2 or -C2 will result in an accumulation of Sgo1 in the nucleus in response to treatment with LMB. Moreover, CRM1 overexpression or

depletion would shed more light on the question whether CRM1 plays a role in recruiting Sgo1 proteins from the nucleus to the cytoplasm and then to the centrosome, respectively.
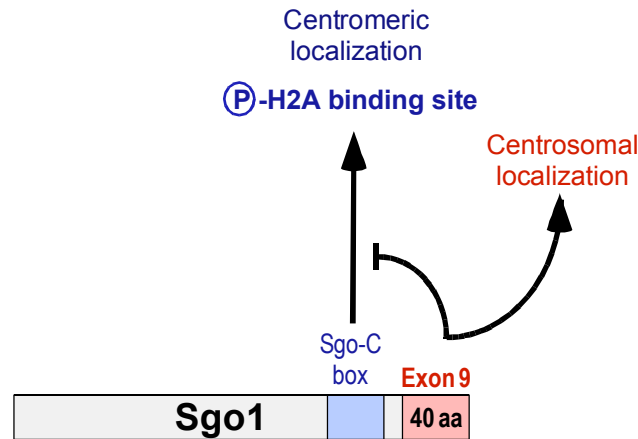
Figure 27. An alternatively spliced bifunctional localization signal specifies the mutually exclusive targeting of Sgo1 isoforms to centromeres *versus* centrosomes. The presence or absence of the exon 9 encoded 40 amino acids at the C-terminus of human Sgo1 determines whether it functions in protection of centromeric or centrosomal cohesin, respectively. This model proposes that the tiny peptide operates in an intramolecular fashion by sterically blocking the C-Box of Sgo1 and, thereby, inhibiting centromeric localization.

4.6.3. Future experiments concerning centrosomal Sgo1

The most revealing insights about the operating principle of this bifunctional localization signal could probably be elucidated by structural analysis. A protein structure could clarify whether the tiny peptide acts in an intramolecular fashion. Until now, nothing is known about the C-terminal structure of Sgo1-A2 and -C2. However, the crystal structure of a small Sgo1-(51-96) peptide in complex with the PP2A holoenzyme has been solved (Xu et al., 2009).

To gain information about folding or intramolecular binding, the bacterial expression of soluble 'core Sgo1' fragments and the C-terminal peptide composed of exon 9 is, however, a prerequisite. The finding that C-terminal Sgo1 fragments including the peptide of exon 9 only, seem to be rather insoluble when expressed in *E. coli* makes this important step even more challenging in the future (Karalus, 2012). In general purification of proteins from inclusion bodies under denaturing conditions is possible but entails improper folding. Therefore, expression of C-terminal Sgo1´s might be improved by using a eukaryotic expression system.

Based on the above findings, it is conceivable that an expression imbalance between the differently specialized Sgo1 isoforms could interfere with the crucial synchrony between the chromosome- and the centrosome cycles. There are several indications from the literature that Sgo1 is up- or down-regulated in certain cancer tissues (Iwaizumi et al., 2009; Scanlan et al., 2001; Yamada et al., 2012). However, none of the studies distinguished between the different Sgo1 isoforms, thus, differences in the expression level of Sgo1 could be due to the varying expression of the different isoforms. The equilibration among the different Sgo1 isoforms could be shifted between normal and cancer tissue. A possible imbalance between the differently specialized Sgo1 isoforms could be tested with a molecular approach using real time PCR and commercially available cDNA of cancer tissue samples.

Together, the above findings facilitate the study of effects of premature centriole disengagement in the absence of simultaneous loss of sister chromatid cohesion. Differently spliced isoforms of one gene regulate two different cellular processes. The crucial role is dedicated to the small peptide encoded by exon 9, as it blocks centromeric targeting and supports centrosomal localization. Thus, an alternatively spliced bifunctional localization signal reprograms Sgo1 to protect centrosomal instead of centromeric cohesin. However, the molecular mechanism of its operating principle is unclear and remains a thrilling quest for further investigations.

5. MATERIAL AND METHODS

5.1. Materials

5.1.1. Hard- and Software

This work was written on an "Apple MacBook2.1" (Apple Inc., Cupertino, CA, USA) using "Microsoft® Word 2008" (Microsoft Corporation, Redmond, WA, USA). "Microsoft® Excel 2008" (Microsoft Corporation, Redmond, WA, USA) and "Open Office" were used for generation of diagrams. Chemiluminescence signals of Western blots as well as Coomassie stained gels were digitized using an "LAS-4000" system (Fuji Film Europe, Düsseldorf). Autoradiographies were digitized using an "FLA-7000" phosphorimager (Fuji Film Europe, Düsseldorf). The image analysis software MultiGauge (Fuji Film Europe, Düsseldorf) was used to visualize chemiluminescence signals from immunoblots and digitized autoradiographies. Image processing was performed with "Adobe Photoshop CS4" (Adobe Systems Inc., San Jose, CA, USA). Generation of figures was done using "CANVAS 9.0.4" (ACD Systems International Inc., Victoria, B.C., Canada), "Adobe Ilustrator CS4" (Adobe Systems Inc., San Jose, CA, USA) and "Microsoft PowerPoint 2008" (Microsoft Corporation, Redmond, WA, USA). "DNASTAR Lasergene" (GATC Biotech, Konstanz) was used for analysis of DNA and protein sequences. Literature and database searches were done with electronic online services provided by the "National Center for Biotechnology Information" (http://www.ncbi.nlm.nih.gov/). A service of the European Bioinformatics Institute was used for sequence alignments ("EMBOSS Pairwise alignment" algorithm, http://www.ebi.ac.uk).

5.1.2. Protocols

The methods described in this section are based on standard techniques (Sambrook, 1989; Sambrook and Russell, 2001) or follow the manufacturer's instructions. When protocols have been modified, detailed information is provided. For all methods, de-ionized sterile water and – when appropriate – sterile solutions and sterile flasks were used.

5.1.3. Chemicals and reagents

Unless otherwise noticed, chemicals and reagents (pro analysis grade) were purchased from AppliChem (Darmstadt), Biomol (Hamburg), Biorad (Munich), Fermentas (St. Leon-Rot), GE Healthcare (Munich), Invitrogen (via Fisher Scientific, Schwerte), Merck/Calbiochem (Darmstadt), Millipore (Schwalbach), New England Biolabs (NEB, Frankfurt a. M.), Pierce/Fisher Scientific (Schwerte), Promega (Mannheim), Roche Diagnostics (Mannheim), Roth (Karlsruhe), Serva (Heidelberg), and Sigma-Aldrich (Steinheim).

5.1.4. Antibodies

Primary Antibody	Application	Source
Mouse anti-α-tubulin	WB	DSHB, clone 12G10
Mouse anti-γ-tubulin	IF, WB	Sigma Aldrich T6557
Mouse anti-phospho-Ser10HistonH3	WB	Sigma Aldrich
Mouse anti-Myc-tag	WB	DSHB, clone 9E10
Mouse anti-Myc-tag	IF, WB	4A6, Upstate
Mouse anti-DNA-Topoisomerase IIa	WB	KAM-CC210, Stressgen
Mouse anti-Hec1	IF	Genetex, Irvine, CA, USA
Mouse anti-GFP	WB	Kind gift of D. van Essen & S. Saccani
Rabbit anti-Smc3	WB	Bethyl
Rabbit anti-Scc1	WB	Stemmann et al. (2001)
Rabbit anti-Smc1	IF, EM, WB	A300-055A, Bethyl
Rabbit anti-Sgo1	IF, WB	Abcam
Rabbit anti-GFP	IP	S. Heidmann (University of Bayreuth)
Rabbit anti-centrin 2	IF	This work (Coring System Diagnostix)
Guinea pig anti-C-Nap1	IF	This work (Charles River Laboratories)

Secondary Antibody	Application	Source
Alexa Fluor 488 goat anti-mouse IgG	IF	Invitrogen
Alexa Fluor 546 goat anti-mouse IgG	IF	Invitrogen
Alexa Fluor 488 goat anti-rabbit IgG	IF	Invitrogen
Alexa Fluor 546 goat anti-rabbit IgG	IF	Invitrogen
Cy3 donkey anti-guinea pig IgG	IF	Jackson Immunoresearch Laboratories
6 nm colloidal Gold goat anti-rabbit IgG (H+L)	EM	Jackson Immunoresearch Laboratories
HRP-conjugated anti-rabbit IgG	WB	Sigma Aldrich
HRP-conjugated anti-rabbit IgG	WB	Sigma Aldrich

WB: Western blot; IF: Immunofluorescence; EM: Electron microscopy

5.1.5. Plasmids

Vector	Origin
pCS2	Turner & Weintraub (1994), MCS modified (FseI/AscI sites inserted)
pcDNA5-FRT-TO	Invitrogen/Fisher Scientific, Schwerte
pRTS-1	Bornkamm, G. W. et al., 2005
pET28a	Novagen, with modified MCS (FseI/AscI sites inserted)

Plasmid	Backbone	Tag	Insert
Scc1			
pOS161	pCS2	-	$hScc1^{WT}$
pOS163	pCS2	-	$hScc1^{NC\ (R172,\ 450A)}$
pLG1966	pCS2	-eGFP-C	$hScc1^{WT}$
pLG1967	pCS2	-eGFP-C	$hScc1^{HRV/WT}$
pLG2208	pCS2	-eGFP-C	$hScc1^{NC}$
pLG2303	pRTS-1	-eGFP-	$hScc1^{WT}$
pLG2305	pRTS-1	-eGFP-	$hScc1^{HRV/WT}$
Smc3			
pLG2294	pCS2	-eGFP-C	$hSmc3^{WT}$
pLG2300	pCS2	-eGFP-C	$hSmc3^{3xTEV}$
Separase			
pOS22	pCS2	$N-ZZ-TEV_4-$	$hSep^{WT}$
pOS41	pCS2	$N-ZZ-TEV_4-$	$hSep^{PD\ (C2029S)}$
pOS337	pCS2	$N-ZZ-TEV_4-$	$hSep^{PM\ (S1126A,\ T1346A,\ \Delta L1391-E1402)}$
pOS338	pCS2	$N-ZZ-TEV_4-$	$hSep^{PM+PD\ (S1126A,\ T1346A,\ C2029S,\ \Delta L1391-E1402)}$
Securin			
pSX100	pCS2	-	$hSecurin^{WT}$
pOS237	pCS2	$-His_6-Flag-His_6-Flag-C$	$hSecurin^{WT}$
pFB1955	pCS2	$-His_6-Flag-His_6-Flag-C$	$hSecurin^{\Delta 92}$
Shugoshin			
pBM2644	pcDNA5-FRT-TO	$N-Myc_6-$	hSgo1-A1
pBM2645	pcDNA5-FRT-TO	$N-Myc_6-$	hSgo1-A2
pBM2646	pcDNA5-FRT-TO	$N-Myc_6-$	hSgo1-C2
pBM2647	pcDNA5-FRT-TO	$N-Myc_6-$	$hSgo1-A1^{N61I}$
pBM2648	pcDNA5-FRT-TO	$N-Myc_6-$	$hSgo1-A2^{N61I}$
pBM2649	pcDNA5-FRT-TO	$N-Myc_6-$	$hSgo1-C2^{N61I}$
pBM2766	pcDNA5-FRT-TO	$N-Myc_6-$	Exon 9 of hSgo1-A2
pBM2767	pcDNA5-FRT-TO	N-GFP-	Exon 9 of hSgo1-A2
others			
pLG2255	pCS2	-	HRV protease
pLG2256	pCS2	-	TEV protease

| pLG2574 | pCS2 | N-His$_6$-Sumo1- | hCentrin 2 |
| pLG2755 | pcDNA5-FRT-TO | N-Myc$_6$- | Exon 9 of hSgo1-A2 fused to hSgo2^{WT} |

Source: pLG – this study; others – Stemmann laboratory plasmid collection

PD: Protease-dead (C2029S)
PM: Phospo-site mutant (S1126A, T1346A, ΔL1391-E1402)
N61I: PP2A-binding resistant

5.1.6. DNA oligonucleotides

Primer	Sequence
MO_hSmc3_5´F	5´-aatggccggcccATGTACATAAAGCAGGTGATTAT-3´
MO_hSmc3_3´A	5´-ttggcgcgcCCATGTGTGGTATCATCTTCTACAA-3´
hSmc3 K245 Tev3_a	5´-ACAGGTTCTCCTTAGCAGAAAGCTCATCAAGTTTG-3´
hSmc3 R246 Tev3_a	5´-CTTCCAGGGCCGAGAGACTAGTGGAGAAAAATCCA-3´
hSmc3 E955 Tev3_a	5´-AGTACAAGTTTTCAAATGCTTCCTGGGGAAGTGAT-3´
hSmc3 K956 Tev3_a	5´-CTTCCAATCTAAGTACCAGACACTGAGCCTCAAAC-3´
hSmc3K245Tev3_b_neu	5´-CACTCTGGAAGTATAAGTTTTCCGTCCCTTGGAAATACAGGTTCTCCTT AGCAGAAAGCT-3´
hSmc3R246Tev3_b_neu	5´-AGGGACGGAAAACTTATACTTCCAGAGTGAGAATCTCTACTTCCAGGGCCGAGAGACTAGT-3´
hSmc3E955Tev3_b_neu	5´-TTCAGTGCCTTGGAAATACAAGTTCTCGCTCTGAAAGTACAAGTTTTCAAATGCTTCCT-3´
hSmc3K956Tev3_b_neu	5´-GCGAGAACTTGTATTTCCAAGGCACTGAAAATCTCTACTTCCAATCTAAGTACCAGACA-3´
hSmc3.seq3	5´-GCTATCATGGTATTGTAATGAATAAC-3´
hSmc3.seq4	5´-CGTTCTTCTTTCTCTTTCACACTGT-3´

5.1.7. Target sequence for dsRNA oligonucleotides

Target mRNA	siRNA seququence	Source
Luciferase (GL2)	5´-CGUACGCGGAAUACUUCGA-3´	Elbashir et al., 2001
hScc1 (3´UTR I)	5´-ACUCAGACUUCAGUGUAUA-3´	Stemmann Laboratory
hScc1 (3´UTR II)	5´-AGGACAGACUGAUGGGAAA-3´	Stemmann Laboratory
hSmc3 (3´UTR I)	5´-UGGGAGAUGUAUAUAGUAA-3´	Stemmann Laboratory
hSmc3 (3´UTR II)	5´-UGUCAUGUUUGUACUGAUA-3´	Stemmann Laboratory
hSgo1	5´-CAGUAGAACCUGCUAGAA-3´	McGuinness et al., 2005
hSgo1 (5´UTR)	5´-GAAGAUAGCUGUUGCAGAA-3´	Stemmann Laboratory
Wapl (I)	5´-CGGACUACCCUUAGCACAA-3´	Kueng et al., 2006
Wapl (II)	5´-GGUUAAGUGUUCCUCUUAU-3´	Kueng et al., 2006

5.2. Microbiological techniques

5.2.1. *E. coli* strains and media

If not indicated otherwise, percentages in buffer recipes are given as v/v.

Strain	Description and origin
XL1-Blue	*E. coli sup*E44, *hsd*R17, *rec*A1, *end*A1, *gyr*A46, *thi*, *rel*A1, *lac*⁻ [F' *pro* AB *lac*I^q, *Lac* ZdM15, Tn10 (*Tet^r*)] (Stratagene/AgilentvTechnologies, Santa Clara, CA, USA)
Rosetta DE3	*E. coli F*⁻, *ompT, hsdSB (rB*⁻ *mB*⁻), gal, dcm, λ) (*DE3* [*lacI, lacUV5-T7 gene 1, ind1, sam7, nin5*]) *Cam^R* (Novagen/Merck)

LB medium:	1% (w/v) Trypton (Difco)
	0,5% (w/v) Yeast extract (Difco)
	1% (w/v) NaCl
	Sterilized by autoclaving

LB agar:	LB medium with 1.5% agar

5.2.2. Cultivation and storage of *E. coli*

E. coli strains were grown in LB medium by shaking at 140-200 rpm at 37°C, LB agar plates were incubated at 37°C. For antibiotic selection, ampicillin and chloramphenicol were added to the media to a final concentration of 100 µg/ml and 34 µg/ml, respectively. Culture densities were determined by measuring the absorbance at a wavelength of 600 nm (OD_{600}). Liquid cultures were supplemented with sterile glycerol to 20% final concentration and subsequently snap frozen in liquid nitrogen for long-term storage at -80°C.

5.2.3. Transformation of plasmid DNA into chemically competent *E. coli*

Competent *E. coli* cells were thawed on ice. For the expression of recombinant proteins, 30 µl of Rosetta DE3 cells were mixed with 100 ng of plasmid DNA. For the production of high amounts of plasmid DNA, 40 µl XL-1 Blue were mixed with 500 ng plasmid DNA or 10 µl ligation reaction and incubated for 30 min on ice. Then, a 42°C heat shock was performed for 45 sec followed by 2 min incubation on ice. For recovery, 300-400 µl LB medium without antibiotics was added and cells were incubated for 15-45 min at 37°C. The XL-1 Blue suspension was directly inoculated into 250 ml LB medium containing ampicillin (100 µg/ml) after recovery and incubated

at 140 rpm at 37°C whereas transformed Rosetta DE3 cells were selected on LB agar plates containing the respective antibiotic(s) and incubated overnight at 37°C.

5.2.4. Expression of proteins in *E. coli*

Rosetta DE3 cells were used for expression of recombinant proteins from pET28a expression plasmids, exclusively. A recent transformed colony was picked from a well grown plate in order to inoculate a preculture containing 15 ml LB Medium supplemented with 0.2% glucose, 100 μg/ml ampicillin and 34 μg/ml chloramphenicol. After 1h of incubation, the preculture was inoculated to the main culture (500 ml LB medium with the same supplements) and grown at 200 rpm at 37°C. At a cell density of OD_{600} = 0.6-0.8, the protein expression was induced by addition of IPTG (1 mM final concentration). After shaking for another 3 h at 37°C, cells were harvested by centrifugation (4°C, 6,000 g, 10 min) and pellets were stored at -80°C after snap freezing in liquid nitrogen.

5.3. Molecular biological methods

5.3.1. Isolation of plasmid DNA from *E. coli*

A single *E. coli* colony harbouring the plasmid DNA of interest was cultivated for 8-14 h, 140 rpm, at 37°C in 4 ml LB medium containing the appropriate antibiotic. Plasmid DNA was purified via alkaline lysis of the bacteria and subsequent isolation by anion exchange columns according to the manufacturer's instructions (QIAGEN Plasmid Purification Handbook, Plasmid Mini Preparation for up to 20 µg DNA). For the transfection of human cells, larger amounts of plasmid DNA were purified from a 250-500 ml overnight culture according to the manufacturer's protocol (QIAGEN Plasmid Purification Handbook, Plasmid Maxi Preparation for up to 800 µg DNA).

5.3.2. Determination of DNA/RNA concentration

After purification of plasmid DNA or RNA, the DNA or RNA concentration was determined by measuring the absorbance at a wavelength of 260 nm with a ND-1000 Spectrophotometer (Peqlab, Erlangen). An OD_{260} = 1 equals a concentration of 50 µg/ml double-stranded DNA or 40 µg/ml single-stranded RNA.

5.3.3. Restriction digestion of DNA

Sequence-specific cleavage of DNA with restriction enzymes was performed according to standard protocols (Sambrook and Russel, 2001) and the instructions of the manufacturer (New England Biolabs, NEB). In general, 5-10 units of restriction enzyme were used for digestion of 1.5 µg DNA. The reaction samples were incubated in appropriate buffer at the recommended temperature for 1-2 h. The restriction digestion was stopped by heat inactivation (15 min/75°C) of the enzyme or by addition of DNA loading buffer.

5.3.4. Dephosphorylation of DNA fragments

For the avoidance of recirculation of linearized vectors, the 5' end of the vector DNA was dephosphorylated by addition of 0.1 units of <u>s</u>hrimp <u>a</u>lkaline <u>p</u>hosphatase (SAP) in the appropriate buffer (Roche, Mannheim). After incubation for 30 min at 37°C, the shrimp alkaline phosphatase was heat-inactivated for 15 min at 75°C.

5.3.5. Separation of DNA fragments by agarose gel electrophoresis

For analytical analysis and preparative isolation, DNA fragments were electrophoretically separated on 1-1.5% agarose gels in TBE buffer containing ethidium bromide (0.5 µg/ml final concentration). DNA samples were mixed with DNA loading buffer and separated at 100 V in TBE-buffer. By intercalation of ethidium bromide into DNA, the DNA fragments could be visualized by using a UV transilluminator (324 nm). Standard DNA size marker (Gene RulerTM, 1kb ladder, 0.1 µg/µl, Fermentas) was used to estimate the size of the fragments.

TBE buffer: 90 mM Tris/NaOH (pH 8.0)
                            90 mM Boric acid
                            2.5 mM EDTA/NaOH

DNA loading buffer (5x):   0.25% Amber G
                            25% Glycerol
                            25 mM EDTA (pH 8.0)

5.3.6. DNA Extraction from agarose gels

After gel electrophoresis, DNA fragments were isolated by excising the corresponding piece of agarose with a scalpel. The DNA extraction was carried out according to manufacturer's instructions using QiaExII Gel Extraction kit (QIAGEN, Hilden). DNA was eluted in 50 µl TE-buffer.

TE buffer: 2.5 mM Tris/HCl (pH 8.0)

                              0.1 mM EDTA/NaOH (pH 8.0)

5.3.7. Ligation of DNA fragments

Amounts of isolated DNA fragments ("inserts") and linearized vectors were estimated on an ethidium bromide-containing agarose gel. For ligation reaction a molar ratio of 1:2.5 of vector to insert was used. With a total volume of 10 µl, the reaction sample contained about 100 ng of vector DNA and 4 units of T4 DNA Ligase (Fermentas, St. Leon-Rot). Ligation reaction was completed after 1-2 h at RT or overnight at 16°C in recommended amounts of reaction buffer (Fermentas, St. Leon-Rot).

5.3.8. DNA Sequencing

A sequencing sample contained 700 ng of plasmid DNA and 20 pmol of sequencing primer in a total volume of 7 µl. DNA sequencing was carried out by an external commercial provider (SeqLab, Göttingen).

5.3.9. Sequence insertion into genes by PCR

Site directed mutagenesis was performed using a fusion PCR based approach using two reverse complementary oligos harboring the desired mutation(s). In two separate PCR reactions each oligo was used to create an upstream and a downstream fragment, respectively. The outer primers were designed to terminate at useful restriction sites. After gel purification the two overlapping products were combined and fused in a PCR reaction with the two outer primers. The resulting fragments were restriction cloned into the respective wild-type sequence. Verification was done by sequencing.

5.3.10. Polymerase chain reaction (PCR)

For DNA amplification, a PCR Mastercycler (Techne, Burlington, USA) was used and PCR samples exhibited a total volume of 50 µl.

PCR reaction: 50-200 ng template plasmid DNA
0.25 µl forward and reverse oligonucleotide primer (100 mM)
1 µl Deoxyribonucleotide mix (10 mM, NEB)
10 µl 5x Phusion HF- or GC-buffer (Finnzyme, Espoo, Finland)
ad 50 µl H_2O
0.3 µl DNA polymerase (Phusion, Finnzyme, Espoo, Finland)

The reaction profile was adjusted according to quantity and quality of template DNA, length and G/C content of the oligonucleotides, the length of the amplified sequences and in view of the manufacturer's instructions (Finnzyme, Espoo, Finland). Usually, the denaturing step was done for 20 sec at 98°C, annealing for 20 sec at a temperature optimized for the individual primer pairs, and elongation at 72°C for 20 sec/kbp.

5.4. Tissue culture methods

5.4.1. Tissue culture cell lines and medium

Cell line	Description and origin
Hek 293T	Human embryonic kidney cell transformed with SV 40 large T antigen
KE-37	Human acute lymphoblastic leukemia T cell line
U2OS	Human osteosarcoma cell line expressing wild type p53 and Rb, but lacking p16
Hek 293 Flp In	Human cervix epithelial cells modified by stable integration of a pFRT/*lac*Zeo plasmid (Invitrogen/Fisher Scientific, Schwerte) carrying the FRT recognition site for transgene integration by Flprecombinase (mediates zeocin resistance), and stable integration of a pcDNA6/TR plasmid (Invitrogen/Fisher Scientific, Schwerte; modified by replacing the *blast*R gene with a *puro*R gene), for constitutive expression of the Tet-repressor (mediates puromycin resistance); This host cell line was kindly provided by Thomas U. Mayer (University of Konstanz)
Hek 293 S1126A	Stable transgenic Hek 293 cell line inducibly overexpressing Phosphomutant-separase (Boos et al., 2008)

All cell lines were cultured in Dulbecco's Modified Eagle Medium (high glucose DMEM; PAA, Pasching, Austria), supplemented with 10% heat-inactivated (40°C, 10 min) fetal calf serum (Biochrom, Lot: 0486G, Berlin), 100 Units/ml penicillin and 100 µg/ml streptomycin (PAA, Pasching, Austria).

5.4.2. Cultivation of mammalian cells

Adherent cells were grown in cell culture dishes at 37°C in a 5% CO_2 atmosphere and split in a ratio of 1:3 to 1:5 twice a week. To passage the cells, the medium was removed; cells were washed with PBS and subsequently incubated for 2-5 min with 16 µl/cm^2 Trypsin/EDTA solution (PAA, Pasching, Austria). Trypsin/EDTA detached the cells from each other as well as from the cell culture dish. The addition of fresh culture medium stopped the reaction. Cells were pelleted by centrifugation (200 g), resuspended in new medium and plated on a new cell culture dish for further cultivation. Cell concentrations of suspensions were determined with a Vi-Cell counter (Beckman Coulter, Krefeld).

Suspension cells, as KE-37, were cultivated in 1-litre spinning flasks. For adequate cell growth, the cell suspension was diluted with fresh medium twice a week.

PBS: 137 mM NaCl
2.7 mM KCl
8 mM Na_2HPO_4
1.4 mM KH_2PO_4 (pH 7.4)

5.4.3. Freezing and thawing of mammalian cells

For long-term storage cells were kept in liquid nitrogen. Then, cells were harvested at 80% confluence as described above. They were resuspended in freezing medium, aliquoted in 1.5 ml cryovials (SARSTEDT, Nürmbrecht) and then frozen in a cardboard box at –80°C. One day later, cryovials were transferred to a liquid nitrogen tank.

Freezing medium: 10% DMSO
90% fetal bovine serum (Biochrom, Berlin)

For thawing, frozen cells were rapidly diluted with pre-warmed (37°C) fresh medium, centrifuged (200 g for 2 min) to remove residual DMSO and plated onto a cell culture dish.

5.4.4. Synchronization of mammalian cells

To arrest cells in early mitosis, first, 2 mM thymidine was added to the culture medium to pre-synchronize cells in early S phase. After 20 h of incubation, cells were washed with PBS and resuspended into fresh medium by washing twice with medium followed by 30 min incubation in the cell culture incubator and another medium change. 3 h after releasing from thymidine block, a 12 h incubation with nocodazole (200 ng/ml) or Taxol (200 ng/ml) containing medium efficiently arrested cells in pro-metaphase.

A double thymidine block was used to arrest cells in early S phase. First, 2 mM thymidine was added for 18 h, cells were then washed with PBS and released for 9 h. The second thymidine (2 mM) block was carried out for 17 h to arrest cells at the beginning of S phase. Cell synchrony was monitored by flow cytometry using propidium iodide (see 5.4.5).

5.4.5. Flow cytometry

For the preparation of FACS samples, about 500,000 cells were washed with 1x PBS and fixed by rapid resuspension in 70% ethanol (–20°C). After storage at 4°C over night or longer, the fixed cells were washed twice in 1x PBS with 0.1% BSA (w/v) and then incubated in 38 mM sodium citrate supplemented with 69 μM propidium iodide and 0.1 μg/ml RNaseA for 1 hour at 37°C. The fluorescence intensity of chromatin bound propidium iodide was analyzed on a Cytometics FC 500 (Beckman Coulter) using CellQuest Pro software.

5.4.6. Transfection of Hek 293T cells

Transfection of Hek 293T cells was performed at 50% density according to the calcium phosphate method. 300.000 cells/ml were seeded in cell culture dishes and grown overnight. Shortly before the transfection mix was added, 25 µM chloroquine was added to the medium to enhance transfection efficiency. For one transfection mix, 5-40 µg (depending on the construct) of plasmid DNA were mixed first with sterile water and then with sterile 2 M CaCl$_2$ (see table below). While gentle

vortexing, 2x HBS was slowly added and the mix was incubated for 5 min at room temperature before dripping onto cultured cells. 5-16 h later the medium was exchanged. 24 h after transfection, nocodazole was added to the medium at a final concentration of 200 ng/ml to arrest cells in mitosis (unless interphase samples were prepared). 36 h after transfection, cells were harvested by rinsing the plate with the used cell culture medium. Following centrifugation at RT (300 g, 3 min) cell pellets were washed once with PBS and subsequently either lysed directly or snap frozen in liquid nitrogen and stored at -80°C for further use.

Transfection mix

Diameter of dish	10 cm	15 cm
Volume of medium	10 ml	25 ml
DNA concentration	16 µg	40 µg
H$_2$O (end volume incl. CaCl$_2$)	800 µl	2000 µl
2M CaCl$_2$	99 µl	248 µl
2x HBS	800 µl	2000 µl
Total volume per dish	1600 µl	4000 µl

2x HBS (500 ml):   8.0 g NaCl
                        0.37 g KCl
                        106.5 mg Na$_2$HPO$_4$
                        1.0 g Glucose
                        5.0 g HEPES/NaOH (pH 7.05)

5.4.7. Generation of stable cell lines

Hek 293 FlpIn cell lines with stable, inducible transgenic expression were generated according to the manufacturer's instructions (Invitrogen/Fisher Scientific, Schwerte). Briefly, transgene plasmid DNA (Myc$_6$ epitope tagged Shugoshin constructs in pcDNA5-FRT-TO vector background) and Flp integrase expression plasmid DNA (pOG44, Invitrogen/Fisher Scientific, Schwerte) were transfected at a ratio of 1:10 according to the calcium phosphate method described in 5.4.5. 24-48 h after transfection, cells were selected for site-specific integration of the transgene with 150 µg/ml hygromycin (PAA, Pasching, Austria). Once hygromycin resistant colonies were large enough to be seen by eye, they were picked, re-plated and inducible expression of the transgene was tested by addition of 5 µg/ml tetracycline (Serva,

Heidelberg) for 12-16 h.

For stable, tetracycline inducible expression of C-terminally GFP-tagged wild-type or HRV Scc1, transfected Hek 293T cells carrying the corresponding pRTS1-based episomes were selected by growth in medium containing 150 µg/ml hygromycin (PAA, Pasching, Austria). Transfection was carried out as described above. Transgene expression was induced with 2 µg/ml tetracycline. The bidirectional, episomal pRTS1 vector is stably inherited in multiple copies by sticking to the chromosome, like the genome of the Ebna virus. Other than genome insertion based stable cell lines, cells transfected with pRTS1 cannot be stored at -80°C and loose the construct after one or two months past transfection.

5.4.8. Transfection of double stranded RNA (siRNA)

For the knock down of endogenous Scc1 and Smc3, mixtures of two 3´UTR-directed siRNAs each were used. The commercial transfection reagent Lipofectamine® RNAi-Max was used for transfection of siRNAs based on nucleic acid packaging into liposomes formed by cationic lipids. Transfections were carried out according to the manufacturer's instructions. For the Sgo1, Wapl and luciferase (GL2, negative control) knock down, siRNA was either transfected according to the calcium phosphate method (see 5.4.5) or using Lipofectamine® RNAiMAX Reagent.

5.4.9. Purification of centrosomes from human cells

Preparative isolation of centrosomes from $1x10^9$ KE-37- or $1x10^8$ Hek293T cells was performed as described (Bornens and Moudjou, 1999) with the difference that prior to lysis cells were synchronized in prometaphase by a thymidine-nocodazole protocol (see 5.4.4) to enrich for fully matured, engaged centrioles. All steps were performed at 4°C except for final sucrose gradient elution. Since centrosomes stick to glass and might be sensitive to shearing, plastic pipettes, beakers, tubes as well as cut-off pipette tips were used. Cells were harvested by centrifugation (280 g, 10 min, 4°C) and washed with half of the initial volume of TBS by gentle swirling. This step was repeated once with 8% sucrose buffer using half of the volume of the previous step. After resuspending cells in 20 ml 8% sucrose buffer, 60-80 ml lysis buffer was slowly added to obtain a final concentration of $1-1.5x10^7$ cells/ml and incubated for 5 min. The swollen nuclei/chromatin were pelleted at 2,500 g for 10 min and the lysate was then filtered through one layer a medical gauze into a 250 ml centrifuge bottle, to

which HEPES and DNase I were added to a final concentration of 10 mM and 10 µg/ml, respectively. After incubation for 30 min, the mixture was transferred into 3-4 Beckman polyallomer tubes (1x3.5 inch; vol=38.5 ml), leaving enough space to place 5 ml 50% sucrose buffer to the bottom of each tube. Thereafter, the centrosomes were sedimented onto the 50% sucrose cushion by spinning at 11,000 g for 20 min at 4°C in a swing out rotor (SW32Ti). After centrifugation, the supernatant was carefully removed from each tube until 8-9 ml remained at the bottom, which were then pooled and mixed. A discontinuous sucrose gradient was prepared in another 38.5 ml tube, which consisted of 5, 3, and 3 ml, respectively, of 70, 50, and 40% sucrose buffer. The centrosomes containing sample was placed on top of the discontinuous sucrose gradient and centrifuged at 25,000g for 75 min at 4°C (same rotor type as above). Finally, centrosomes were recovered by puncturing the tube at the bottom with a hot 20G needle. Then, 0.5 ml fractions were collected. Fractions were snap frozen in liquid nitrogen and stored at –80°C. The presence of centrosomes was tested by immunoblotting (see 5.5.2) and immunofluorescence (see 5.4.10).

Sucrose buffer:	8% (w/v) Sucrose in 0.1x TBS:
	100 ml TBS
	80 g Sucrose
	H_2O ad 1 liter
Lysis buffer:	1 mM HEPES/KOH (pH 7.2)
	0.5% NP-40
	0.5 mM $MgCl_2$
	0.1% β-Mercaptoethanol
	Complete protease inhibitor cocktail (EDTA-free)
	(Roche, Mannheim)
Gradient buffer:	10 mM PIPES/KOH (pH 7.2)
	0.1% Triton X-100
	0.1% β-Mercaptoethanol
Sucrose buffer:	i.e. 70% sucrose in gradient buffer (w/w):
	70 g sucrose plus gradient buffer to a final weight of 100 g

To isolate centrosomes from less cells (one 10 cm petri dish corresponding to about $4x10^6$ cells) for direct imaging, a modified version of the centrosome purification

protocol was established. Cells were lysed in LP2 supplemented with complete protease inhibitor cocktail (Roche, Mannheim), 500 ng/ml nocodazole and 10 µg/ml DNaseI. Lysed cells were further treated with 14 strokes in a glass dounce homogenizer with a "tight" pestle (Wheaton, Millville, NJ, USA) and incubated for 20 min on ice. Then, the chromatin was pelleted by centrifugation (2,500 g, 10 min, 4°C, swing out rotor) and then the supernatant containing centrosomes was centrifuged (13,000 g, 25 min, 4°C, swing-out rotor) through a 3.5 ml sucrose cushion directly onto coverslips. Specimen were fixed in -20°C methanol and processed for immunofluorescence as described in 5.4.10. For some experiments, lysates were supplemented with HRV-protease (2.5 ng/µl) and incubated for 45 minutes at RT prior to centrosome isolation.

To assess centriole disengagement in intact cells, cell lines Tet-induced to express WT- or HRV-Scc1 were transfected with siRNA against endogenous Scc1 for 3 days and then transfected in nocodazole containing medium with expression plasmids coding for non-degradable securinΔN and HRV-protease. 16 hours thereafter, mitotic cells were harvested by shake-off, released into fresh medium and further grown for 4 hours on coverslips. Finally, G1-phase cells were fixed with -20°C methanol and processed for IF (see 5.4.11).

Centrosome dilution buffer:	400 mM PIPES/KOH (pH 6.8)
	5 mM MgCl$_2$
	5 mM EGTA
	20 mM EDTA
	0.01% Triton X-100

Sucrose cushion:	Centrosome dilution buffer with 40% (w/v) sucrose

5.4.10. Immunofluorescence of centrosomes

To test the presence of centrosomes, 10 µl from each fraction were dispersed in 5 ml 10 mM PIPES/KOH (pH 7.2) by vortexing and transferred into COREX centrifuge tubes (15 ml), which carried at their bottoms a coverslip on top of an adaptor. After centrifugation (13,000 g, 10 min, 4°C, JS 13.1 swing-out rotor), the coverslips were carefully lifted out from the COREX tubes and the centrosomes on the coverslips were fixed in –20°C methanol over night. Afterwards, the specimen was blocked in

PBS, 1% BSA (w/v) for 30 min at RT followed by incubation with the primary antibodies (centrin 2 and C-Nap1) in blocking solution for 1 h at RT. Coverslips were then washed 3 times with blocking solution, incubated with appropriate fluorescently labeled secondary antibodies in blocking solution for 1 h at RT and washed again as before. Finally coverslips were mounted with 3 µl mounting medium, placed on a microscope slide and then fixed with nail polish on the slide. Immunostained centrosomes were visualized by fluorescence microscopy. Images were aquired using an Axiovert upright microscope equipped with a Plan-APOCHROMAT 100x/0.4 objective (Carl Zeiss MicroImaging, Jena), a 23.0 1.4 MP monochrome Spot Persuit camera system and Spot 4.5.9.1 software (Diagnostic Instruments, Sterling Heights, MI, USA).

Mounting medium: 0.5% p-Phenylenediamine
                          20 mM Tris/HCl (pH 9.0) in 90% Glycerol

5.4.11. Immunofluorescence of Hek 293T cells

For IF staining, cells grown on coverslips were washed once with PBS in a 6-well culture plate. The samples were then fixed with either 3.7% formaldehyde in PBS for 10 min or with methanol (-20°C) overnight at -20°C. Cells were permeabilized by incubation in 0.5% Triton X-100 in PBS for 5 min. After washing once with 0.1% Triton X-100 in PBS, samples were blocked in 3% BSA in PBS (w/v) for 1 h. Coverslips were transferred onto parafilm and placed in a wet chamber. Staining was done by incubation with a dilution of primary antibodies in 3% BSA in PBS (w/v) for 2 h followed by 4 washes with 1% BSA in PBS (w/v). After incubation with a dilution of fluorescently labeled secondary antibodies for 1 h, samples were washed twice with 1% BSA in PBS (w/v), incubated with 1 µg/ml Hoechst 33342 in PBS for 15 min and then again washed twice with PBS. Coverslips were finally mounted with 3 µl mounting medium and placed on a glass slide. Immunostained cells were visualized by IF-microscopy. Images were aquired using an Axiovert upright microscope equipped with a Plan-APOCHROMAT 100x/0.4 objective (Carl Zeiss MicroImaging, Jena), a 23.0 1.4 MP monochrome Spot Persuit camera system and Spot 4.5.9.1 software (Diagnostic Instruments, Sterling Heights, MI, USA). Cell imaging was also carried out on a DMI 6000 inverted microscope stand equipped with a digital camera and with an HCX PL FUOTAR L 100x/0.4 objective (Leica Microsystems, Wetzlar).

5.4.12. Chromosome spreads

Cells were synchronized with nocodazole (200 ng/ml) containing medium for 12 hours. About 5×10^5 mitotic cells were harvested by shake-off and resuspended in 250 µl hypotonic medium by carefully pipetting up and down. After 3 min at RT, another 250 µl and then 2 ml were zestful added to the cell suspension in order to minimize cell loss. After another 5 min incubation, swollen cells were pelleted at 100 g for 5 min and carefully resuspended in 20 µl hypotonic medium. Thereafter, 250 µl, 250 µl, and 2 ml of Canoy´s solution were added to the suspension in a stepwise manner, followed by 30 min incubation at RT. For further dehydration, cells were twice pelleted at 300 g for 4 min and washed with 1 ml Canoy´s solution. After final resuspension in 250 µl Canoy´s solution, samples could be stored at –20°C. To proceed, 2 x 7.5 µl aliquots were dropped onto a microscope slide, which was cooled down to 0°C on top of an ice-submersed metal block and moisturized by breath. Following proper spreading of the sample, the slide was dried at 60°C on a metal block covered with a wet tissue. Afterwards, the chromosomal content of lysed cells was stained by incubation in Hoechst 33342 (1 µg/ml in PBS) for 10 min. Then, samples were washed twice with PBS, desalinated with H_2O and air-dried. Finally, 5 µl mounting medium was put on top of the slide which was carefully covered with a 24 x 60 mm coverslip. Spread chromosomes were visualized by IF-microscopy. Images were aquired using an Axiovert upright microscope equipped with a Plan-APOCHROMAT 100x/0.4 objective (Carl Zeiss MicroImaging, Jena), a 23.0 1.4 MP monochrome Spot Persuit camera system and Spot 4.5.9.1 software (Diagnostic Instruments, Sterling Heights, MI, USA).

Hypotonic medium: 40% FCS-free medium (e.g. DMEM)
                                 60% desalinated water
                                 500 ng/ml Nocodazole

Canoy´s solution: Methanol : Acetic acid = 3:1

5.4.13. Isolation of chromatin

About 0.5 to 1×10^6 cells were harvested by pipetting medium over the cell cultivation plates followed by centrifugation for 3 min at 200 g and two PBS washing steps. After washing, cells were resuspended in 100 µl buffer A. 0.5 µl 20% Triton X-100 was

added followed by 8 min incubation on ice. Lysed cells were spun down at 1,300g for 5 min at 4°C. The supernatant was separated from the pellet and centrifuged at 16,000 g for 5 min. The soluble fraction resembles the cytosolic fraction of the cells. It was mixed with 100 µl 2xSDS-sample buffer and heated at 95°C for 10 min. The pellet of the lysed cells, which contains the chromatin, was washed once more with 100 µl buffer A and resuspended in 100 µl buffer B followed by an incubation of 30 min on ice. Chromatin was then centrifuged at 1,700 g for 5 min at 4°C. The pellet was washed 1-2 times with buffer B and finally resuspended in 100 µl buffer B. 100 µl 2xSDS-sample buffer was added and samples were heated at 95°C for 10 min. SDS-PAGE (5.5.1) and immunoblotting (5.5.2) was performed.

Buffer A: 10 mM HEPES/KOH (pH 7.9)
                 10 mM KCl
                 1.5 mM $MgCl_2$
                 0.34 M Sucrose
                 10% Glycerol
                 100 mM NaCl
                 1 mM DTT

Buffer B: 3 mM EDTA
                 0.2 mM EGTA
                 1 mM DTT

5.4.14. Preparation of *Xenopus laevis* egg extracts

The *Xenopus* egg extract was prepared as previously described by Murray (1991). To obtain frog eggs, 1 ml <u>h</u>uman <u>c</u>horionic <u>g</u>onadotropin (hCG; Sigma CG-10, 1000 U/ml in H_2O) was injected into the dorsal lymph sac of a female frog one day before extract preparation. The frogs were transferred to 1x MMR buffer 6 h later and typically laid mature eggs 20-24 h after injection. First, all vessels were rinsed with bidestilled water to prevent contamination with Ca^{2+} and frog eggs were kept at 18°C. Once prepared, extracts were kept on ice until use. The jelly coats (*zona pellucida*) of the oocytes were removed by 5-10 min incubation in cysteine solution. Afterwards, all activated and amorphous eggs were removed and eggs were washed 4x in CSF-XB to quantitatively remove all dejellying solution. Afterwars, the eggs were carefully transferred into centrifuge tubes containing 1 ml CSF-XB and 100 µg/ml of

cytochalasin B. By sequential centrifugation at 18°C for 1 min at 200 g and 1 min at 600 g (JS 13.1 swing-out rotor, Beckmann) eggs were tightly packed and buffer displaced. All supernatant on top of the packed eggs was removed. Then, the eggs were destroyed at 18°C by a crushing spin at 13,000 g for 10 min. By puncturing the centrifuge tube with a syringe (18G), the light brown cytoplasmic fraction was collected. Cytochalasin B was added to a final concentration of 10 µg/ml to inhibit actin polymerization. At this stage, the extract is arrested in metaphase of meiosis II (CSF-extract). To inhibit translation, cycloheximide (Calbiochem 239764, dissolved in H_2O) was added in a final concentration of 100 µg/ml.

Before further experiments were carried out, the CSF-arrest was tested by incubation of 50 µl CSF-extract with 1 µl sperm nuclei (1.3×10^5 per µl) at 30°C for 5 min. Then, 1 µl Ca^{2+} (stock solution: 15 mM $CaCl_2$ in sperm dilution buffer) was put in a new tube and mixed with 24 µl of the sperm-supplemented extract while the remaining 25 µl were left untreated. After incubation for 30 min at 30°C, 1 µl of each sample was mixed with 3 µl of DAPI-Fix and investigated by fluorescence microscopy in regards to chromatin morphology.

Stable anaphase extracts with active APC/C, Cdk1 and separase were produced by addition of cyclin B1Δ90 (80 nM for low Δ90 anaphase extract) prior Ca^{2+}-mediated release from CSF arrest. They were used either directly or snap-frozen in aliquots and stored at –80°C.

CSF-XB: 100 mM KCl
          0.1 mM $CaCl_2$
          2 mM $MgCl_2$
          10 mM HEPES/KOH (pH 7.7)
          50 mM Sucrose
          5 mM EGTA/KOH (pH 8.0)
          pH 7.7, adjusted with KOH

MMR (25x):   2.5 M NaCl
          50 mM KCl
          25 mM $MgCl_2$
          50 mM $CaCl_2$
          2.5 mM EDTA/NaOH (pH 8.0)
          125 mM HEPES/NaOH (pH 7.8)
          pH 7.8, adjusted with NaOH

DAPI-Fix: 48% Glycerol
                       11% Formaldehyde
                       1x MMR
                       1µg/ml Hoechst 33342 (Sigma B-2261)

XB-salts (20x):   2 M KCl
                       2 mM CaCl$_2$
                       20 mM MgCl$_2$

Cysteine solution: 2% (w/v) Cysteine (free base)
                       0.5x XB-salts
                       pH 7.8, adjusted with KOH

Sperm dilution buffer: 5 mM HEPES/KOH (pH 7.7)
                       100 mM KCl
                       150 mM Sucrose
                       1 mM MgCl$_2$

5.5. Protein biochemistry methods

5.5.1. SDS-polyacrylamide gel electrophoresis (SDS-PAGE)

For the separation of proteins under denaturing conditions, commercially available neutral gels (Serva, Heidelberg) with a continuous polyacrylamide gradient from 4-12% were used. Prior to loading, the protein samples were mixed with sample buffer and denatured for 5 min at 95°C. As a molecular weight standard, PageRuler Prestained Protein Ladder (Fermentas, St. Leon-Rot) was used. Electrophoresis was carried out at constant electric current of 25-30 mA in Laemmli running buffer.

Sample buffer (4x):   40% Glycerol
                       250 mM Tris/HCl (pH 6.8)
                       8% (w/v) SDS
                       2M β-Mercaptoethanol
                       0.04% (w/v) Bromphenol blue

Laemmli running buffer: 25 mM Tris
                        192 mM Glycine
                        3.5 mM SDS

5.5.2. Immunoblotting

After separation by SDS-PAGE, proteins were transferred electrophoretically to a polyvinylidene fluoride (PVDF) membrane (Immobilon P, Millipore, Schwalbach) by semi-dry blotting. Prior to protein transfer, the hydrophobic PVDF membrane was made accessible for the aqueous blotting buffer by a brief incubation in 100% methanol. Then, the membrane was rinsed with distilled water to remove the methanol and equilibrated with blotting buffer.

Proteins were transferred at a constant voltage of 15 V for 30-45 min at RT or 13 V for 85 min, respectively. Afterwards, the membrane was blocked for unspecific binding with 5% skim milk in PBS (w/v) for 30 min at RT. This was followed by incubation with the primary antibody diluted in 1% BSA in PBS (w/v) for 1 h at RT or overnight at 4°C. Having washed the membrane three times with PBS-Tween for 15 min each, it was incubated with the appropriate HRP-conjugated (horseradish peroxidase) secondary antibody directed to the primary antibody diluted in 1% BSA in PBS (w/v) for 1 h at RT and then washed again as before. For detection the ECL-plus chemiluminescence detection kit was used according to the manufactures protocol (ECL, GE Healthcare, Munich) and a LAS-4000 camera system (Fuji).

Blotting buffer: 25 mM Tris
                                   192 mM Glycine
                                   20% Methanol

PBS-Tween: 0.05% Tween-20 in PBS

5.5.3. Coomassie staining

For coomassie staining, SDS-gels were incubated in coomassie solution for several hours after protein separation. To remove unspecific staining, coomassie solution was exchanged by destaining solution for 5 to 12 h. For storage, coomassie-stained gels were vacuum-dried onto a Whatman 3MM blotting paper (GE Healthcare, Munich) in a slab gel dryer (GD2000, Hoefer, Holliston, MA, USA).

Coomassie solution: 0.4% Coomassie Brilliant Blue R250
                                     0.4% Coomassie Brilliant Blue G250
                                     (Sigma-Aldrich, Steinheim)
                                     20% Methanol

Destaining solution: 30% Methanol
                            70% Acetic acid

5.5.4. Autoradiography

When radioactive samples were used, proteins were separated via SDS-PAGE (see 5.5.1) and the gels incubated in destaining solution for 30 min followed by washing with water for 10 min. This treatment fixed proteins and washed out unincorporated ^{35}S-methionine. Gels were dried on Whatman 3MM blotting paper (GE Healthcare, Munich) in a slab gel dryer (GD2000, Hoefer, Holliston, MA, USA) and exposed to a film (BioMax MR, Kodak) for 3 h to 3 days, depending on expected signal intensity. Autoradiographies were digitized using FLA-7000 phosphorimager (Fuji Film Europe, Düsseldorf).

5.5.5. *In vitro* translation (IVT)

For coupled *in vitro* transcription-translation (IVTT) of cohesin subunits, corresponding pCS2 based plasmids were combined with ^{35}S-methionine and TNT SP6 Quick rabbit reticulocyte lysate (Promega, Mannheim) according to the manufacturer's recommendations. Subsequent cleavage reactions were done by incubation of equal volumes of IVTT and protease (separase, HRV, or TEV) for 30 minutes at RT. Optionally, the IVTT was pre-incubated with Plk1.

5.5.6. Generation of whole cell extracts

0.5 to 1×10^6 cells were harvested by pelleting for 3 min at 200g. The pellet was washed once with PBS and resuspended in 100-200 µl LP2 lysis buffer. After an incubation of 5 min, 100-200 µl 2x SDS sample buffer was added. Samples were heated at 95°C for 5-10 min. SDS-PAGE (5.5.1) and immunoblotting (5.5.2) was performed sequentially.

LP2 (lysis buffer):   20 mM Tris/HCl (pH 7.7)
                           100 mM NaCl
                           10 mM NaF
                           20 mM β-glycerophosphate
                           5 mM MgCl$_2$
                           0.1% Triton X-100
                           5% glycerol
                           Complete protease inhibitor cocktail (Roche, Mannheim)

5.5.7. Immunoprecipitation experiments from transfected Hek 293T cells

For immunoprecipitations (IP), 1×10^7 transfected Hek 293T cells were harvested by pipetting medium over the cell culture dishes followed by centrifugation for 3 min at 300 g. From here on all steps were carried out either on ice or at 4°C. Cells were resuspended in 1 ml LP2 supplemented with complete protease inhibitor cocktail (Roche, Mannheim) and lysed with 14 strokes in a glass dounce homogenizer with a "tight" pestle (Wheaton, Millville, NJ, USA). Lysates were clarified by centrifugation at 16,000 g for 30 min and the supernatant was transferred to a new tube. An input sample of 20 µl was mixed with 40 µl 2x SDS-PAGE sample buffer. Cleared lysates were then combined with 10 µg of rabbit anti-GFP antibody DMP-crosslinked to Affi-prep protein A beads (BioRad). Following rotation for 3 h at 4°C or over night at 4°C, beads were pelleted briefly in a tabletop micro-centrifuge and then washed 6 times with 1 ml LP2. Subsequently, the beads were resuspended in 250 µl LP2 and transferred to a Mobicol microcolumn (Mobitec, Göttingen). The column was allowed to drain, capped at the bottom and proteins bound to the beads were eluted by gentle shaking with 35 µl of 2x SDS-PAGE sample buffer (without β-mercaptoethanol) at 85°C for 5 min. The bottom plug was removed and the eluate centrifuged into a 1.5 ml reaction tube at 200 g for 1 min. Samples were mixed with 0.2 µl β-mercaptoethanol, incubated for 5 min at 95°C and then subjected to SDS-PAGE on pre-cast gels (Serva, Heidelberg) followed by Western blot analysis.

5.5.8. Purification of active recombinant human separase

After transfection of 293T cells with different expression constructs for human ZZ-TEV$_4$-tagged separase and securin (Stemmann et al., 2001), synchronized cells (see 5.4.4) from 10 large cell culture dishes ($\varnothing$ 15 cm) were harvested, resuspended in 30 ml LP2 supplemented with complete protease inhibitor cocktail (plus EDTA, Roche, Mannheim) and treated with a glass homogenisator (Dounce, Wheaton, Millville, NJ, USA). Following 10 min on ice and centrifugation (15,000 rpm, JA 25.50, 30 min, 4°C), the supernatant was rotated overnight at 4°C with 300 µl IgG-Sepharose 6 Fast Flow (GE Healtcare, Munich) to affinity purify ZZ-TEV$_4$-tagged separase/securin-complexes. Beads with immobilized separase/securin complexes were washed twice with CSF-XB prior to their incubation in *Xenopus laevis* egg extract (see 5.6.1). *X. laevis* anaphase egg extract was used for degradation of securin (100 ng/ml of His-tagged human cyclin B1Δ90 isolated from baculovirus-infected insect cells, calcium

chloride from 25x stock). Usually, 300 µl beads were rotated in 3 ml extract for 45 min at RT. After washing, the beads were incubated in new extract for another 45 min to ensure complete securin degradation. Finally, the beads were washed with CSF-XB, twice with modified XB-buffer containing additional 250 mM NaCl and 0.1% Triton X100 and TEV-buffer. Separase was detached from IgG Sepharose after incubation with 100 µl TEV-protease (12.5U/µl provided by the core facility of the MPI of Biochemistry, Martinsried). The separase eluate was recovered by spinning the suspension through 35 mm filters in small columns (MoBiTec) to remove the beads. The eluate was either used for activity assays directly or aliquoted, snap-frozen in liquid N_2 and stored at –80°C.

XB buffer:	10 mM HEPES/KOH (pH 7.7)
	100 mM KCl
	1 mM $MgCl_2$
	0.1 mM $CaCl_2$
	50 mM Sucrose

TEV buffer:	10 mM HEPES/KOH (pH 7.7)
	50 mM NaCl
	25 mM NaF
	1 mM EGTA
	20% Glycerol

5.5.9. Separase activity assay

To examine the activity of separase, 2 µl of eluted separase were mixed with 2 µl of *in-vitro* translated ^{35}S-labelled human Scc1 and incubated for 30 min at 37°C. The reaction was stopped by addition of sample buffer. Samples were denatured for 5 min at 95°C and proteins separated by SDS-Page (see 5.5.1.). After autoradiography processing (see 5.5.4), Scc1 cleavage products were detected when separase was active.

5.5.10. Centriole disengagement assays

For standard egg extract based centriole disengagement assays, 10 µl centrosomes were combined with 50 µl CSF-extract (containing 5 ng/ml nocodazole), which had been previously supplemented with: Cyclin B1ΔN (2-20 ng/µl); *Xenopus laevis* securinΔN (3-300 ng/µl); or Cyclin B1ΔN, *X.l.* securinΔN, and securin-less human

WT- or mutant separase (43, 300, and 5 ng/µl, respectively). After incubation for 10 min at RT, 2 µl $CaCl_2$ (15 mM in sperm dilution buffer) were added to abrogate the CSF arrest. 45 min thereafter, samples were resuspended in 500 µl centrosome dilution buffer. Centrosomes were re-isolated by pelleting them through a sucrose cushion and analyzed by IF as described in 5.4.10. Instead of centrosomes purified from untransfected KE-37 cells, centrosomes from Hek 293T expressing C-terminally eGFP-tagged Scc1 or Smc3 were used, respectively. In these cases, the egg extract based assay was modified in that the CSF-extract was supplemented with proteolytically active WT-separase (5 ng/µl), HRV-protease (7 ng/µl), TEV-protease (0.625 U/µl), and BI2536 (200 nM) and not released by calcium addition.

For centriole disengagement assays in a purified system, centrosomes (15 µl) isolated from Hek 293T cells, which had endogenous Scc1 or Smc3 replaced by WT- or HRV-Scc1-GFP or WT- or TEV-Smc3-GFP, were diluted in 200 µl HRV- or TEV cleavage buffer. After addition of 10 µl HRV- (7 ng/µl) or TEV protease (0.625 U/µl) the mixture was incubated for 40 min at 30°C. Then, centrosomes were centrifuged directly onto coverslips and analyzed by IF (see 5.4.10).

Depending on arrest efficiency and individual preparation, 15-35% of isolated centrosomes appeared disengaged in the control sample. Background centriole disengagement in mock- or untreated samples was therefore subtracted from other samples according to the formula:

$$100 \times (N_{sample}^{diseng.} - background) / (N_{sample}^{total} - background)$$

with: $background = N_{control}^{diseng.} \times N_{sample}^{total} / N_{control}^{total}$

HRV cleavage buffer: 50 mM Tris/HCl (pH 8.0)
                        300 mM NaCl
                        10 mM EDTA
                        1 mM DTT

TEV cleavage buffer: 10 mM HEPES/KOH (pH 7.7)
                        50 mM NaCl
                        25 mM NaF
                        1 mM EGTA
                        20% Glycerol

5.5.11. Electron microscopy of centrosomes

Fixation and embedding for standard electron microscopy

Isolated centrosomes were resuspended in MT buffer (1:20), pelleted (13,000g, 30 min, 4°C, JS 13.1, swing-out rotor) to remove sucrose followed by two fixation steps: First, tightly pelleted centrosomes were incubated with MT buffer supplemented with 2.5% glutaraldeyde (pH 7.0-7.2) for 45 min on ice. During the second fixation step for 45 min at 18°C, MT buffer was supplemented with 1.25% glutaraldehyde and 0.5% tannic acid (pH 7.2). After two washes with 15 ml in ddH$_2$O for 15 min, centrosome pellets were osmicated (1% OsO$_4$ in ddH$_2$O (w/v)) for 60 min on ice. Pellets were washed twice in ddH$_2$O, transferred to 1.5-2% agar, dehydrated in an ascending alcohol sequence and embedded in Epon 812 (Serva, Heidelberg) as described by McFadden and Melkonian (1986).

MT buffer: 30 mM PIPES/KOH (pH 7.2)
                    5 mM Na/EDTA
                    15 mM KCl

Fixation and preembedding of isolated and immunogold labeled centrosomes

Several fractions of isolated centrosomes were resuspended in 10 mM PIPES/KOH (pH 7.2) buffer to dilute out the sucrose, centrifuged (13,000g, 20 min, 4°C, JS 13.1, swing-out rotor) onto coverslips and fixed using 4% formaldehyde/0.5% glutaraldehyde in Na/PBS for 30 min at RT. Coverslips were carefully washed 5x with 1 ml Na/PBS. After blocking for 1h at RT, coverslips were washed as before and the first antibody was diluted in blocking buffer and incubated for 2h at RT in a wet chamber. Afterwards, centrosomes on coverslips were washed 5x (5-10 min incubation) with blocking buffer and Na/PBS (1:1 mixture) and incubated with the 6 nm immunogold labeled secondary antibody diluted in blocking buffer. After 2h at RT and additional extensive washing in Na/PBS with 5-10 min incubation, a second fixation step for 40 min at 4°C with MT buffer containing 2.5% glutaraldehyde was carried out. After two washes with ddH$_2$O for 15 min, centrosomes were overlayed with 1% osmium tetroxide (1% OsO$_4$ in ddH$_2$O (w/v)) for 60 min at 4°C followed by further washing steps with ddH$_2$O before dehydration in an ascending alcohol sequence and embedment in Epon 812 (Serva, Heidelberg). Further steps including

infiltration, flat embedding and embedding in Epon 812 was carried out according to standard procedures described in Geimer (2009).

Na/PBS: 8.1 mM Na_2HPO_4
                 1.5 mM NaH_2PO_4
                 150 mM NaCl (pH 7.4)

Blocking buffer: 2% BSA (w/v)
                 0.1% cold water fish skin gelantin (v/v)
                 0.05% Tween 20 (v/v) in Na/PBS (pH 7.4)

Ultrathin sectioning and electron microscopy

Ultrathin serial sections (~70 nm) were cut with a diamond knife (Diatome, Biel, Schweiz) on a Ultracut UCT microtome (Leica Microsystems, Vienna, Austria) and mounted on Pioloform-coated copper grids (Plano, Wetzlar, Germany). The sections were stained with lead citrate and uranyl acetate (Reynolds, 1963). Micrographs were taken with a JEM-2100 transmission electron microscope (Jeol, Tokio, Japan) and documented using Gatan UltraScan 4000 CCD-camera (4k x 4k Pixel, Gatan Inc., Pleasanton, CA, USA). Ultrathin sectioning and electron microscopy were carried out by PD Dr. Stefan Geimer (Cell Biology, University of Bayreuth).

6.   ABBREVIATIONS

Δ	delta (deletion of a protein binding domain)
A	Ampere or alanine
aa	amino acid(s)
Ala	alanine
APC/C	Anaphase promoting complex/cyclosome (E3 ligase)
ATP	adenosine 5'-triphosphate
bp	base pairs
BSA	bovine serum albumin
C-terminal	carboxyterminal
C-terminus	carboxy terminus (C-terminal: carboxyterminal)
ca.	circa
CBB	Coomassie brilliant blue staining
Cdc	cell division cycle
Cdk1	Cyclin-dependent kinase 1
CLD	Cdc6-like domain
CLS	centrosomal localization signal
CMV	cytomegalovirus
CSF	cytostatic factor
CSF-extract	*X. laevis* egg extract arrested in metaphase II by CSF
cyclin B1ΔN	mutant stabilized via an N-terminal deletion of 90 aa (Δ90)
D-box	destruction box (aa sequence RxxL; x: any amino acid)
D. melanogaster	*Drosophila melanogaster*
DAPI	4',6'-diamino-2-phenylindol
dd	double distilled
DMSO	dimethylsulfoxide
DNA	deoxyribonucleic acid
dNTP	deoxynucleotide
DSHB	Developmental Studies Hybridoma Bank
DTT	dithiothreitol
E. coli	*Escherichia coli*
EDTA	ethylendiamine tetraacetic acid
eGFP	enhanced green fluorescent protein
EGTA	ethylen glycol tetraacetic acid
EM	electron microscopy
Fig.	figure
g	gram or gravitational constant (9.81 m/sec^2)
h	hour(s) or human
HBS	HEPES buffered saline
HEPES	4-(2-hydroxyethyl)-1piperazineethansulfonic acid

His	histidine
HRP	horseradish peroxidase
HRV	HRV protease recognition sequence (aa: LEVLFQ/GP)
HRV protease	human rhinovirus 3C protease
i.e.	*id est* ('in other words')
IF	immunofluorescence
IgG	immunoglobulin G
IP	immunoprecipitation
IPTG	isopropyl-β-D-thiogalactopyranoside
IVT	*in vitro* transcription/translation
kb	kilo base pairs
kDa	kilo dalton
KT	kinetochore
l	liter
LB	Luria-Bertani
m	milli, meter or mouse
M	Molar (mol/l) or molecular weight
MBP	maltose binding protein
MCAK	mitotic centromere associated kinesin
MCC	mitotic checkpoint complex
MCS	multiple cloning site
min	minute(s)
MMR	Marc's modified Ringer
mRNA	messenger RNA
MT	microtubules
MTOC	main microtubule organizing center
Myc	c-Myc oncogene, tag (aa sequence: EQKLISEEDL)
n	nano
N-terminal	aminoterminal
N-terminus	amino terminus
NBD	nucleotide binding domain
NC	non-cleavable
Noc	nocodazole
NTA	nitrilotriacetic acid
OD	optical density
ORF	open reading frame
p.a.	*pro analysi*
PAGE	polyacrylamide gel electrophoresis
PBS	phoshate buffered saline
PCR	polymerase chain reaction
PD	protease-dead
PIPES	piperazine-N,N′-bis(2-ethanesulfonic acid)
Plk1	polo-like kinase 1

PP2A	protein phosphatase 2 A
PVDF	polyvinylidene fluoride
Rel.	release
RING	really interesting new gene
RNA	ribonucleic acid
RNAi	RNA interference
RNase	ribonuclease
rpm	rounds per minute
RT	room temperature
S. cerevisiae	*Saccharomyces cerevisiae* (budding yeast)
S. pombe	*Schizosaccharomyces pombe*
SA	phosphorylation-site mutant separase (Ser1126Ala)
SAC	spindle assembly checkpoint
SAP	shrimp alkaline phosphatase
SDS	sodium dodecylsulfate
sec	seconds
securin ΔN	mutant stabilized via an N-terminal deletion of 90 aa (Δ90)
Sgo	shugoshin
siRNA	small interference RNA
SMC	structural maintenance of chromosomes
SPB	spindle pole body
Tet	tetracycline
TEV	TEV protease recognition sequence (aa: EXXYXQG/S)
TEV protease	tobacco etch virus protease
Thym.	thymidine
Tris	tris(hydroxymethyl)aminomethane
U	unit
V	volt
v/v	volume per volume
w/v	weight per volume
Wapl	wings apart-like
WB	Western blot
WCE	whole cell extract
WT	wild-type
x	any amino acid
X. laevis	*Xenopus laevis*
XB	extract buffer
XErp1	*Xenopus* Emi1-related protein 2
ZZ	IgG binding domain of protein A
μ	micro

7.   REFERENCES

Alliegro, M.C., Alliegro, M.A. and Palazzo, R.E. (2006). Centrosome-associated RNA in surf clam oocytes. *Proc Natl Acad Sci U S A.* 103(24): 9034-9038.

Anderson, D.E., Losada, A., Erickson, H.P. and Hirano, T. (2002). Condensin and cohesin display different arm conformations with characteristic hinge angles. *J Cell Biol.* 156(3): 419-424.

Azimzadeh, J. and Marshall, W.F. (2010). Building the centriole. *Curr Biol.* 20(18): R816-25.

Bacac, M., Fusco, C., Planche, A., Santodomingo, J., Demaurex, N., Leemann-Zakaryan, R., Provero, P. and Stamenkovic, I. (2011). Securin and separase modulate membrane traffic by affecting endosomal acidification. *Traffic.* 12(5): 615-626.

Bahe, S., Stierhof, Y.D., Wilkinson, C. J., Leiss, F., and Nigg, E.A. (2005). Rootletin forms centriole-associated filaments and functions in centrosome cohesion. *J Cell Biol.* 171(1): 27–33.

Ballabeni, A., Melixetian, M., Zamponi, R., Masiero, L., Marinoni, F. and Helin, K. (2004). Human geminin promotes pre-RC formation and DNA replication by stabilizing CDT1 in mitosis. *EMBO J.* 23(15): 3122-3132.

Bastiaens, P., Caudron, M., Niethammer, P. and Karsenti, E. (2006). Gradients in the self-organization of the mitotic spindle. *Trends Cell Biol.* 16(3): 125-134.

Basto, R., Lau, J., Vinogradova, T., Gardiol, A., Woods, C.G., Khodjakov, A. and Raff, J.W. (2006). Flies without centrioles. *Cell* 125(7): 1375-1386.

Beauchene, N.A., Díaz-Martínez, L.A., Furniss, K., Hsu, W.S., Tsai, H.J., Chamberlain, C., Esponda, P., Giménez-Abián, J.F. and Clarke, D.J. (2010). Rad21 is required for centrosome integrity in human cells independently of its role in chromosome cohesion. *Cell Cycle.* 9(9): 1774-1780.

Beisson, J. and Wright, M. (2003). Basal body/centriole assembly and continuity. *Curr Opin Cell Biol.* 15(1): 96-104.

Ben-Shahar, T.R., Heeger, S., Lehane, C., East, P., Flynn, H., Skehel, M. and Uhlmann, F. (2008). Eco1-dependent cohesin acetylation during establishment of sister chromatid cohesion. *Science.* 321: 563-566.

Bernard, P., Schmidt, C.K., Vaur, S., Dheur, S., Drogat, J., Genier, S., Ekwall, K., Uhlmann, F. and Javerzat, J.P. (2008). Cell-cycle regulation of cohesin stability along fission yeast chromosomes. *EMBO J.* 27(1): 111-121.

Berns, M.W. and Richardson, S.M. (1977). Continuation of mitosis after selective laser microbeam destruction of the centriolar region. *J Cell Biol.* 75(3): 977-982.

Bettencourt-Dias, M. and Glover, D.M. (2007). Centrosome biogenesis and function: centrosomics brings new understanding. *Nat Rev Mol Cell Biol.* 8(6): 451-463.

Bettencourt-Dias, M., Hildebrandt, F., Pellman, D., Woods, G. and Godinho, S.A. (2011). Centrosomes and cilia in human disease. *Trends Genet. 27*(8): 307-315.

Blow, J.J., and Dutta A. (2005). Preventing re-replication of chromosomal DNA. Nat Rev Mol Cell Biol 6, 476 *Nat Rev Mol Cell Biol.* 6(6): 476-486.

Bobinnec, Y., Moudjou, M., Fouquet, J.P., Desbruyères, E., Eddé, B. and Bornens, M. (1998). Glutamylation of centriole and cytoplasmic tubulin in proliferating non-neuronal cells. *Cell Motil Cytoskeleton.* 39(3): 223-32.

Boos, D., Kuffer, C., Lenobel, R., Körner, R. and Stemmann, O. (2008). Phosphorylation-dependent binding of cyclin B1 to a Cdc6-like domain of human separase. *J Biol Chem.* 283(2): 816-823.

Borges, V., Lehane, C., Lopez-Serra, L., Flynn, H., Skehel, M., Rolef Ben-Shahar, T. and Uhlmann, F. (2010). Hos1 deacetylates Smc3 to close the cohesin acetylation cycle. *Mol Cell.* 39(5): 677-688.

Bornens, M. (2002). Centrosome composition and microtubule anchoring mechanisms. *Curr Opin Cell Biol.* 14(1): 25-34.

Bornens, M., and M. Moudjou. (1999). Studying the composition and function of centrosomes in vertebrates. *Methods Cell Biol.* 61: 13–34.

Bornkamm, G.W., Berens, C., Kuklik-Roos, C., Bechet, J.M., Laux, G., Bachl, J., Korndoerfer, M., Schlee, M., Hölzel, M., Malamoussi, A., Chapman, R.D., Nimmerjahn, F., Mautner, J., Hillen, W., Bujard, H. and Feuillard J. (2005). Stringent doxycycline-dependent control of gene activities using an episomal one-vector system. *Nucleic Acids Res.* 33(16): e137.

Boyarchuk, Y., Salic, A., Dasso, M. and Arnaoutov, A. (2007). Bub1 is essential for assembly of the functional inner centromere. *J Cell Biol.* 176(7): 919-928.

Brar, G. A., Kiburz, B. M., Zhang, Y., Kim, J. E., White, F., und Amon, A. (2006). Rec8 phosphorylation and recombination promote the step-wise loss of cohesins in meiosis. *Nature.* 441: 532-536.

Brito, D.A., Gouveia, S.M. and Bettencourt-Dias, M. (2012). Deconstructing the centriole: structure and number control. *Curr Opin Cell Biol*. 24(1): 4-13.

Brodie, K.M. and Henderson, B.R. (2012). Characterization of BRCA1 centrosome targeting, dynamics and function: A role for the nuclear export signal, CRM1 and Aurora A kinase. *J Biol Chem.* 287(10): 7701-7716.

Carazo-Salas, R.E., Guarguaglini, G., Gruss, O.J., Segref, A., Karsenti, E., and Mattaj, I.W. (1999). Generation of GTP-bound Ran by RCC1 is required for chromatin-induced mitotic spindle formaiton. *Nature*. 400: 178-181.

Carvalho-Santos, Z., Azimzadeh, J., Pereira-Leal, J.B. and Bettencourt-Dias, M. (2011). Evolution: Tracing the origins of centrioles, cilia, and flagella. *J Cell Biol.* 194(2): 165-175.

Caudron, M., Bunt, G., Bastiaens, P. and Karsenti, E. (2005). Spatial coordination of spindle assembly by chromosome-mediated signaling gradients. *Science.* 309(5739): 1373-1376.

Cimini, D. and Degrassi, F. (2005). Aneuploidy: a matter of bad connections. *Trends Cell Biol.* 15(8): 442-451.

Ciosk, R., Shirayama, M., Shevchenko, A., Tanaka, T., Toth, A. and Nasmyth, K. (2000). Cohesin's binding to chromosomes depends on a separate complex consisting of Scc2 and Scc4 proteins. *Mol Cell.* 5: 243-254.

Cleveland, D.W., Mao, Y., and Sullivan, K.F. (2003). Centromeres and kinetochores: from epigenetics to mitotic checkpoint signaling. *Cell.* 112: 407-421.

Cordingley, M.G., Callahan, P.L., Sardana, V.V., Garsky, V.M. and Colonno, R.J. (1990). Substrate requirements of human rhinovirus 3C protease for peptide cleavage in vitro. *J Biol Chem.* 265(16): 9062-9065.

Cox, J., Jackson, A.P., Bond, J. and Woods, C.G. (2006) What primary microcephaly can tell us about brain growth. *Trends Mol Med.* 12(8): 358-366.

Crasta, K., Huang, P., Morgan, G., Winey, M. and Surana, U. (2006). Cdk1 regulates centrosome separation by restraining proteolysis of microtubule-associated proteins. *EMBO J.* 25(11): 2551-2563.

Cunha-Ferreira, I., Bento, I., Bettencourt-Dias, M. (2009). From zero to many: control of centriole number in development and disease. *Traffic.* 10(5): 482-498.

Dammermann, A., Müller-Reichert, T., Pelletier, L., Habermann, B., Desai and A., Oegema, K. (2004). Centriole assembly requires both centriolar and pericentriolar material proteins. *Dev Cell.* 7(6): 815-829.

Debec, A., Szöllösi, A. and Szöllösi, D. (1982). A Drosophila melanogaster cell line lacking centriole. *Biol Cell.* 44: 133-138.

Delattre, M., Spierer, A., Jaquet, Y. and Spierer, P. (2004). Increased expression of Drosophila Su(var)3-7 triggers Su(var)3-9-dependent heterochromatin formation. *J Cell Sci.* 117(Pt 25): 6239-6247.

Deng, C.X. (2001). Tumorigenesis as a consequence of genetic instability in Brca1 mutant mice. *Mutat Res.* 477(1-2): 183-189.

Dictenberg, J.B., Zimmerman, W., Sparks, C.A., Young, A., Vidair, C., Zheng, Y., Carrington, W., Fay, F.S. and Doxsey, S. J. (1998). Pericentrin and gamma-tubulin form a protein complex and are organized into a novel lattice at the centrosome. *J Cell Biol.* 141: 163–174.

Dirksen, E.R. (1991). Centriole and basal body formation during ciliogenesis revisited. *Biol Cell.* 72(1-2): 31-38.

Doxsey, S., McCollum, D. and Theurkauf, W. (2005). Centrosomes in cellular regulation. *Annu Rev Cell Dev Biol.* 21: 411-434.

Elbashir, S.M., Harborth, J., Lendeckel, W., Yalcin, A., Weber, K., Tuschl, T. (2001). Duplexes of 21-nucleotide RNAs mediate RNA interference in cultured mammalian cells. *Nature.* 411(6836): 494-498.

Faragher, A.J., and Fry, A.M. (2003). Nek2A kinase stimulates centrosome disjunction and is required for formation of bipolar mitotic spindles. *Mol Biol Cell.* 14(7): 2876-2889.

Farcas, A.M., Uluocak, P., Helmhart, W. and Nasmyth, K. (2011). Cohesin's concatenation of sister DNAs maintains their intertwining. *Mol Cell.* 44(1): 97-107.

Ferguson, R.L., and Maller, J.L. (2008). Cyclin E-dependent localization of MCM5 regulates centrosome duplication. *J Cell Sci.* 121(Pt 19): 3224-3232.

Ferguson, R.L., Pascreau, G. and Maller, J.L.. (2010). The cyclin A centrosomal localization sequence recruits MCM5 and Orc1 to regulate centrosome reduplication. *J Cell Sci.* 123(Pt 16): 2743-2749.

Flegg, C.P., Sharma, M., Medina-Palazon, C., Jamieson, C., Galea, M., Brocardo, M.G., Mills, K. and Henderson, B.R. (2010). Nuclear export and centrosome targeting of the protein phosphatase 2A subunit B56alpha: role of B56alpha in nuclear export of the catalytic subunit. *J Biol Chem.* 285(24): 18144-18154.

Forgues, M., Difilippantonio, M.J., Linke, S.P., Ried, T., Nagashima, K., Feden, J., Valerie, K., Fukasawa, K. and Wang, X.W. (2003). Involvement of Crm1 in hepatitis B virus X protein-induced aberrant centriole replication and abnormal mitotic spindles. *Mol Cell Biol.* 23: 5282-5292.

Fukasawa K. (2007). Oncogenes and tumour suppressors take on centrosomes. *Nat Rev Cancer.* 7(12): 911-924.

Gadde, S. and Heald, R. (2004). Mechanisms and molecules of the mitotic spindle. *Curr Biol.* 14: R797–R805.

Gandhi, R., Gillespie, P.J. and Hirano, T. (2006). Human Wapl is a cohesin-binding protein that promotes sister-chromatid resolution in mitotic prophase. *Curr Biol.* 16(24): 2406-2417.

Ganem, N.J., Godinho, S.A. and Pellman, D. (2009). A mechanism linking extra centrosomes to chromosomal instability. *Nature.* 460(7252): 278-282.

Gard, D.L., Hafezi, S., Zhang, T. and Doxsey, S.J. (1990). Centrosome duplication continues in cycloheximide-treated Xenopus blastulae in the absence of a detectable cell cycle. *J Cell Biol.* 110(6): 2033-2042.

Geimer, S. (2009). Immunogold Labeling of Flagellar Components In Situ. *Methods in Cell Biol.* 91:63-80. (S.M. King and G.J. Pazour, eds., Academic Press, San Diego)

Gerlich, D., Hirota, T., Koch, B., Peters, J.M. and Ellenberg, J. (2006). Condensin I stabilizes chromosomes mechanically through a dynamic interaction in live cells. *Curr Biol.* 16(4): 333-344.

Gillingham, A.K. and Munro, S. (2000). The PACT domain, a conserved centrosomal targeting motif in the coiled-coil proteins AKAP450 and pericentrin. *EMBO Rep.* 1: 524-529.

Giménez-Abián, J.F., Sumara, I., Hirota, T., Hauf, S., Gerlich, D., de la Torre, C., Ellenberg, J. and Peters, J.M. (2004). Regulation of sister chromatid cohesion between chromosome arms. *Curr Biol.* 14(13): 1187-1193.

Glotzer, M., Murray, A.W. and Kirschner, M.W. (1991). Cyclin is degraded by the ubiquitin pathway. *Nature. 349*(6305): 132-138.

Gómez, R., Valdeolmillos, A., Parra, M.T., Viera, A., Carreiro, C., Roncal, F., Rufas, J.S., Barbero, J.L. and Suja, J.A. (2007). Mammalian SGO2 appears at the inner centromere domain and redistributes depending on tension across centromeres during meiosis II and mitosis. *EMBO Rep.* 8(2): 173-180.

Gorr, I.H., Boos, D., and Stemmann, O. (2005). Mutual inhibition of separase and cdk1 by two-step complex formation. *Mol Cell.* 19(1): 135–141.

Gorr, I.H., Reis, A., Boos, D., Wuehr, M., Madgwick, S., Jones, K.T., and Stemmann, O. (2006). Essential cdk1-inhibitory role for separase during meiosis in vertebrate oocytes. *Nat Cell Biol.* 8(9): 1035–1037.

Gregson, H.C., Schmiesing, J.A., Kim, J.S., Kobayashi, T., Zhou, S. and Yokomori, K. (2001). A potential role for human cohesin in mitotic spindle aster assembly. *J Biol Chem.* 276(50): 47575-47582.

Gruber, S., Arumugam, P., Katou, Y., Kuglitsch, D., Helmhart, W., Shirahige, K. and Nasmyth, K. (2006). Evidence that loading of cohesin onto chromosomes involves opening of its SMC hinge. *Cell*. 127: 523-537.

Gruber, S., Haering, C.H. and Nasmyth, K. (2003). Chromosomal cohesin forms a ring. *Cell.* 112(6): 765-777.

Guacci, V., Koshland, D. and Strunnikov, A. (1997). A direct link between sister chromatid cohesion and chromosome condensation revealed through the analysis of MCD1 in S. cerevisiae. *Cell*. 91(1): 47-57.

Guan, J., Ekwurtzel, E., Kvist, U. and Yuan, L. (2008). Cohesin protein SMC1 is a centrosomal protein. *Biochem Biophys Res Commun.* 372(4): 761-764.

Gueth-Hallonet, C., Antony, C., Aghion, J., Santa-Maria, A., Lajoie-Mazenc, I., Wright, M., Maro, B. (1993). gamma-Tubulin is present in acentriolar MTOCs during early mouse development. *J Cell Sci.* 105: 157-166.

Guillou, E., Ibarra, A., Coulon, V., Casado-Vela, J., Rico, D., Casal, I., Schwob, E., Losada, A. and Méndez, J. (2010). Cohesin organizes chromatin loops at DNA replication factories. *Genes Dev.* 24(24): 2812-2822.

Güttler, T., Madl, T., Neumann, P., Deichsel, D., Corsini, L., Monecke, T., Ficner, R., Sattler, M. and Görlich, D. (2010). NES consensus redefined by structures of PKI-type and Rev-type nuclear export signals bound to CRM1. *Nat Struct Mol Biol* 17: 1367-1376.

Habedanck, R., Stierhof, Y.D., Wilkinson, C.J. and Nigg,. E. A. (2005). The polo kinase plk4 functions in centriole duplication. *Nat. Cell Biol.* 7(11): 1140-1146.

Haering, C.H., Farcas, A.M., Arumugam, P., Metson, J., Nasmyth, K. (2008). The cohesin ring concatenates sister DNA molecules. *Nature.* 454(7202): 297-301.

Haering, C.H., Lowe, J., Hochwagen, A., and Nasmyth, K. (2002). Molecular architecture of SMC proteins and the yeast cohesin complex. *Mol Cell.* 9: 773-788.

Haering, C.H., Schoffnegger, D., Nishino, T., Helmhart, W., Nasmyth, K. and Löwe, J. (2004). Structure and stability of cohesin's Smc1-kleisin interaction. *Mol Cell.* 15(6): 951-964.

Hagiwara, D., Yamashino, T. and Mizuno, T. (2004. A Genome-wide view of the Escherichia coli BasS-BasR two-component system implicated in iron-responses. *Biosci Biotechnol Biochem.* 68(8): 1758-1767.

Hauf, S., Roitinger, E., Koch, B., Dittrich, C.M., Mechtler, K., and Peters, J. (2005). Dissociation of cohesin from chromosome arms and loss of arm cohesion during early mitosis depends on phosphorylation of SA2. *PLoS Biol.* 3(3): e69.

Hauf, S., Waizenegger, I.C. and Peters, J.M. (2001). Cohesin cleavage by separase required for anaphase and cytokinesis in human cells. *Science.* 293(5533): 1320-1323.

Heald, R. and McKeon, F. (1990). Mutations of phosphorylation sites in lamin A that prevent nuclear lamina disassembly in mitosis. *Cell.* 61(4): 579-589.

Heald, R., Tournebize, R., Blank, T., Sandaltzopoulos, R., Becker, P., Hyman, A. and Karsenti, E. (1996). Self-organization of microtubules into bipolarspindles around artificial chromosomes in Xenopus egg extracts. *Nature.* 382: 420-425.

Hemerly, A.S., Prasanth, S.G., Siddiqui, K. and Stillman, B. (2009). Orc1 Controls Centriole and Centrosome Copy Number in Human Cells. *Science.* 323 (5915): 789-793.

Hinchcliffe, E. H., Li, C., Thompson, E. A., Maller, J. L., and Sluder, G. (1999). Requirement of cdk2-cyclin e activity for repeated centrosome reproduction in Xenopus egg extracts. *Science.* 283(5403): 851-854.

Hinchcliffe, E.H., Miller, F.J., Cham, M., Khodjakov, A. and Sluder, G. (2001). Requirement of a centrosomal activity for cell cycle progression through G1 into S phase. *Science.* 291(5508): 1547-1550.

Hirano, T. (2005). Condensins: organizing and segregating the genome. *Curr Biol.* 15, R265-R275.

Holland, A.J. and Taylor, S.S. (2006). Cyclin-B1-mediated inhibition of excess separase is required for timely chromosome disjunction. *J Cell Sci.* 119: 3325-3336.

Holland, A.J., Böttger, F., Stemmann, O. and Taylor, S.S. (2007). Protein phosphatase 2A and separase form a complex regulated by separase autocleavage. *J Biol Chem.* 282(34): 24623-24632.

Holt, L.J., Krutchinsky, A.N., and Morgan, D.O. (2008). Positive feedback sharpens the anaphase switch. *Nature* 454: 353-357.

Hornig, N.C. and Uhlmann, F. (2004). Preferential cleavage of chromatin-bound cohesin after targeted phosphorylation by Polo-like kinase. *EMBO J.* 23: 3144–3153.

Hu, B., Itoh, T., Mishra, A., Katoh, Y., Chan, K.L., Upcher, W., Godlee, C., Roig, M.B., Shirahige, K. and Nasmyth, K. (2011). ATP hydrolysis is required for relocating cohesin from sites occupied by its Scc2/4 loading complex. *Curr Biol.* 21. 12-24.

Huang, H., Feng, J., Famulski, J., Rattner, J. B., Liu, S.T., Kao, G.D., Muschel, R., Chan, G.K.T., und Yen, T.J. (2007). Tripin/hSgo2 recruits MCAK to the inner centromere to correct defective kinetochore attachments. *J Cell Biol.* 177: 413-424.

Huang, X., Andreu-Vieyra, C.V., Wang, M., Cooney, A.J., Matzuk, M.M. and Zhang, P. (2009). Preimplantation mouse embryos depend on inhibitory phosphorylation of separase to prevent chromosome missegregation. *Mol Cell Biol*. 29(6): 1498-1505.

Huang, X., Andreu-Vieyra, C.V., York, J.P., Hatcher, R., Lu, T., Matzuk, M.M. and Zhang, P. (2008). Inhibitory phosphorylation of separase is essential for genome stability and viability of murine embryonic germ cells. *PLoS Biol.* 6(1): e15.

Huang, X., Hatcher, R., York, J.P., and Zhang, P. (2005). Securin and separase phosphorylation act redundantly to maintain sister chromatid cohesion in mammalian cells. *Mol Biol Cell.* 16: 4725-4732.

Ibañez-Tallon, I., Heintz, N., Omran, H. (2003). To beat or not to beat: roles of cilia in development and disease. *Hum Mol Genet.* 12 Spec No 1: R27-35.

Ivanov, D. and Nasmyth, K. (2005). A topological interaction between cohesin rings and a circular minichromosome. *Cell.* 122(6): 849-860.

Ivanov, D. and Nasmyth, K. (2007). A physical assay for sister chromatid cohesion in vitro. *Mol Cell.* 27(2): 300-310.

Iwaizumi, M., Shinmura, K., Mori, H., Yamada, H., Suzuki, M., Kitayama, Y., Igarashi, H., Nakamura, T., Suzuki, H., Watanabe, Y., Hishida, A., Ikuma, M. and Sugimura, H. (2009). Human Sgo1 downregulation leads to chromosomal instability in colorectal cancer. *Gut.* 58: 249-260.

Jager, H., Herzig, B., Herzig, A., Sticht, H., Lehner, C.F. and Heidmann, S. (2004). Structure predictions and interaction studies indicate homology of separase N-terminal regulatory domains and Drosophila THR. *Cell Cycle.* 3: 182-188.

Jallepalli, P.V., Waizenegger, I.C., Bunz, F., Langer, S., Speicher, M. R., Peters, J., Kinzler, K.W., Vogelstein, B. and Lengauer, C. (2001). Securin is required for chromosomal stability in human cells. *Cell.* 105: 445-457.

Jensen, S., Segal, M., Clarke, D.J. and Reed, S.I. (2001). A novel role of the budding yeast separin Esp1 in anaphase spindle elongation: evidence that proper spindle association of Esp1 is regulated by Pds1. *J Cell Biol.* 152(1): 27-40.

Jiang, N., Wang, X., Jhanwar-Uniyal, M., Darzynkiewicz, Z. and Wei Dai. (2006). Polo-box domain of PLK3 functions as a centrosome localization signal, over-expression of which causes mitotic arrest, cytokinesis defects, and apoptosis. *J Biol Chem.* 281(15): 10577-10582.

Karalus, D. (2012). Master thesis. University of Bayreuth.

Katis, V.L., Galova, M., Rabitsch, K.P., Gregan, J. and Nasmyth, K. (2004). Maintenance of cohesin at centromeres after meiosis I in budding yeast requires a kinetochore-associated protein related to MEI-S332. *Curr Biol.* 14(7): 560-572.

Katis, V.L., Lipp, J.J., Imre, R., Bogdanova, A., Okaz, E., Habermann, B., Mechtler, K., Nasmyth, K. and Zachariae, W. (2010). Rec8 phosphorylation by casein kinase 1 and Cdc7-Dbf4 kinase regulates cohesin cleavage by separase during meiosis. *Dev Cell.* 18(3): 397-409.

Kawashima, S.A., Yamagishi, Y., Honda, T., Ishiguro, K. and Watanabe, Y. (2010). Phosphorylation of H2A by Bub1 prevents chromosomal instability through localizing shugoshin. *Science.* 327(5962): 172-177.

Kemp, C.A., Kopish, K.R., Zipperlen, P., Ahringer, J. and O'Connell, K.F. (2004). Centrosome maturation and duplication in *C. elegans* require the coiled-coil protein SPD-2. *Dev Cell*. 6(4): 511-523.

Keryer, G., Ris, H. and Borisy, G.G. (1984). Centriole distribution during tripolar mitosis in Chinese hamster ovary cells. *J Cell Biol.* 98(6): 2222-2229.

Khodjakov, A. and Rieder, C.L. (2001). Centrosomes enhance the fidelity of cytokinesis in vertebrates and are required for cell cycle progression. *J Cell Biol.* 153(1): 237-242.

Khodjakov, A., Cole, R.W., Oakley, B.R., Rieder, C.L. (2000). Centrosome-independent mitotic spindle formation in vertebrates. *Curr Biol.* 10(2): 59-67.

Kim, K.P., Weiner, B.M., Zhang, L., Jordan, A., Dekker, J. and Kleckner, N. (2010). Sister cohesion and structural axis components mediate homolog bias of meiotic recombination. *Cell*. 143(6): 924-937.

Kirschner, M.W. and Mitchison, T. (1986). Microtubule dynamics. *Nature.* 324(6098): 621.

Kitagawa, D., Vakonakis, I., Olieric, N., Hilbert, M., Keller, D., Olieric, V., Bortfeld, M., Erat, M.C., Flückiger, I., Gönczy, P. and Steinmetz, M.O. (2011). Structural basis of the 9-fold symmetry of centrioles. *Cell*. 144(3): 364-375.

Kitajima, T.S., Hauf, S., Ohsugi, M., Yamamoto, T., und Watanabe, Y. (2005). Human Bub1 defines the persistent cohesion site along the mitotic chromosome by affecting shugoshin localization. *Curr Biol*. 15: 353-359.

Kitajima, T.S., Kawashima, S.A., and Watanabe, Y. (2004*).* The conserved kinetochore protein shugoshin protects centromeric cohesion during meiosis. *Nature*. 427(6974): 510–517.

Kitajima, T.S., Sakuno, T., Ishiguro, K., Iemura, S., Natsume, T., Kawashima, S.A., and Watanabe, Y. (2006). Shugoshin collaborates with protein phosphatase 2A to protect cohesin. *Nature*. 441: 46–52.

Klein, F., Mahr, P., Galova, M., Buonomo, S.B., Michaelis, C., Nairz, K. and Nasmyth, K. (1999). A central role for cohesins in sister chromatid cohesion, formation of axial elements, and recombination during yeast meiosis. *Cell*. 98(1): 91-103.

Knockleby, J., and Lee, H. (2010). Same partners, different dance: involvement of DNA replication proteins in centrosome regulation. *Cell Cycle.* 9(22): 4487-4491.

Kogut, I., Wang, J., Guacci, V., Mistry, R.K., and Megee, P.C. (2009). The Scc2/Scc4 cohesin loader determines the distribution of cohesin on budding yeast chromosomes. *Genes Dev.* 23: 2345-2357.

Kollman, J.M., Merdes, A., Mourey, L. and Agard, D.A. (2011). Microtubule nucleation by γ-tubulin complexes. *Nat Rev Mol Cell Biol.* 12(11): 709-721.

Kong, X., Ball, A.R. Jr., Sonoda, E., Feng, J., Takeda, S., Fukagawa, T., Yen, T.J., Yokomori, K. (2009). Cohesin associates with spindle poles in a mitosis-specific manner and functions in spindle assembly in vertebrate cells. *Mol Biol Cell.* 20(5): 1289-1301.

Koshland, D. and Hartwell, L.H. (1987). The structure of sister minichromosome DNA before anaphase in Saccharomyces cerevisiae. *Science* 238: 1713–1716.

Kosugi, S., Hasebe, M., Matsumura, N., Takashima, H., Miyamoto-Sato, E., Tomita, M., and Yanagawa, H. (2009). Six classes of nuclear localization signals specific to different binding grooves of importin α. *J Biol Chem.* 284: 478-485.

Kudo, N., Matsumori, N., Taoka, H., Fujiwara, D., Schreiner, E.P., Wolff, B., Yoshida, M. and Horinouchi, S. (1999). Leptomycin B inactivates Crm1/exportin 1 by covalent modification at a cysteine residue in the central conserved region. *Proc Natl Acad Sci U S A.* 96: 9112–9117.

Kudo, N.R., Anger, M., Peters, A.H., Stemmann, O., Theussl, H.C., Helmhart, W., Kudo, H., Heyting, C. and Nasmyth, K. (2009). Role of cleavage by separase of the Rec8 kleisin subunit of cohesin during mammalian meiosis I. *J Cell Sci.* 122(Pt 15): 2686-2698.

Kudo, N.R., Wassmann, K., Anger, M., Schuh, M., Wirth, K.G., Xu, H., Helmhart, W., Kudo, H., Mckay, M., Maro, B., Ellenberg, J., de Boer, P., und Nasmyth, K. (2006). Resolution of chiasmata in oocytes requires separase-mediated proteolysis. *Cell* 126: 135-146.

Kueng, S., Hegemann, B., Peters, B.H., Lipp, J.J., Schleiffer, A., Mechtler, K. and Peters, J.M. (2006). Wapl controls the dynamic association of cohesin with chromatin. *Cell.* 127(5): 955-967.

Kurze, A., Michie, K.A., Dixon, S.E., Mishra, A., Itoh, T., Khalid, S., Strmecki, L., Shirahige, K., Haering, C.H., Löwe, J. and Nasmyth, K. (2011). A positively charged channel within the Smc1/Smc3 hinge required for sister chromatid cohesion. *EMBO J.* 30(2): 364-378.

La Terra, S., English, C.N., Hergert, P., McEwen, B.F., Sluder, G. and Khodjakov, A. (2005). The de novo centriole assembly pathway in HeLa cells: cell cycle progression and centriole assembly/maturation. *J Cell Biol.* 168(5): 713-722.

Lafont, A.L., Song, J. and Rankin, S. (2010). Sororin cooperates with the acetyltransferase Eco2 to ensure DNA replication-dependent sister chromatid cohesion. *Proc Natl Acad Sci U S A.* 107(47): 20364-20369.

Lambert, W., Söderberg, C.A., Rutsdottir, G., Boelens, W.C., Emanuelsson, C. (2011). Thiol-exchange in DTSSP crosslinked peptides is proportional to cysteine content and precisely controlled in crosslink detection by two-step LC-MALDI MSMS. *Protein Sci.* 20(10): 1682-1691.

Lee, J., Kitajima, T.S., Tanno, Y., Yoshida, K., Morita, T., Miyano, T., Miyake, M. and Watanabe, Y. (2008). Unified mode of centromeric protection by shugoshin in mammalian oocytes and somatic cells. *Nat Cell Biol.* 10(1): 42-52.

Leidel, S. and Gönczy, P. (2003). SAS-4 is essential for centrosome duplication in C elegans and is recruited to daughter centrioles once per cell cycle. *Dev Cell.* 4(3): 431-439.

Leidel, S., Delattre, M., Cerutti, L., Baumer, K. and Gönczy, P. (2005). SAS-6 defines a protein family required for centrosome duplication in C. elegans and in human cells. *Nat Cell Biol.* 7(2): 115-125.

Lénárt, P., Petronczki, M., Steegmaier, M., Di Fiore, B., Lipp, J.J., Hoffmann, M., Rettig, W.J., Kraut, N. and Peters, J.M. (2007). The small-molecule inhibitor BI 2536 reveals novel insights into mitotic roles of polo-like kinase 1. *Curr Biol.* 17(4): 304-315.

Lengronne, A., Katou, Y., Mori, S., Yokobayashi, S., Kelly, G.P., Itoh, T., Watanabe, Y., Shirahige, K., and Uhlmann, F. (2004). Cohesin relocation from sites of chromosomal loading to places of convergent transcription. *Nature.* 430: 573–578.

Lin, W., Wang, M., Jin, H. and Yu, H.G. (2011). Cohesin plays a dual role in gene regulation and sister-chromatid cohesion during meiosis in Saccharomyces cerevisiae. *Genetics.* 187(4): 1041-1051.

Liu, Q., Jiang, Q. and Zhang, C. (2009). A fraction of Crm1 locates at centrosomes by its CRIME domain and regulates the centrosomal localization of pericentrin. *Biochem Biophys Res Commun.* 384: 383-388.

Llano, E., Gómez, R., Gutiérrez-Caballero, C., Herrán, Y., Sánchez-Martín, M., Vázquez-Quiñones, L., Hernández, T., de Alava, E., Cuadrado, A., Barbero, J.L., Suja, J.A. and Pendás A.M. (2008). Shugoshin-2 is essential for the completion of meiosis but not for mitotic cell division in mice. *Genes Dev.* 22(17): 2400-2413.

Loncarek, J., Hergert, P. and Khodjakov, A. (2010). Centriole reduplication during prolonged interphase requires procentriole maturation governed by Plk1. *Curr Biol.* 20(14): 1277-1282.

Loncarek, J., Hergert, P., Magidson, V. and Khodjakov, A. (2008). Control of daughter centriole formation by the pericentriolar material. *Nat Cell Biol.* 10(3): 322-328.

Losada, A., Hirano, M. and Hirano, T. (1998). Identification of Xenopus SMC protein complexes required for sister chromatid cohesion. *Genes Dev.* 12(13): 1986-1997.

Losada, A., Yokochi, T. and Hirano, T. (2005). Functional contribution of Pds5 to cohesin-mediated cohesion in human cells and Xenopus egg extracts. *J Cell Sci.* 118(Pt 10): 2133-2141.

Losada, A., Yokochi, T., Kobayashi, R., and Hirano, T. (2000). Identification and characterization of SA/Scc3p subunits in the Xenopus and human cohesin complexes. *J Cell Biol.* 150: 405–416.

Lu, F., Lan, R., Zhang, H., Jiang, Q. and Zhang, C. (2009). Geminin is partially localized to the centrosome and plays a role in proper centrosome duplication. *Bio Cell.* 101(5): 273-285.

Macy, B., Wang, M. and Yu, H.G. (2009). The many faces of shugoshin, the "guardian spirit," in chromosome segregation. *Cell Cycle.* 8(1): 35-37.

Mahoney, N.M., Goshima, G., Douglass, A.D. and Vale, R.D. (2006). Making microtubules and mitotic spindles in cells without functional centrosomes. *Curr Biol.* 16: 564-569.

Maiato, H., Rieder, C.L. and Khodjakov, A. (2004). Kinetochore-driven formation of kinetochore fibers contributes to spindle assembly during animal mitosis. *J Cell Biol.* 167: 831-840.

Manandhar, G., Schatten, H. and Sutovsky, P. (2005). Centrosome reduction during gametogenesis and its significance. *Biol Reprod.* 72(1): 2-13.

Marshall, W.F. and Nonaka, S. (2006). Cilia: tuning in to the cell's antenna. *Curr Biol.* 16(15): R604-614.

Matsumoto, Y. and Maller, J.L. (2004). A centrosomal localization signal in cyclin E required for Cdk2-independent S phase entry. *Science*. 306: 885-888.

Matsuo, K., Ohsumi, K., Iwabuchi, M., Kawamata, T., Ono, Y., Takahashi, M. (2012). Kendrin is a novel substrate for separase involved in the licensing of centriole duplication. *Curr Biol.* 22: 1-7.

Mayor, T., Stierhof, Y.D., Tanaka, K., Fry, A.M. and Nigg, E.A. (2000). The centrosomal protein C-Nap1 is required for cell cycle-regulated centrosome cohesion. *J Cell Biol.* 151: 837–846.

Mazia, D. (1987). The chromosome cycle and the centrosome cycle in the mitotic cycle. *Int Rev Cytol.* 100: 49-92.

Mc Intyre, J., Muller, E.G., Weitzer, S., Snydsman, B.E., Davis, T.N. and Uhlmann, F. (2007). In vivo analysis of cohesin architecture using FRET in the budding yeast Saccharomyces cerevisiae. *EMBO J.* 26(16): 3783-3793.

McFadden, G.I., and Melkonian, M. (1986). Use of Hepes buffer for microalgal culture media and fixation for electron microscopy. *Phycologia*. 25: 551-557.

McGuinness, B.E., Hirota, T., Kudo, N.R., Peters, J.M., and Nasmyth, K. (2005). Shugoshin prevents dissociation of cohesin from centromeres during mitosis in vertebrate cells. *PLoS Biol.* 3(3): e86.

Megraw, T.L., Sharkey, J.T. and Nowakowski, R.S. (2011). Cdk5rap2 exposes the centrosomal root of microcephaly syndromes. *Trends Cell Biol.* 21(8): 470-480.

Mei, J., Huang X., and Zhang, P. (2001). Securin is not required for cellular viability, but is required for normal growth of mouse embryonic fibroblasts. *Curr Biol.* 11(15): 1197-1201.

Meraldi, P., Lukas, J., Fry, A.M., Bartek, J. and Nigg, E.A. (1999). Centrosome duplication in mammalian somatic cells requires E2F and Cdk2-cyclin A. *Nat Cell Biol.* 1: 88-93.

Michaelis, C., Ciosk, R., and Nasmyth, K. (1997). Cohesins: Chromosomal proteins that prevent premature separation of sister chromatids. *Cell.* 91: 35-45.

Möckel, M. (2010). Master thesis. University of Bayreuth.

Moutinho-Pereira, S., Debec, A. and Maiato, H. (2009). Microtubule cytoskeleton remodeling by acentriolar microtubule-organizing centers at the entry and exit from mitosis in Drosophila somatic cells. *Mol Biol Cell.* 20(11): 2796-2808.

Mueller, P.R., Coleman, T.R. and Dunphy, W.G. (1995). Cell cycle regulation of a Xenopus Wee1-like kinase. *Mol Biol Cell.* 6(1): 119-134.

Murray, M.T., Krohne, G., Franke, W.W. (1991). Different forms of soluble cytoplasmic mRNA binding proteins and particles in Xenopus laevis oocytes and embryos. *J Cell Biol* 112(1): 1-11.

Nakamura, A., Arai, H. and Fujita, N. (2009). Centrosomal Aki1 and cohesin function in separase-regulated centriole disengagement. *J Cell Biol.* 187(5): 607-614.

Nakanishi, A., Han, X., Saito, H., Taguchi, K., Ohta, Y., Imajoh-Ohmi, S. and Miki, Y. (2007). Interference with BRCA2, which localizes to the centrosome during S and early M phase, leads to abnormal nuclear division. *Biochem Biophys Res Commun.* 355: 34-40.

Narasimhachar, Y. and Coué, M. (2009). Geminin stabilizes Cdt1 during meiosis in Xenopus oocytes. *J Biol Chem.* 284(40): 27235-27242.

Nasmyth, K. (2011). Cohesin: a catenase with separate entry and exit gates? *Nat Cell Biol.* 13(10): 1170-1177.

Nasmyth, K. and Haering, C.H. (2005). The structure and function of smc and kleisin complexes. *Annu Rev Biochem.* 74: 595–648.

Nasmyth, K. and Haering, C.H. (2009). Cohesin: its roles and mechanisms. *Annu Rev Genet.* 43: 525-558.

Nasmyth, K., Peters, J.M. and Uhlmann, F. (2000). Splitting the chromosome: cutting the ties that bind sister chromatids. *Science.* 288(5470): 1379-1385.

Nigg, E.A. (2002). Centrosome aberrations: cause or consequence of cancer progression? *Nat Rev Cancer.* 2(11): 815-825.

Nigg, E.A. (2006). Origins and consequences of centrosome aberrations in human cancer. *Int J Cancer.* 119: 2717-2723.

Nigg, E.A. (2007). Centrosome duplication: of rules and licenses. *Trends Cell Biol.* 17 (5): 215-221.

Nigg, E.A. and Raff, J.W. (2009). Centrioles, centrosomes, and cilia in health and disease. *Cell.* 139(4): 663-678.

Nigg, E.A., and Stearns, T. (2011). The centrosome cycle: Centriole biogenesis, duplication and inherent asymmetries. *Nat Cell Biol.* 13(10): 1154-1160.

Nishiyama, T., Ladurner, R., Schmitz, J., Kreidl, E., Schleiffer, A., Bhaskara, V., Bando, M., Shirahige, K., Hyman, A.A., Mechtler, K. and Peters, J.M. (2010). Sororin mediates sister chromatid cohesion by antagonizing Wapl. *Cell.* 143(5): 737-749.

Ohba, T., Nakamura, M., Nishitani, H. and Nishimoto, T. (1999). Self-Organization of microtubule asters induced in Xenopus egg extracts by GTP-bound Ran. *Science.* 284: 1356-1358.

Panizza, S., Tanaka, T., Hochwagen, A., Eisenhaber, F. and Nasmyth, K. (2000). Pds5 cooperates with cohesin in maintaining sister chromatid cohesion. *Curr Biol.* 10(24): 1557-1564.

Parker, L.L., Atherton-Fessler, S. and Piwnica-Worms, H. (1992). p107wee1 is a dual-specificity kinase that phosphorylates p34cdc2 on tyrosine 15. *Proc Natl Acad Sci USA.* 89(7): 2917-2921.

Pascreau, G., Eckerdt, F., Churchill, M.E. and Maller, J.L. (2010). Discovery of a distinct domain in cyclin A sufficient for centrosomal localization independently of Cdk binding. *Proc Natl Acad Sci. U.S.A.* 107: 2932-2937.

Pelletier, L., Ozlü, N., Hannak, E., Cowan, C., Habermann, B., Ruer, M., Müller-Reichert, T. and Hyman, A.A. (2004). The Caenorhabditis elegans centrosomal protein SPD-2 is required for both pericentriolar material recruitment and centriole duplication. *Curr Biol.* 14(10): 863-873.

Peters, J.M., Tedeschi, A., and Schmitz, J. (2008). The cohesin complex and its roles in chromosome biology. *Genes Dev. 22*: 3089-3114.

Petronczki, M., Siomos, M.F. and Nasmyth, K. (2003). Un ménage à quatre: the molecular biology of chromosome segregation in meiosis. *Cell.* 112(4): 423-440.

Pfleger, C.M., and Kirschner, M.W. (2000). The KEN box: an APC recognition signal distinct from the D box targeted by Cdh1. *Genes Dev.* 14(6): 655-665.

Pfleghaar, K., Heubes, S., Cox, J., Stemmann, O., and Speicher, M.R. (2005). Securin is not required for chromosomal stability in human cells. *PloS Biol.* 3(12): e416.

Piel, M., Meyer, P., Khodjakov, A., Rieder, C.L. and Bornens, M. (2000). The respective contributions of the mother and daughter centrioles to centrosome activity and behavior in vertebrate cells. *J Cell Biol.* 149(2): 317-330.

Pines, J. (2011). Cubism and the cell cycle: the many faces of the APC/C. *Nat Rev Mol Cell Biol.* 12: 427-438.

Porter, A.C., and Farr, C.J. (2004). Topoisomerase II: untangling its contribution at the centromere. *Chromosome Res.* 12(6): 569-583.

Pouwels, J., Kukkonen, A.M., Lan, W., Daum, J.R., Gorbsky, G.J., Stukenberg, T., and Kallio, M.J. (2007). Shugoshin-1 plays a central role in kinetochore assembly and is required for kinetochore targeting of Plk1. *Cell Cycle.* 6: e1-e7.

Praetorius, H.A., and Spring, K.R. (2005). A physiological view of the primary cilium. *Annu Rev Physiol.* 67: 515-29.

Prasanth, S.G., Prasanth, K.V., Siddiqui, K., Spector, D.L. and Stillman, B. (2004). Human Orc2 localizes to centrosomes, centromeres and heterochromatin during chromosome inheritance. *EMBO J.* 23(13): 2651-2663.

Quintyne, N.J. and Schroer, T. (2002). Distinct cell cycle–dependent roles for dynactin and dynein at centrosomes. *J Cell Biol.* 159(2): 245-254.

Rabitsch, K.P., Gregan, J., Schleiffer, A., Javerzat, J.P., Eisenhaber, F. and Nasmyth, K. (2004). Two fission yeast homologs of Drosophila Mei-S332 are

required for chromosome segregation during meiosis I and II. *Curr Biol.* 14(4): 287-301.

Rankin, S., Ayad, N.G. and Kirschner, M.W. (2005). Sororin, a substrate of the anaphase-promoting complex, is required for sister chromatid cohesion in vertebrates. *Mol Cell.* 18(2): 185-200.

Rappleye, C.A., Tagawa, A., Lyczak, R., Bowerman, B. and Aroian, R.V. (2002). The anaphase-promoting complex and separin are required for embryonic anterior-posterior axis formation. *Dev Cell.* 2(2): 195-206.

Rauh, N.R., Schmidt, A., Bormann, J., Nigg, E.A. and Mayer, T.U. (2005). Calcium triggers exit from meiosis II by targeting the APC/C inhibitor XErp1 for degradation. *Nature.* 437: 1048-1052.

Resnick, T.D., Satinover, D.L., MacIsaac, F., Stukenberg, P.T., Earnshaw, W.C., Orr-Weaver, T.L. and Carmena, M. (2006). INCENP and Aurora B promote meiotic sister chromatid cohesion through localization of the Shugoshin MEI-S332 in Drosophila. *Dev Cell.* 11(1): 57-68.

Reynolds, E.S. (1963). The use of lead citrate at high pH as an electron-opaque stain in electron microscopy. *J Cell Biol.* 17: 208-212.

Riedel, C.G., Katis, V.L., Katou, Y., Mori, S., Itoh, T., Helmhart, W., Gálová, M., Petronczki, M., Gregan, J., Cetin, B., Mudrak, I., Ogris, E., Mechtler, K., Pelletier, L., Buchholz, F., Shirahige, K. and Nasmyth, K. (2006). Protein phosphatase 2A protects centromeric sister chromatid cohesion during meiosis I. *Nature.* 441(7089): 53-61.

Rieder, C.L., Faruki, S., and Khodjakov, A. (2001). The centrosome in vertebrates: more than a microtubule-organizing center. *Trends Cell Biol.* 11(10): 413–419.

Rivera, T. and Losada, A. (2006). Shugoshin and pp2a, shared duties at the centromere. Bioessays. 28(8): 775–779.

Salic, A., Waters, J.C. and Mitchison, T.J. (2004). Vertebrate shugoshin links sister centromere cohesion and kinetochore microtubule stability in mitosis. *Cell.* 118(5): 567-578.

Salisbury, J.L., Suino, K.M., Busby, R. and Springett, M. (2002). Centrin-2 is required for centriole duplication in mammalian cells. *Curr Biol.* 12(15): 1287-1292.

Sambrook, J., and Russell, D.W. (2001). Molecular cloning: a laboratory manual, 3rd *(Cold Spring Harbor, N.Y., Cold Spring Harbor Laboratory Press).*

Sambrook, J., Fritsch, E.F. and Maniatis, T. (1989). Molecular Cloning *(Cold Spring Harbor, CSH Laboratory Press).*

Scanlan, M.J., Gout, I., Gordon, C.M., Williamson, B., Stockert, E., Gure, A.O., Jäger, D., Chen, Y.T., Mackay, A., O'Hare, M.J., and Old, L.J. (2001). Humoral immunity to human breast cancer: antigen definition and quantitative analysis of mRNA expression. *Cancer Immun.* 1. 4-20.

Schleiffer, A., Kaitna, S., Maurer-Stroh, S., Glotzer, M., Nasmyth, K., and Eisenhaber, F. (2003). Kleisins: A superfamily of bacterial and eukaryotic SMC protein partners. *Mol Cell.* 11: 571–575.

Schmidt, A., Duncan, P. I., Rauh, N. R., Sauer, G., Fry, A. M., Nigg, E. A. and Mayer, T. U. (2005). Xenopus polo-like kinase Plx1 regulates XErp1, a novel inhibitor of APC/C activity. *Genes Dev.* 19: 502-513.

Schmidt, A., Rauh, N. R., Nigg, E. A. and Mayer, T. U. (2006). Cytostatic factor: an activity that puts the cell cycle on hold. *J Cell Sci.* 119: 1213-1218.

Schmitz, J., Watrin, E., Lénárt, P., Mechtler, K. and Peters, J.M. (2007). Sororin is required for stable binding of cohesin to chromatin and for sister chromatid cohesion in interphase. *Curr Biol.* 17(7): 630-636.

Schöckel, L. (2009). Master thesis. Lausitz University of Applied Science (LUAS), Senftenberg.

Schuh, M., and Ellenberg, J. (2007). Self-organization of MTOCs replaces centrosome function during acentrosomal spindle assembly in live mouse oocytes. *Cell.* 130(3): 484-98.

Severin, F., A.A. Hyman, and Piatti, S. (2001). Correct spindle elongation at the metaphase/anaphase transition is an APC-dependent event in budding yeast. *J Cell Biol.* 155 (5): 711-718.

Silkworth, W.T., Nardi, I.K., Scholl, L.M. and Cimini., D. (2009). Multipolar spindle pole coalescence is a major source of kinetochore mis-attachment and chromosome mis-segregation in cancer cells. *PLoS One.* 4(8): e6564.

Simons, M. and Walz, G. (2006). Polycystic kidney disease: cell division without a c(l)ue? *Kidney Int.* 70(5): 854-864.

Siomos, M.F., Badrinath, A., Pasierbek, P., Livingstone, D., White, J., Glotzer, M. and Nasmyth, K. (2001). Separase is required for chromosome segregation during meiosis I in Caenorhabditis elegans. *Curr Biol.* 11(23): 1825-1835.

Sjögren, C. and Nasmyth, K. (2001). Sister chromatid cohesion is required for postreplicative double-strand break repair in Saccharomyces cerevisiae. *Curr Biol.* 11(12): 991-995.

Sluder, G. and Nordberg, J.J. (2004). The good, the bad and the ugly: the practical consequences of centrosome amplification. *Curr Opin Cell Biol.* 16(1): 49-54.

Sontag, E., Nunbhakdi-Craig, V., Bloom, G.S., and Mumby, M.C. (1995). A Novel Pool of Protein Phosphatase 2A Is Associated with Microtubules and Is Regulated dudng the Cell Cycle. *J Cell Biol.* 128(6): 1131-1144.

Starita, L.M., Machida, Y., Sankaran, S., Elias, J.E., Griffin, K., Schlegel, B.P., Gygi, S.P. and Parvin, J.D. (2004). BRCA1-dependent ubiquitination of gamma-tubulin regulates centrosome number. *Mol Cell Biol.* 24(19): 8457-8466.

Stegmeier, F., Visintin, R. and Amon, A. (2002). Separase, polo kinase, the kinetochore protein Slk19, and Spo12 function in a network that controls Cdc14 localization during early anaphase. *Cell.* 108: 207-220.

Stemmann, O., Boos, D. and Gorr, I.H. (2005). Rephrasing anaphase: separase FEARs shugoshin. *Chromosoma.* 113(8): 409-417.

Stemmann, O., Zou, H., Gerber, S.A., Gygi, S.P., and Kirschner, M.W. (2001). Dual inhibition of sister chromatid separation at metaphase. *Cell.* 107(6): 715-726.

Strnad, P., Leidel, S., Vinogradova, T., Euteneuer, U., Khodjakov, A. and Gönczy, P. (2007). Regulated HsSAS-6 levels ensure formation of a single procentriole per centriole during the centrosome duplication cycle. *Dev Cell.* 13(2): 203-213.

Stuermer, A., Hoehn, K., Faul, T., Auth, T., Brand, N., Kneissl, M., Pütter, V., Grummt, F. (2007). Mouse pre-replicative complex proteins colocalise and interact with the centrosome. *Eur J Cell Biol.* 86(1): 37-50.

Sullivan, M., C. Lehane, and Uhlmann, F. (2001). Orchestrating anaphase and mitotic exit: separase cleavage and localization of Slk19. *Nat Cell Biol.* 3(9): 771-777.

Sumara, I., Vorlaufer, E., Gieffers, C., Peters, B.H. and Peters, J.M. (2000). Characterization of vertebrate cohesin complexes and their regulation in prophase. *J Cell Biol.* 151(4): 749-762.

Sumara, I., Vorlaufer, E., Stukenberg, P.T., Kelm, O., Redemann, N., Nigg, E.A. and Peters, J.M. (2002). The dissociation of cohesin from chromosomes in prophase is regulated by polo-like kinase. *Mol Cell.* 9(3): 515–525.

Sun, Y., Kucej, M., Fan, H.Y., Yu, H., Sun, Q.Y. and Zou H. (2009). Separase is recruited to mitotic chromosomes to dissolve sister chromatid cohesion in a DNA-dependent manner. *Cell.* 137(1): 123-132.

Sun, Y., Yu, H., and Zou, H. (2006). Nuclear exclusion of separase prevents cohesin cleavage in interphase cells. *Cell Cycle.* 5(21): 2537-2542.

Sundin, O., and Varshavsky, A. (1981). Arrest of segregation leads to accumulation of highly intertwined catenated dimers: dissection of the final stages of SV40 DNA replication. *Cell.* 25(3): 659-669.

Surosky, R.T., Newlon, C.S. and Tye, B.K. (1986). The mitotic stability of deletion derivatives of chromosome III in yeast. *Proc Natl Acad Sci U S A.* 83(2): 414-418.

Szöllösi, D., Calarco, P. and Donahue, R.P. (1972). Absence of centrioles in the first and second meiotic spindles of mouse oocytes. *J Cell Sci.* 11(2): 521-541.

Tachibana, K.E., Gonzalez, M.A., Guarguaglini, G., Nigg, E.A. and Laskey, R.A. (2005). Depletion of licensing inhibitor geminin causes centrosome overduplication and mitotic defects. *EMBO Rep.* 6(11): 1052-1057.

Tada, S., Li, A., Maiorano, D., Méchali, M., Blow, J.J. (2001). Repression of origin assembly in metaphase depends on inhibition of RLF-B/Cdt1 by geminin. *Nat Cell Biol.* 3(2): 107-113.

Takahashi, T.S., Yiu, P., Chou, M.F., Gygi, S., and Walter, J.C. (2004). Recruitment of Xenopus Scc2 and cohesin to chromatin requires the pre-replication complex. *Nat Cell Biol.* 6: 991-996.

Tanaka, T., Cosma, M.P., Wirth, K. and Nasmyth, K. (1999). Identification of cohesin association sites at centromeres and along chromosome arms. *Cell.* 98(6): 847-858.

Tang, Z., Shu, H., Qi, W., Mahmood, N.A., Mumby, M.C., Yu, H. (2006). PP2A is required for centromeric localization of Sgo1 and proper chromosome segregation. *Dev Cell.* 10(5):575-585.

Tang, Z., Sun, Y., Harley, S.E., Zou, H., Yu, H. (2004). Human Bub1 protects centromeric sister-chromatid cohesion through Shugoshin during mitosis. *Proc Natl Acad Sci U S A.* 101(52): 18012-18017.

Thein, K.H., Kleylein-Sohn, J., Nigg, E.A. and Gruneberg, U. (2007). Astrin is required for the maintenance of sister chromatid cohesion and centrosome integrity. *J Cell Biol.* 178(3): 345-354.

Tsou, M. F. and Stearns, T. (2006). Mechanism limiting centrosome duplication to once per cell cycle. *Nature.* 442 (7105): 947-951.

Tsou, M.F., Wang, W.J., George, K.A., Uryu, K., Stearns, T. and Jallepalli, P.V. (2009). Polo kinase and separase regulate the mitotic licensing of centriole duplication in human cells. *Dev Cell.* 17(3): 344-354.

Turner, D.L. and Weintraub, H. (1994). Expression of achaete-scute homolog 3 in Xenopus embryos converts ectodermal cells to a neural fate. *Genes Dev.* 8(12): 1434-1447.

Uhlmann, F. (2003). Separase regulation during mitosis. *Biochem Soc Symp.* 70: 243-251.

Uhlmann, F., Lottspeich, F. and Nasmyth, K. (1999). Sister-chromatid separation at anaphase onset is promoted by cleavage of the cohesin subunit Scc1. *Nature.* 400 (6739): 37-42.

Uhlmann, F., Wernic, D., Poupart, M.A., Koonin, E.V. and Nasmyth, K. (2000). Cleavage of cohesin by the CD clan protease separin triggers anaphase in yeast. *Cell.* 103(3): 375-386.

Unal, E., Heidinger-Pauli, J.M., Kim, W., Guacci, V., Onn, I., Gygi, S.P. and Koshland, D.E. (2008). A molecular determinant for the establishment of sister chromatid cohesion. *Science.* 321. 566-569.

van Breugel, M., Hirono, M., Andreeva, A., Yanagisawa, H.A., Yamaguchi, S., Nakazawa, Y., Morgner, N., Petrovich, M., Ebong, I.O., Robinson, C.V., Johnson, C.M., Veprintsev, D. and Zuber, B. (2011). Structures of SAS-6 suggest its organization in centrioles. *Science.* 331(6021): 1196-1199.

Verde, F., Labbé, J.C., Dorée, M. and Karsenti, E. (1990). Regulation of microtubule dynamics by cdc2 protein kinase in cell-free extracts of Xenopus eggs. *Nature.* 343(6255): 233-238.

Vernì, F., Gandhi, R., Goldberg, M.L. and Gatti, M. (2000). Genetic and molecular analysis of wings apart-like (wapl), a gene controlling heterochromatin organization in Drosophila melanogaster. *Genetics.* 154(4): 1693-1710.

Vladar, E.K., and Stearns, T. (2007). Molecular characterization of centriole assembly in ciliated epithelial cells. *J Cell Biol.* 178(1): 31-42.

Waizenegger, I.C., Hauf, S., Meinke, A., and Peters, J.M. (2000). Two distinct pathways remove mammalian cohesin from chromosome arms in prophase and from centromeres in anaphase. *Cell.* 103: 399-410.

Wang, L.H.C., Mayer, B., Stemmann, O., Nigg, E.A. (2010). Centromere DNA decatenation depends on cohesin removal and is required for mammalian cell division. *J Cell Sci.* 123: 806-813.

Wang, W.J., Soni, K.R., Uryu, K. and Tsou, M. F. (2011). The conversion of centrioles to centrosomes: essential coupling of duplication with segregation. *JCB.* 193(4): 727-739.

Wang, X., Yang, Y. and Dai, W. (2006). Differential subcellular localizations of two human Sgo1 isoforms: implications in regulation of sister chromatid cohesion and microtubule dynamics. *Cell Cycle.* 5(6): 635-640.

Wang, X., Yang, Y., Duan, Q., Jiang, N., Huang, Y., Darzynkiewicz, Z. and Dai, W. (2008). sSgo1, a major splice variant of Sgo1, functions in centriole cohesion where it is regulated by Plk1. *Dev Cell.* 14(3): 331-341.

Warren, W.D., Steffensen, S., Lin, E., Coelho, P., Loupart, M., Cobbe, N., Lee, J.Y., McKay, M.J., Orr-Weaver, T., Heck, M.M. and Sunkel, C.E. (2000). The Drosophila RAD21 cohesin persists at the centromere region in mitosis. *Curr Biol.* 10(22): 1463-1466.

Watanabe, Y. (2005). Shugoshin: guardian spirit at the centromere. *Curr Opin Cell Biol.* 17(6): 590-595.

Watanabe, Y., Shirahige, K., and Uhlmann, F. (2004). Cohesin relocation from sites of chromosomal loading to places of convergent transcription. *Nature.* 430: 573-578.

Weber, S.A., Gerton, J.L., Polancic, J.E., DeRisi, J.L., Koshland, D. and Megee, P.C. (2004). The kinetochore is an enhancer of pericentric cohesin binding. *PLoS Biol.* 2(9): e260.

Wendt, K.S., Yoshida, K., Itoh, T., Bando, M., Koch, B., Schirghuber, E., Tsutsumi, S., Nagae, G., Ishihara, K., Mishiro, T., Yahata, K., Imamoto, F., Aburatani, H., Nakao, M., Imamoto, N., Maeshima, K., Shirahige, K. and Peters, J.M. (2008). Cohesin mediates transcriptional insulation by CCCTC-binding factor. *Nature.* 451(7180): 796-801.

Wittmann, T., Hyman, A., und Desai, A. (2001). The spindle: A dynamic assembly of microtubules and motors. *Nat Cell Biol.* 3: e28-34.

Wohlschlegel, J.A., Dwyer, B.T., Dhar, S.K., Cvetic, C., Walter, J.C., Dutta, A. (2000). Inhibition of eukaryotic DNA replication by geminin binding to Cdt1. *Science.* 290(5500): 2309-2312.

Wong, C. and Stearns, T. (2003). Centrosome number is controlled by a centrosome-intrinsic block to reduplication. *Nat Cell Biol.* 5: 539-544.

Wong, R.W., and Blobel, G. (2008). Cohesin subunit SMC1 associates with mitotic microtubules at the spindle pole. *Proc Natl Acad Sci.* 105: 15441-15445.

Xu, X., Weaver, Z., Linke, S.P., Li, C., Gotay, J., Wang, X.W., Harris, C.C., Ried, T. and Deng, C.X. (1999). Centrosome amplification and a defective G2-M cell cycle checkpoint induce genetic instability in BRCA1 exon 11 isoform-deficient cells. *Mol Cell.* 3(3): 389-395.

Xu, Z., Cetin, B., Anger, M., Cho, U.S., Helmhart, W., Nasmyth, K. and Xu, W. (2009). Structure and function of the PP2A-shugoshin interaction. *Mol Cell.* 35(4): 426-441.

Yamada, H.Y., Yao, Y., Wang, X., Zhang, Y., Huang, Y., Dai, W. and Rao, C.V. (2012). Haploinsufficiency of SGO1 results in deregulated centrosome dynamics, enhanced chromosomal instability and colon tumorigenesis. *Cell Cycle.* 11(3): 479-488.

Zou, H., McGarry, T.J., Bernal, T. and Kirschner, M.W. (1999). Identification of a vertebrate sister-chromatid separation inhibitor involved in transformation and tumorigenesis. *Science*. 285: 418-422.

Zou, H., Stemmann, O., Anderson, J.S., Mann, M., and Kirschner, M.W. (2002). Anaphase specific auto-cleavage of separase. *FEBS Lett.* 528 (1-3): 246-250.

8. PUBLIKATIONSLISTE

Im Rahmen dieser Arbeit sind folgende Veröffentlichungen entstanden:

Schöckel, L., Möckel, M., Mayer, B., Boos, D. and Stemmann, O. (2011). Cleavage of cohesin rings coordinates the separation of centrioles and chromatids. *Nat Cell Biol,* **13**, 966-972.

Schöckel, L., Karalus, D., Mayer, B. and Stemmann, O. (2012). An alternatively spliced bifunctional localization signal reprograms shugoshin 1 to protect centrosomal instead of centromeric cohesin. Manuscript in preparation.

9. DANKSAGUNG

10. LEBENSLAUF

PERSÖNLICHE DATEN

Name:	**LAURA SCHÖCKEL**
Geburtsdatum:	11.12.1983
Geburtsort:	Cottbus
Adresse:	Hölderlin Anlage 3, 95447 Bayreuth

PROMOTION

04/2009 – 2012   **Universität Bayreuth**

Doktorarbeit am Lehrstuhl für Genetik in der Arbeitsgruppe von Prof. Dr. Olaf Stemmann

STUDIUM

Masterstudium   **Hochschule Lausitz (Senftenberg)**
03/2007 – 04/2009   Studium der Biotechnologie
Abschluss: **Master of Science** (M.Sc.)

Master Thesis   **Max-Planck-Institut für Biochemie (Martinsried/München)**
04/2008 – 04/2009   Abteilung Zellbiologie bei Prof. Dr. Olaf Stemmann

Bachelorstudium   **Hochschule Lausitz (Senftenberg)**
03/2003 – 04/2007   Studium der Biotechnologie
Abschluss: **Bachelor of Science** (B.Sc.)

Bachelor Thesis   **Charité (Berlin)**
08/2006 – 03/2007   Abteilung Dermatologie bei PD Dr. Ingo Nindl

Praxissemester   **Deutsches Krebsforschungszentrum (DKFZ) (Heidelberg)**
08/2005 – 02/2006   Abteilung Tumorvirologie bei Dr. Nathalie Salomé

SCHULAUSBILDUNG

07/2000 – 06/2001   Schüleraustausch (Oklahoma, USA)
08/1996 – 06/2003   Heinrich-Heine Gymnasium (Cottbus)
Abschluss: **Abitur**

Hiermit erkläre ich, dass ich die Arbeit selbständig verfasst und keine anderen als die von mir angegebenen Quellen und Hilfsmittel benutzt habe.

Ferner erkläre ich, dass ich anderweitig mit oder ohne Erfolg nicht versucht habe, diese Dissertation einzureichen. Ich habe keine gleichartige Doktorprüfung an einer Hochschule endgültig nicht bestanden.

Bayreuth, den 02.05.2012